DEVELOPMENT AND IMPLEMENTATION OF A COMPOSITE MODEL FOR WAVE, CIRCULATION, AND SEDIMENT PROCESSES IN IBAKA DEEP SEAPORT IN NIGERIA

A Dissertation

by

EPHRAIM UDO PAUL

Submitted to the Office of Graduate and Professional Studies of
Texas A&M University
in partial fulfillment of the requirements for the degree of

DOCTOR OF PHILOSOPHY

Chair of Committee,	David A. Brooks
Co-Chair of Committee,	Benjamin S. Giese
Committee Members,	Steven F. DiMarco
	James M. Kaihatu
Head of Department,	Debbie J. Thomas

August 2014

Major Subject: Oceanography

ABSTRACT

In-depth knowledge of nearshore wave, circulation, and sediment processes are vital to effective and efficient management, operation, and regulation of ports and harbors. The scientific knowledge of these processes is currently lacking in Ibaka, Nigeria and this work was designed to assess these processes, thereby filling the existing gap in the literature. Even after seven decades of discovery of Ibaka bay as a leading natural harbor in Nigeria, no proactive efforts have been made to harness this resource. This dissertation aimed at developing a composite modeling system that would provide accurate and reliable information on circulation and sediment processes in Ibaka. This information will facilitate the speedy development of the deep seaport for economic empowerment of both local residents and the state. This study has three segments: field experiments, numerical experiments and data analyses.

NearCoM-TVD was chosen as the base model for this study because of its efficiency, accuracy, and robustness in simulating the processes of interest in Ibaka. This study has undertaken a detailed investigation of the impacts of different channel designs on the erosion and/or accretion of adjacent Ibaka beach and provided the optimum channel size and location. Maps and time series of wave action attenuation based on the optimum channel design have been produced. Analyses of relative contribution of various forcing mechanisms to the total sediment budget showed that wave height variations have the greatest impact on sediment transport in Ibaka. Significant wave height above 1.0 m initiated sediment transport and morphological changes in Ibaka. The effects of wave-current interactions on sediment

processes have been investigated and found to be significant for wave heights near 1.0 m in Ibaka bay. Examination of seasonal bias on sediment processes showed that only rainy season (April to October) wave climate caused sediment transport in the bay. Reduction of wave action, due to the dredged channel, resulted in wave refocusing towards the nearby Tom Shot Island. Finally, a five-year maintenance dredging time window has been estimated for this port and harbor site.

DEDICATION

This dissertation is dedicated to my beloved parents, Chief Udo Paul Ukpabio and Chief (Mrs.) Charity Udo Akpabio. They have been my source of inspiration in everything I accomplished in life.

ACKNOWLEDGEMENTS

I would like to thank all my advisory committee co-chairs, Dr. Brooks and Dr. Giese, and my committee members, Dr. DiMarco and Dr. Kaihatu, for their patience, guidance and support throughout the duration of this study. A special thank you also goes to my former advisor, Dr. Robert E. Randall of Ocean Engineering Division at Texas A&M University for his patience and direction during my Master of Science program. I equally thank Dr. Hamm C. Chen of Ocean Engineeering department, who introduced me to the numerical modeling world.

Thanks also to Dr. Fengyan Shi of the Center for Applied Coastal Research, University of Deleware, Newark for his guidance and support in the modeling aspect of the study. I owe much gratitude to my parent in-laws, Bishop Udoh Etim Ukpong and Reverend (Mrs.) Grace Udoh Ukpong for their continued support, prayers and encouragements throughout the duration of my graduate studies at Texas A&M University. I sincerely thank my beloved wife, Mfon Paul, and my daughters, Idaraobong and Unwana Paul for their understanding and cooperation. Much time was spent outside home during this study.

Lastly, I thank my siblings and friends especially Mr. Daniel Ukpong, Mrs. Victoria Udoh, Mrs. Itoro Umoh, Mr. Edet Ekanem, Mrs. Margaret Udoh, Chief Edet Udoh, Mr. Anietie UdoEkpe, Mr. Effiong Ukpabio, Mr. Ime Udong, Mrs. Florence Udong, Mr. Lawrence Isung, and Dr. Aniefiok Ukommi for their numerous supports. I also thank some of my former teachers and professors: Professor Akpan H. Ekpo, Professor Ini A. Udoka, Mr. Godwin E. Udoh, Mr. Okon U. Udo, Mr. Edem E. Esara, Engr. Uwemedimo Ebong, Mr. Etim J. Akpan, Mr. Ime A. Udo, Mrs.

Esther J. Efrenie, Dr. (Mrs.) G. A. Chukwudebe, Professor Sam Ogbogu, Dr. Michael Ndinechi, and Professor Johnson I. Ejimiah of blessed memory. You prepared me for these achievements.

This list will be incomplete if I fail to mention the initiator of the graduate training program, Architect (Obong) Victor B. Attah, the immediate past executive governor of Akwa Ibom State, Nigeria. I equally thank Obong Attah's successor, Chief Godswill O. Akpabio for the sustenance of the program.

TABLE OF CONTENTS

LIST OF FIGURES

FIGURE Page

LIST OF TABLES

CHAPTER I

INTRODUCTION

Ibaka is one of Nigerian coastal communities. It is centered on Latitude 4.65^{o}N and Longitude 8.32^{o}E with an approximate land area of 50 km^{2} and estimated population of 19,600 people (NPC, 2011). It is situated along the Gulf of Guinea (GoG) in the Southern end of Nigeria and has maritime boundaries with Cameroon to the east, Cross River State, Nigeria to the north, and Equatorial Guinea to the south. The average annual land and surface water temperature is 28^{o}C. Ibaka bay (the project site) is adjacent to and situated Northeast of Ibaka community. Figure 1 is a physical map of Africa indicating Ibaka bay (letter "A" in the map). This figure indicates the proximity of Ibaka to other countries in Africa. At least six other countries could have direct access to this deep seaport. The countries are Cameroon, Equatorial Guinea, Garbon, Congo, Benin Republic, and Togo. None of these countries has its own deep seaport or any other operational deep seaport closer to it than Ibaka. Ibaka and its environs have two main seasons, namely: rainy season (April to November) and dry season (December to March). Stormy rains characterize the rainy season while the dry season has mild weather conditions.

Figure 1. Physical map of Africa showing the location of Ibaka bay ("A" in the map). (Courtesy: www.mapsofworld.com/africa)

The region's predominant, rainy season, wind direction is southwest with a typical speed of 7 m/s at 10 meters above sea level. Swells from the South Atlantic Ocean also enter the study domain from the southwest direction (≈200^{o} using the Nautical convention). Ibaka bay has a non-dredged draft of 13.5 meters in most part of the bay (AKSG Official Site, 2012). Water level at the bay is approximately five meters (5 m) above mean lowest low water datum (MLLW) in the region (Antia, 2012: Personal Communication). The water in the bay is well mixed throughout the year with an average salinity of 28. Maximum spring tidal range observed

in the bay was 3.5 meters (AKSG Official Site, 2012). Higher tidal ranges (approximately 3 meters) occur during rainy season spring tides. The dominant tidal constituents in the region are M_2 and S_2. Other semi-diurnal tidal harmonics, M_4, M_6, etc. can also be seen in a cross shelf current analysis (Rider, 2004). The yearly average tidal range at the offshore boundary of the bay is 1.7 meters. Figure 2 is a map showing major cities, rivers, RDI 300 kHz Workhorse Acoustic Doppler Current Profiler (ADCP) moorings, QuickSCAT wind stations and cross shelf Conductivity, Temperature, and Depth (CTD) stations during a Joint Industry Project (JIP, 2000) in southern Nigerian coastal areas. Ibaka is about twenty-three kilometers (fifteen miles) south of Calabar, which is located on the southeastern end of the map. The map also shows the 100-meter bathymetric contour along the Nigerian coastline. This 100 m depth contour clearly shows that the continental shelf is widened (≈ 120 km) at the southeast end of Nigeria, when compared to the width of the continental shelf on the western coast (≈ 30 km) in Nigeria. This can shed some light on why the wave climate and tidal processes in the two regions are significantly different (as reported in the literature: Awosika and Ibe (1993), Awosika et al., (2000)).

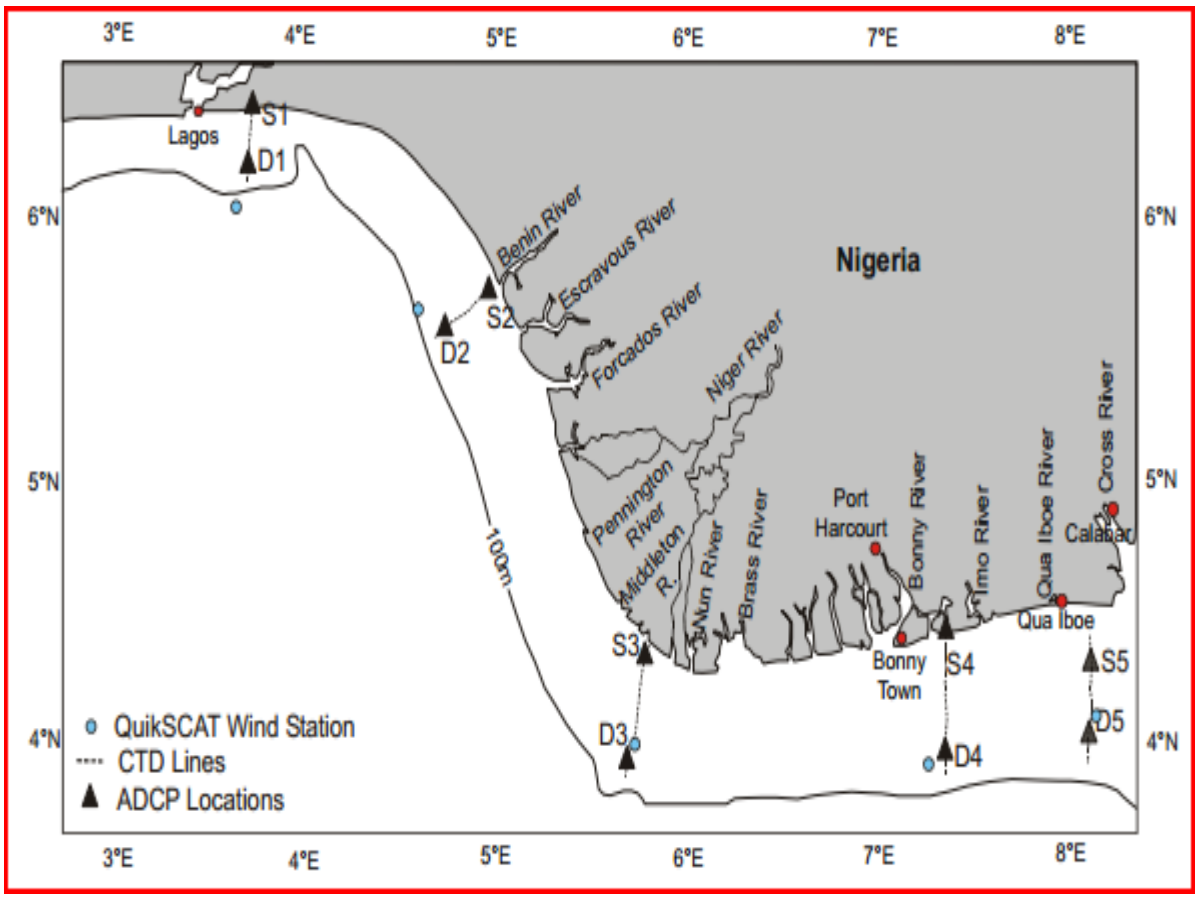

Figure 2. Map of southern Nigeria coastline and continental shelf showing major cities, rivers, RDI ADCP moorings, QuickSCAT wind stations, and CTD stations. (Courtesy: Rider (2004)).

Figure 3 shows the bathymetry of the study site and the locations where some model calibration, validation, and verification data are available. The locations are indicated as JIP and Ekundu in the map.

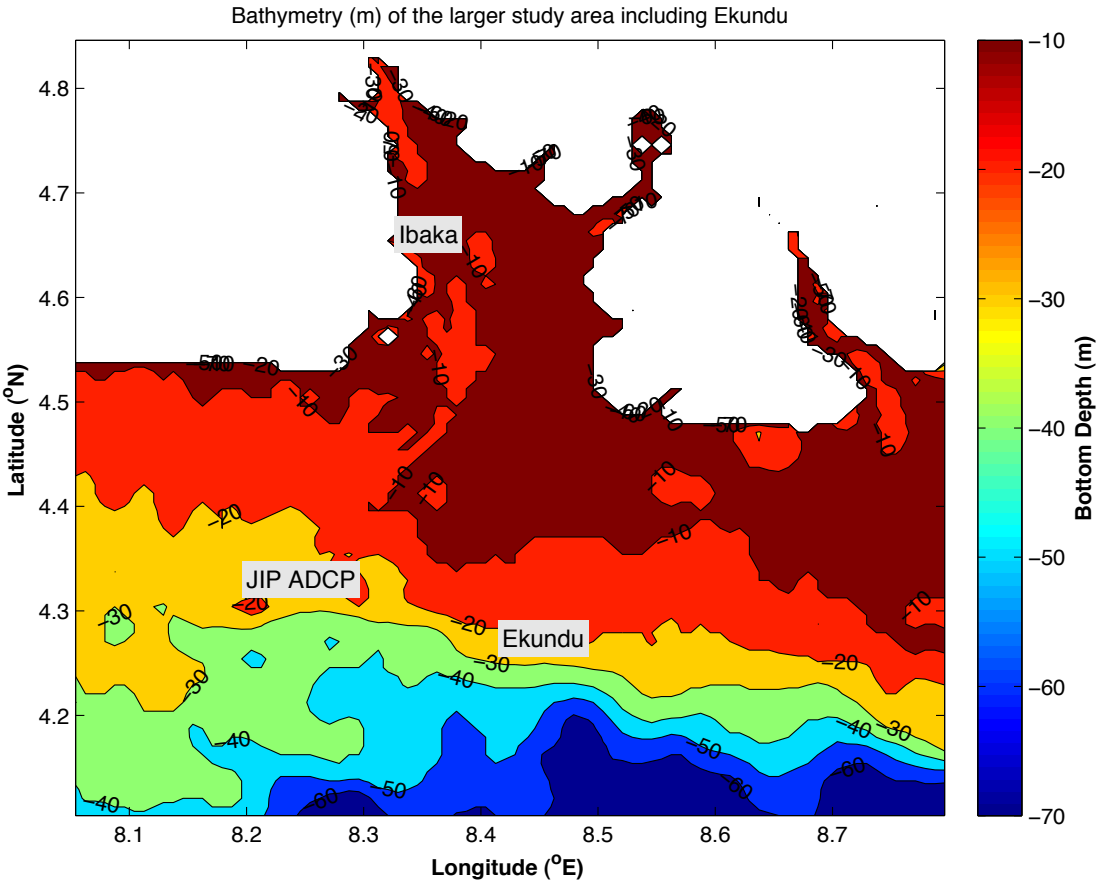

Figure 3. Study site bathymetry and its proximity to locations of model validation data (JIP and Ekundu).

Ibaka is one of the active fishing settlements in Nigeria. Southeastern coastal region of Nigeria has a wider (≈ 120 km) continental shelf when compared to the western Nigeria continental shelf (≈ 30 km) (Awosika and Ibe, 1993; Awosika, 1994; and Awosika et al., 2000). Energetic waves (swells) from the open ocean break at a further distance before they get to Ibaka bay. This is one of the reasons boat mishap and wave breaking related hazards are minimized in Ibaka. The moderate wave climate, combined with continuously upwelled nutrient-rich waters (Ibaka coast is on the left and predominant wind direction is from the

south), makes Ibaka a home to fishermen. About 70% of Ibaka residents engage in fishing for livelihood and fishing activities account for 65% of Ibaka total annual revenue (BNRCC, 2011). Other major occupations of Ibaka people are subsistence farming and fuelwood production, which account for about 15% and 10% of Ibaka total revenue respectively.

Ibaka hosts one of the Nigerian Naval bases (Forward Operation Base, Ibaka). The Navy helps to secure Ibaka against external invasion and sea pirates. They also collaborate with civilian researchers to conduct some Oceanographic and environmental research in Ibaka and surrounding waters. Some fine resolution depth sounding data in Ibaka are archived by the Navy. Unfortunately, most of the data from the naval research are currently not available for public use. Some of these Ibaka near shore data are not classified but they are not processed into formats that can be assessed and used by the general public.

The project site also has an adjacent beach, The Ibaka Beach. The sediment on the beach is mostly coarse ($d_{50} \approx 0.32$ mm) sand. This shiny coarse sand gives the beach an aesthetic look. The beach is not yet developed for tourism and other recreational activities. The beach nourishment is an integral part of the deep seaport project. When the deep seaport is operational and the beach fully developed, the strategic location of Ibaka beach will make it the preferred vacation resort for both local and international tourists. The beach will bring substantial revenue to local communities and Akwa Ibom state government. For instance, a class project done in 2008 (Paul, 2008) by this author revealed that the United State Federal Government made a net profit of $700 for every $1 it invested in Miami Beach, Florida. Further details about the benefits of beach development and nourishment processes can be found in a paper by González and his colleagues (González et al., 2007). This study intends to look at alternative designs of the port channel and other structures that will have the least negative

impacts on the erosion of Ibaka beach and make recommendations to beach developers, stakeholders, and policy makers.

Akwa Ibom State International airport (Ibom Airport) is about 40 Km North-West of this project site. Currently, Ibom airport has the longest runway (6 Km) in West Africa. It is the only airport in the West African sub-region designed with maintenance, repair and overhaul (MRO) facility. According to the official press release from the airport management in December 2013, the MRO facility (still under construction) was 90% completed. The anticipated completion date for all construction work at the airport is May 2015. Ibom international airport is scheduled to commence full operations by the third quarter of 2015.

A review of archival records of the British Colonial government in Nigeria, (1914 to 1960) shows that this natural deep seaport and harbor site in Nigeria was discovered more than a decade before Nigeria's independence in October 1, 1960. There are documented evidences that the British pre-colonial administrators had recommended Ibaka bay for prioritized investments in port- related activities in Nigeria (AKSG Official Site, 2012). Due to political and other vested interests, such recommendations had been ignored and more public funds were channeled into ports and harbors developments in locations where such infrastructures require huge initial capital investments and are also more expensive to maintain. Also, some lives and goods (worth millions of dollars) that have been wasted on Nigerian ports can be attributed entirely to siting of such ports in hazardous locations.

Moreover, the dredged drafts in existing ports in Nigeria cannot support high tonnage vessels (> 100,000 Dead Weight Tonnage (DWT)). Extra costs are incurred by offloading these high tonnage vessels in high seas. All the costs incurred in this long chain of products delivery are transferred to the final consumers. Nigerians and citizens of other neighboring countries

(Cameroon, Equatorial Guinea, Garbon, Benin Republic, and Togo) will soon overcome these additional costs in business, as the successful completion of Ibaka deep seaport project will provide a long-term solution to these problems.

Apart from the additional cost, there are many safety issues with offloading ships in high seas. Most of the reported cases of water pollution in Nigerian coastal waters (outside the Niger Delta region where major Oil and Gas Producers spill crude oil into the coastal waters with impunity) are directly linked to offshore offloading of high tonnage vessels. Sometimes the unpredictable nature of waves can destroy the offshore moorings that keep these vessels in place during the offloading opearations, and the oceans consume the goods in that vessel. Some tankers spill their contents and/or intentionally wash and drain their tanks into the water and pollute it during offloading in high seas (NPA, 2012). These pollutions have grave consequences on fish production and harvesting in Nigerian coastal waters. The health conditions of people who consume these poisoned fishes are also a major concern.

There have been some reported cases where vessels have been lost to ocean waves due to prediction errors in Nigerian territorial waters. These have resulted in economic losses amounting to millions of dollars. Another consequence of this forecast error (which is often overlooked) is the environmental hazard posed by these lost vessels. The ocean currents sometimes drift the vessels, or their parts, into navigation channels or routes, thereby grounding subsequent vessels on that route (NPA, 2013).

There is need to investigate all physical factors associated with circulation and sediment transport/bed morphological changes in Ibaka deep seaport site and Ibaka beach. Detailed scientific studies should be conducted to provide adequate knowledge of the dynamics in the domain. A better understanding of these processes will lead to a cost-effective

port and harbor design. A detailed documentation of the benefits of committing resources to improve existing Oceanographic techniques for better infrastructural designs can be found in Flather, 2000 and Panigrahi et al., 2009. Several studies (Moeini and Etemad-Shahidi (2009), Lin et al. (2002), Ris et al. (1999), etc.) have confirmed that slight perturbations in physical forcing can significantly upset the equilibrium state of an estuary. Thus, it is pertinent to devote resources (time, financial and human resources) to identify the dominant physical forcing mechanisms of circulation in Ibaka bay. Scientific and Engineering experiments must be conducted to evaluate how the port infrastructures would alter the current or existing circulation patterns. These experimental outcomes should guide the final design and construction of the deep seaport infrastructures.

The motivation for this study is my desire to properly understand and provide improved information on Ibaka bay wave climate, circulation and sediment transport/morphological changes. This information and data will facilitate the proper planning, design, construction, maintenance, and operation of the proposed Ibaka deep seaport. This study also aims at developing a predictive or operational model for waves and transport processes in Ibaka. This kind of study has never been done in Ibaka by any investigator. The main challenge of the predictability aspect of this study is the acquisition of long record, high-resolution data for detailed model verification.

The hypotheses for this study are:

1. Wave forcing has a significant influence on the circulation pattern and sediment processes in Ibaka bay.

2. Port infrastructures will refocus wave energy and alter the prevailing circulation patterns in Ibaka bay.

3. Tidal modulation of the refocused waves will erode the adjacent Ibaka beach and transport sediment into the dredged ship channel and harbor on annual time scales.

The goal of this study is to provide answers to relevant scientific and engineering questions, formulated in the above hypotheses, and then recommend a seaport channel design that will preserve adjacent Ibaka beach, have the greatest cost-effective channel maintenance cost, and still keep the local fishermen in business. This study comprises three components: field study, numerical experiments, and data analyses.

This dissertation is organized in the following sequence. Chapter two reviews some literature related to wave, current, and sediment processes in coastal oceans. Chapter three focuses on detailed methodology used in carrying out the research. Chapter four assesses the sensitivity of forcing functions on model predictions. Chapter five presents the results of the physical and numerical studies. Discussion of the results is done in chapter six. Chapter seven provides a summary of conclusions and recommendations for future studies in Ibaka.

CHAPTER II

LITERATURE REVIEW

The bathymetry and water depth exert major influence on nearshore wave transformation. Although high winds can increase wave height, the nearshore wave heights will adjust to local water depth immediately through breaking. Other important factors controlling coastal wave climate are exposure to offshore wave height, coastal steepness, site geometry, and tidal range (Haller et al., 1997; Ajao and Houghton, 1998; Booij et al., 1999 and Ris et al., 1999). However, if the coastal bathymetry profile is complex, modeled wave energy climate could entirely depend on which output location within the model domain is selected (Eckart, 1952; Booij et al., 1985; Dean, 2001; Fredsoe and Deigaard, 1992; Nielsen, 1992; Geeraerts et al., 2009).

Brown and Wolf have demonstrated the importance of including surge in nearshore models with non-uniform bathymetry (Brown and Wolf, 2009 and Wolf, 2009). Their result showed that negligence of surge in the model, in areas where surges are significant, could give a very inaccurate representation of waves and current patterns in the region.

Proper representation of major driving forces is essential for effective model predictions. The JERICHO (Joint Evaluation of Remote sensing Information for Coastal defense and Harbor Organizations) project found that tide estimation affects SWAN model output more than any other source of error in boundary parameter specification in their research domain. The JERICHO project also found that coastal wave heights are mostly limited by local water depth; hence increasing offshore wave heights do not have much additional wave impact at the coasts of most nearshore study sites (Wolf, Hargreaves, & Flather, 2000). However, the

JERICHO project did not quantify the impact of radiation stress associated with the waves on long shore transport and rip current generation near the coast.

The SWAN (Simulating WAves Nearshore) wave model employed in this study is a spectral wave model, which cannot simulate diffraction around obstacles explicitly. Herman et al. in 2002 as reported in Holthuijsen et al. (2004) developed an approximate diffraction algorithm for use in spectral models. It is important to point out that this so-called approximate diffraction formulation was phase decoupled. Since the incidence and diffracted/reflected waves in this model did not have phase coherence, this formulation cannot be applied in domains where nodal wave patterns (standing waves) are significant. This limitation of approximate diffraction formulation was also found in the parabolic approximation to the phase-resolving mild slope equation (Berkhoff, 1972; Panchang et al., 1990). Lin and his colleagues tested the inclusion of reflection and diffraction as well as wave-current interaction in WABED wave model (Lin et al., 2006). They found better agreement with laboratory data within the wave and current conditions the model was evaluated. Booij (2012) included Herman's approximate diffraction formulation in SWAN and compared the output with typical SWAN output and data from Yu et al. (2010). Booij concluded that although model results with the inclusion of approximate diffraction agreed better with data, the added complexity (due to the diffraction module) might not be justified if the model domain of interest has little or a few obstacles.

The modifications of nearshore circulation due to the presence of waves had been studied and quantified by some researchers (Stive and Wind, 1982; Horsburgh and Wilson, 2007; and Zhang and Liu, 2009). These investigators based their works on radiation stress theories developed by Longuet-Higgins and Stewart (1960, 1961, 1962, and 1964). The

researchers concluded that the excess flux of horizontal momentum due to wave breaking and other transformations in nearshore regions could be a major driver of the nearshore circulation on varied time and spatial scales. Stive and Wind assessed the non-linearity of the radiation stress concept while Zhang and Liu extended the concept to standing waves and then included the new derivation in modeling sediment transport in nearshore regions. Nonlinear wave-current interactions explained a significant variation in sediment transport patterns in shallow water in Zhang and Liu's experiment.

Rider and Ewa-Oboho had identified tides as the major forcing component that modulates waves (both the locally wind-generated waves and incoming offshore swells) and other circulation forcing functions in the Cross River estuary (Rider, 2004; Ewa-Oboho, 2012). Previous field studies and data analyses had revealed that tides in most Nigerian coastal waters are predominantly semidiurnal. The major tidal constituent was found to be M_2 with a period of 12.42 hours (Rider, 2004; Houghton; 1976, Picaut, 1983; Ibe and Quelennec, 1989; Awosika et al., 1993; Awosika and Ibe, 1994; Awosika, 1995; Folorunsho and Awosika, 1995; Awosika et al., 2000; Folorunsho, 2006 and Williams and Benson, 2010). Some of these studies had documented that M_2 tidal constituent account for more than 50% of tidal energy in the eastern continental shelf in Nigeria. Most of these studies were conducted by field experiments and some site-specific measured water surface elevation had been published. The interested reader can use these surface elevation data to extract the tidal constituents and see which of the constituents dominate over the others.

A review of available literature shows that several efforts had been made by researchers to employ low-cost Lagrangian drifters to study circulation and dispersion of constituents in coastal shallow waters. Some investigators used passive drifters (Pape and

Garvine, 1982; Ebbesmeyer and Coomes, 1993; Brooks, Personal Communication) while others use active drifters (George and Largier, 1996; Johnson et al., 2003; Perez et al., 2003; Austin and Atkinson, 2004) in acquiring surface circulation data. Passive drifters do not have the facilities to transmit sampled data to land station for archiving whereas active drifters were equipped with periodic data transmitting facility. Some of these authors borrowed their drifter design from a manual by Sybrandy and Niller, 1990.

The cost of most active drifters in the market was high (≈$4,000.00 per piece) and far beyond the budget of this study. I decided to design and construct locally made low-cost surface drifters for this work. Austin and Atkinson's work (Austin and Atkinson, 2004) on design and construction of low-cost drifters served as a guide to my drifter design for the field experiment. Austin and Atkinson used Garmin GPS RINO 110 series, as the electronic facility, in their surface drifter construction. An external timing circuitry was required in their design because of fewer facilities available in Garmin's RINO 110 series when compared to Garmin's RINO 120 series (used in this study). The effective transmission range of the RINO 110 GPS was 1.2 kilometers (0.75 miles) and the data transmission to ground station equipment was done every 4 minutes. This transmission range placed a limit on the use of RINO 110 series based drifters for sampling circulation data in nearshore waters. The four minutes time resolution was also coarse. Some fast varying currents were not sampled. Data storage and battery capacity of the RINO 110 series GPS were also low. Periodic survey of the study domain was required to obtain periodic fixes on the drifters to facilitate their recovery. Time and location information on these drifters were downloaded after the recovery of the drifters. If the drifter were lost to the open ocean, no data at spatial extent beyond a radius of 1.2 km (0.75 miles) would be

available. Garmin RINO 120 series transceiver that was used for this study overcame these limitations of RINO 110 series.

Sediment transport predictions are very sensitive to model input and forcing functions. Different model formulations have their merits, demerits, and varying levels of uncertainties. Getting accurate measurement of waves, current, and sediment data near the seafloor is a herculean task. This makes it very difficult to validate and verify sediment models. Several authors and sediment modelers (Soulsby, 1997; Shapiro et al., 2004; Soulsby and Clarke, 2005; Morteza et al., 2006; Balson and Collins, 2007; Sivakholundu et al., 2009; Carbajal and Montano-Ley, 2011; Kranenburg et al., 2011; Sandra et al., 2011; etc.) have documented their model agreement with existing data. Most verified sediment models have reasonable agreements with data qualitatively (but quantitatively deviate by a factor of 2 on the average). Some of the referred authors ascribed the observed low model skill (low coefficient of determination, r^2, between model output and data) to factors such as inaccurate representation of wave streaming, Stokes drift, residual tidal current direction, and wave velocity asymmetry and acceleration skewness. Even the ground truth data used to verify the model performance also have a high level of uncertainty in the accuracy of the measured data.

Soulsby (1987) suggested that long-term sediment transport could have a very different direction from the residual current because of observed wave stirring effects and non-linear relationship of the sediment flux and current speed. Thus, Soulsby opined that current speed and direction should not be used as a proxy for sediment transport pattern without site-specific experimental verifications. In emphasizing the importance of accounting for small-scale non-linear processes in accurate prediction of sediment transport/ morphology, Soulsby stated that

these sub grid non-linear processes could cause chaotic behavior in sediments similar to the randomness observed in weather due to small perturbations in atmospheric forcing functions.

Komarova and Newell (2000) investigated the processes affecting the formation of sand banks. They found that these bottom features were caused by the interaction between the tides and sea floor in their study domain. They identified two mechanisms responsible for the generation of sand banks and sand waves as: “linear instability and non-linear coupling between long sand banks and short waves”. Their results depicted that the coupling of long sand banks and short sand waves was the major contributor to the generation and evolution of sand banks. This study revealed that long wave modulation of smaller waves is an important forcing function affecting bottom processes in near shore regions.

Balson and Collins (2007) observed that the strongest (but short duration) currents and very large waves did not make significant contributions to the long-term sediment transport in their study location. They suggested that the transition region between storm induced processes at the coastlines and non-linear wave-current interaction process in the offshore region could be the more focused research area in sediment dynamics for a better understanding and prediction of these processes.

Kranenburg et al. (2011) determined that real wave streaming was not the only major process that contributed to onshore sediment transport in flume experiments. These authors also realized that vertical advection of sediments in flumes played a lesser role to onshore sediment transport when compared to the contributions from additional onshore current due to real wave streaming. Interestingly, the authors found that horizontal gradient in horizontal sediment flux due to real wave contributed significantly (same order of magnitude) to sediment

transport as the real wave streaming. Therefore, real wave streaming should be included in sediment models as a spatially varying quantity.

In order to achieve longer channel dredging windows in near shore harbors, sediment exporting channel design (ebb-dominated transport) is desirable since it avoids long-term buildups of sediments towards the upstream section of the channel (Sivakholundu et al. (2009)). Sivakholundu et al. also found that channel designs for extended dredging windows required the longitudinal gradient of the transport rate to be minimized as much as possible. These authors did not quantify the cost implications of minimizing the along channel transport rate gradient.

Kaihatu et al. (1989) found that alternative designs of the entrance channel could minimize wave impacts at Morro Bay, California. Morro Bay had recurring incidence of wave-induced damages (including death of experienced fishermen and other bay users). The wave model they use, RCPWAVE, confirmed some observations reported by the U.S. Army Corps of Engineers (USACE), Los Angeles, 1988. Hence RCPWAVE could be used to predict wave-induced processes in the bay with high level of confidence. Analyses of the USACE reports showed that the location of incident wave breaking (relative to the Morro Bay entrance channel) correlated positively with the number of catastrophic incidence recorded in the bay. This study came up with alternative channel designs that could shift locations of wave breaking further offshore and thus minimize wave-induced damages in the bay. These alternative channel designs increased dredging cost but could save some lives and properties if fully implemented. The scope of the project did not cover analysis of benefit-cost implications of executing the recommendations contained in that report.

Many researchers have identified bed shear stress as the main hydrodynamic parameter that controls transport of sediment in nearshore regions (Grant and Madsen, 1979; Sleath, 1990; Soulsby and Clarke 2005; Van den Boogaard et al., 2009b; Humbyrd and Madsen, 2010; Van der A, et al., 2010; O'Donoghue and Van der A, 2012). Bed shear stress is defined as the frictional force per unit area, imparted to the seabed by the flow or current. Accurate model predictions of near bed sediment processes depend heavily on the proper parametization and/or calculation of the bed shear stress. Sediment transport formulations using bed shear stress are preferred to the ones using mean stream velocities.

The feedback effects of sedimentary processes on bed shear stress had been examined by a couple of investigators (Sheremet and Stone, 2003; Quaresma et al., 2007). They found that bed roughness specification was a critical parameter in the accurate determination of bed shear stress in sediment models.

Oumeraci (1999) assessed the strengths and limitations of physical modeling and then evaluated the usefulness of physical modeling to numerical experiments. Other researchers have emphasized the importance of composite (combining theoretical, physical and numerical modeling) modeling for engineering designs and analyses (Van den Boogaard et al., 2009; Van den Boogaard et al., 2009b; Sutherland and Obhrai, 2009; Barthel and Funke, 1989; Booij and Holthuijsen, 1987; Elgar and Guza, 1985; Birkemeier and Dalrymple, 1975).

Proper parameterization of the sub-grid scale processes in hydrodynamic and transport models is a vital aspect of the modeling work. Good agreements of model result to data or theoretic solutions are highly dependent on how accurate these small-scale processes are calculated. Gent and his colleagues have some publications with a large number of references on this subject matter (Gent, 2011; Gent et al., 1995).

CHAPTER III

METHODOLOGY

This study has three major components: field study, data processing and analyses, and numerical modeling using NearCoM-TVD as the base model. The methods used to conduct these three components of the study are described in the following paragraphs.

FIELD STUDY

The field experiment was designed to obtain forcing, calibration, validation, and verification data for the NearCoM-TVD numerical model. Low-cost (and/or disposable) surface drifters were designed, constructed, and then deployed to sample surface current data in Ibaka estuary, along the Nigerian southeastern coastal waters. The surface drifter construction followed the design of drifters used in previous estuarine work by my advisor, Dr. David Brooks (Figure 4). The major modification to Brooks' surface drifters was the inclusion of data transmitting facility from the estuary to land stations. With this new facility, Brooks' passive prototype drifter was upgraded to an active surface drifter. The major difference between a passive drifter and an active drifter is that data from an active drifter are backed up whereas passive drifters have no backed up facility. The difference is mostly felt if certain events occurred suddenly and the drifter is lost to the open ocean. In such circumstance, all efforts will have been wasted if a passive drifter was deployed since none of the sampled data can be retrieved. For an active drifter, at least all the data transmitted (at specified frequencies) to the ground station could be retrieved. The experiment was carried out in December 2012. Garmin

RINO 120 series Global Positioning System (GPS) formed the electronic system of the surface drifters.

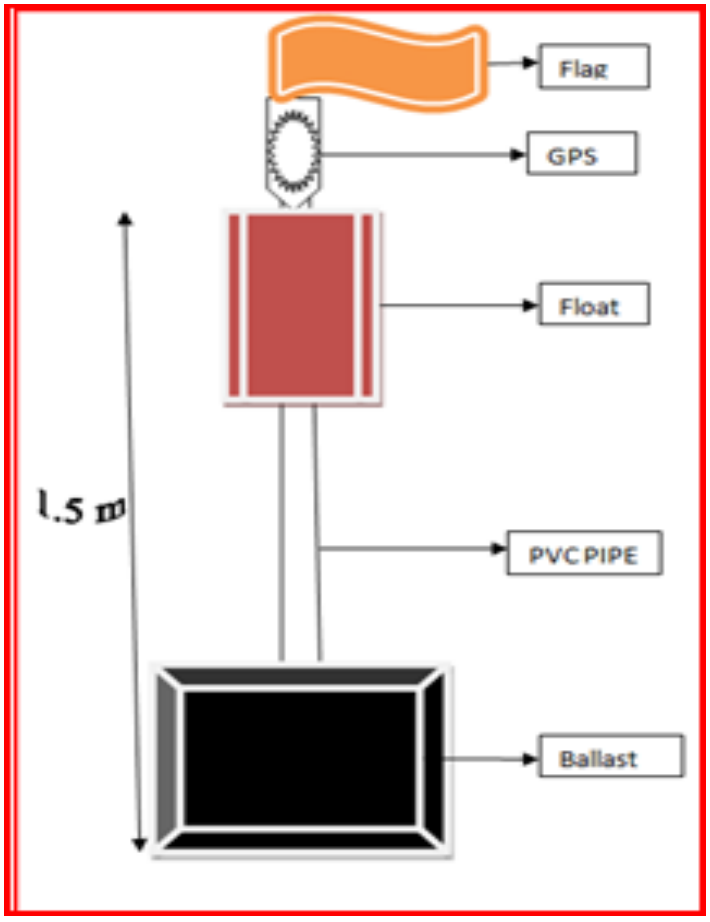

Figure 4. Sketch of the surface drifter used in the field experiment. The flag is for easy identification and recovery purposes. The GPS unit encloses the electronic system in a watertight compartment. The float prevents GPS from being submerged in water. The ballast ensures that the drifter is always floating on the water surface.

The RINO 120 GPS series includes a two-way radio (transmit-receive) capability with 30 transmission channels (14 Family Radio Service (FRS) channels on 462.5625 to 467.7125 MHz, 8 General Mobile Radio Service (GMRS) channels on 462.550 to 462.725 MHz, and 8 GMRS

repeater channels). The radio is also equipped with 38 squelch codes that allow selective blocking out of some unwanted transmissions. It transmits by line of sight (LOS) operation (signals radiate in a straight line from the transmitting antennas to the receiving antennas, hence the antennas should not be blocked by waves or submerged in water) with a maximum transmission range of 8 kilometers (≈5 miles). It has an internal storage that can store up to 4096 acquired position points (enough to store position information sampled at 15 seconds over a semi-diurnal tidal cycle). The user can specify the sampling frequency (that best suits the experiment) in RINO 120 series. With proper tuning of the channels, RINO 120 can transmit its position (at user-specified frequency) to another RINO 120 that is tuned to the appropriate frequency band (using the channel and squelch codes). The RINO 120 GPS transceiver uses three 1.5 Volt AA alkaline batteries which can last up to 15 hours in continuous operation of the device. This battery life was sufficient to acquire and transmit position (longitude and latitude) and time data throughout one tidal cycle (semi-diurnal tidal regime) in my study domain. The GPS can determine positions to an accuracy of 3 meters. This functionality made the RINO 120 GPS package an ideal instrument for the field study because Ibaka bay has a comparable radius as the RINO 120 transceiver range. The average cost of building one surface drifter unit was $200. This cost was within the budget for this study, thus a total of ten (10) surface drifter units were built for this study.

The drifter casing and drogues were designed such that their combined resonant buoyancy frequency was higher than the frequency of the energetic part of the wave spectrum in the study region. This was to ensure that the drifter always stayed on the surface of the water. With the relatively high buoyancy frequency, the drifters will not be displaced

significantly from their neutrally buoyant positions by the passage of the low frequency waves. Using the formula:

$$f = 1/ \{2\pi [(L/g) (\rho_c/\rho_0)]\}^{1/2} \quad \ldots\ldots\ldots\ldots\ldots\ldots\ldots\ldots\ldots\ldots\ldots\ldots\ldots\ldots\ldots\ldots \quad (1)$$

where f is the resonant buoyancy frequency, L is the length of the cylindrical PVC pipe, g is the gravitational acceleration, ρ_c is the density of the PVC pipe, and ρ_0 is the density of the ambient fluid (Ibaka bay water in this case); f turned out to be ≈0.7 Hertz (faster than the site's energetic wave frequency of ≈0.15 Hertz, as estimated from the analyses of TOTAL data obtained from the System of Industry metocean data for the Offshore and Research Community (SIMORC) archive).

The field experiment was designed such that the drifters were released at different stages of the tide and at different spatial locations within the bay. The drifters would then be monitored over complete tidal cycles. Some local fishermen in Ibaka were consulted and engaged in tracking the drifters so that they did not drift into the open ocean and get lost. After a few complete tidal cycles, the drifters were recovered. Time and position data acquired by the Garmin (RINO 120 Series) Global Positioning System (GPS) with two-way radio devices were downloaded to the computer via RS232 DB9-pin serial adapter (note that RINO 120 GPS comes with DB9 female adapter and most modern laptop computers (including the ones used for this study) are also equipped with DB9 female or 15-pin adapters; in such cases an RS 232 to USB converter is required to download the data). The downloaded data was further processed into current and circulation data using first order difference operator. Alternatively, the surface

circulation of the bay can be plotted directly from the Garmin RINO 120 GPS via the menu option, 'Track'.

Five surface drifters were deployed at different stages of the tide and different spatial locations within the bay on December 17, 2012. Some local fishermen were paid to use their fishing boats and monitor the drifters so that the instruments were not drifted into the open ocean and lost (in case of a sudden surge event). Most importantly, the engagement of the local fishermen was to ensure that the local residents secured the drifters against theft. Figure 5 shows the surface drifter while figure 6 shows one of the local fishing boats used in tracking the drifter positions in Ibaka bay during the December 2012 field experiments.

Figure 5. Prototype surface drifter used in sampling surface current in Ibaka bay (December 2012). Garmin RINO 120 series GPS is housed in the white plastic seal on top (Courtesy: Dr. Brooks)

Figure 6. Local fishermen using their fishing boat to monitor surface drifters deployed in Ibaka bay.

However, the field experiment did not go as smoothly as planned. Some aggrieved local residents obstructed the exercise by removing some drifters that were deployed to sample the currents out of the bay. The local 'boys' claimed that they were not involved in the deep seaport project implementation. They informed me that none of the phases of the project has sought any input from them. They said that no role has been set aside for them to play in the project execution. Their large acre of land was snatched away from them without any form of compensation. No alternative means of livelihood is planned for them since the port infrastructures will obstruct their fishing terminals and route to the open sea. They sought to

know how they would benefit from the proposed Ibaka deep seaport project. They vowed to continually obstruct all projects on the site as long as the project development partners fail to identify them as major stakeholders on the project.

The ugly situation was aggravated as some Ibaka residents erroneously portrayed me as the Akwa Ibom State government representative on the planning and designing phase of the project. They considered the field campaign as being funded by the state government and then they decided to seize the surface drifters to register their protest. Those who were ignorant of the drifters' function might have stolen some of the missing deployed drifters. This incident hindered the progress of my field experiment as it took a few days to re-negotiate with the local dwellers and retrieve some of the seized surface drifters.

I put in all time and other resources in my disposal into the scientific/engineering design of the experiment. I failed to look at the human aspects/contributions to the success of the experiment. If I had thoroughly searched the literature of previous investigators (conducting environmental research in similar terrain), I would have been well armed to handle the challenges I faced during the exercise. For instance, Awosika et al. (1994) reported that fishermen just because of the aesthetic worth of the drifters collected most drifters his team deployed into the shelf waters off Nigeria. Also during the Joint Industry Project (JIP), by some major Oil and Gas companies in Nigeria, in 2000, local fishermen also removed most of the surface drifters deployed, as reported in Rider (2004).

Adequate resources should be committed to develop effective communication network in coastal areas (such as a broadcast email system, broadcast text messaging system or town crier communications system in areas without modern communication facilities) to ensure that every stakeholder and interest/pressure groups are on the same page, before embarking on

field study. It is a truism that all scientific and engineering research studies share one fundamental objective in common: “a better understanding of the system processes which will translate into improved living conditions for mankind”. With this objective in mind, no amount of resources can be tagged a waste, if they are used to inform, educate, and restore confidence of the local residents and integrate them as partners in the research program. Effective communication is needed for a successful project everywhere in the world as documented by Lawrence Patella in his opening remarks at the Midwest Chapter Meeting of Western Dredging Association in St. Louis, Missouri. “ … I also find it bothersome that in today’s Global economy, most are un-aware that if for some reason we were unable to dredge so that “Ships May Pass”, shelves in grocery and other commercial outlets would be empty in a relatively short period of time (excerpt from opening remarks by Larry Patella, Executive Director for Communications, Western Dredging Association (WEDA), in St. Louis, Missouri on April 17, 2013).

Nevertheless, I gained a lot of knowledge of the physical processes driving circulation in Ibaka during the field experiment. My interactions with the local fishermen gave me an idea and estimates of the dominant wave directions, significant wave height (SWH), typical tidal range, seasonal changes, and the sediment characteristics of Ibaka bay. Significant wave height is defined as the average of the highest one-third of waves in a wave group. This knowledge will be vital in qualitative validation of the numerical model, especially when maps of extreme events are analyzed. Also, I transformed some of these challenges into a rare opportunity where I educated the local residents on the benefits that an operational deep seaport project will bring to their community. I enlightened them on the type of job opportunities they will have as well as other indirect revenues, such as improved market for their produce, which will accrue to them. I was able to re-establish and build trust (which was lost due to long years of

negligence) between Ibaka residents and the state government. This achievement was measured by the way the residents shifted their ground and released the surface drifters in their possession. They pledged never to obstruct work in the site again as long as they are properly informed before the commencement of such work. A cordial relationship has been established between my research team and the Ibaka community.

My field study research team comprised myself, as the Principal Investigator (PI), and some undergraduate students of Akwa Ibom State University (AKSU), Nigeria. The undergraduate students were drawn from the Naval Architecture, Marine Engineering, and Ocean Science Departments. The AKSU students assisted me in assembling the drifters (cut the PVC pipes, housed the Garmin RINO 120 GPS unit in waterproofed container, and fixed the drogues). The students were excited to learn how to construct equipment that can sample currents in the estuary using simple everyday materials they play around with in the laboratory.

One of the most successful and exciting part of this field campaign was the engagement of some undergraduate students in Akwa Ibom State University. Some curious students asked pertinent questions about the working principle of the drifters during the construction phase. I answered all the general questions instantly and promised to address the technical questions on site, since I thought they would better understand the technical issues, when they were conducting the experiments on the field. The students developed keen interest for the project. Some of the students informed me that they would like to design a similar experiment and study other coastal estuaries for their final undergraduate projects.

The RINO 120 GPS FRS radio channels were carefully selected to ensure that the sampled data were correctly transmitted to the coastal stations. The maximum transmission range of the RINO 120 series radio is 8 kilometers (5 miles). The coastal stations were selected

to overcome this range limitation. Five GPS units were set aside for archiving the data on land. These land stations serve as a back-up data in the event that the drifter is drifted by severe wave event (such as storms) into the open ocean. The sampling rate was set to 15 seconds. Each set of drifter deployment and recovery was designed for a complete tidal period. The available tidal information showed that Ibaka bay has mixed tidal signal but with strong M_2 and S_2 semidiurnal constituent signals. The drifters were deployed at different tidal phases to examine the correlation of tidal phases with the current intensities in Ibaka.

Data were downloaded and circulation map plotted using the built-in algorithms of the Garmin GPS. Appropriate software from Garmin website was installed on the PC notebook computer to facilitate the processing of the data. The current information obtained from the experiment was used as part of the input to the SHORECIRC numerical model. Parts of the data were also used to calibrate, validate and verify the circulation model performance (skill) for the bay.

Akwa Ibom State University (AKSU), Nigeria, provided the major funding for these field experiments.

DATA PROCESSING AND ANALYSES

Global data archives were searched for bathymetric, waves, currents, and sediment data in Cross River Estuary. Cross River Estuary is located off the Gulf of Guinea on the eastern border of Nigeria. It has a length of about 200 kilometers (125 miles) and a maximum width of about 30 kilometers (18.8 miles) at the mouth of the estuary. Ibaka bay is part of the Cross River Estuary system and it empties directly into the open Gulf of Guinea. Some of the public data archives visited were the System of Industry Metocean data for the Offshore and Research

Community (SIMORC), Global Level of the Sea Surface (GLOSS), Nigerian Institute of Oceanography and Marine Research (NIOMR), Ocean Data and Information Network for Africa (ODINAFRICA), and the University of California, San Diego (USCD) TOPEX database for 30 arc second resolution bathymetry data. Figure 7 shows the distribution of sea surface elevation gauges for ODINAFRICA network.

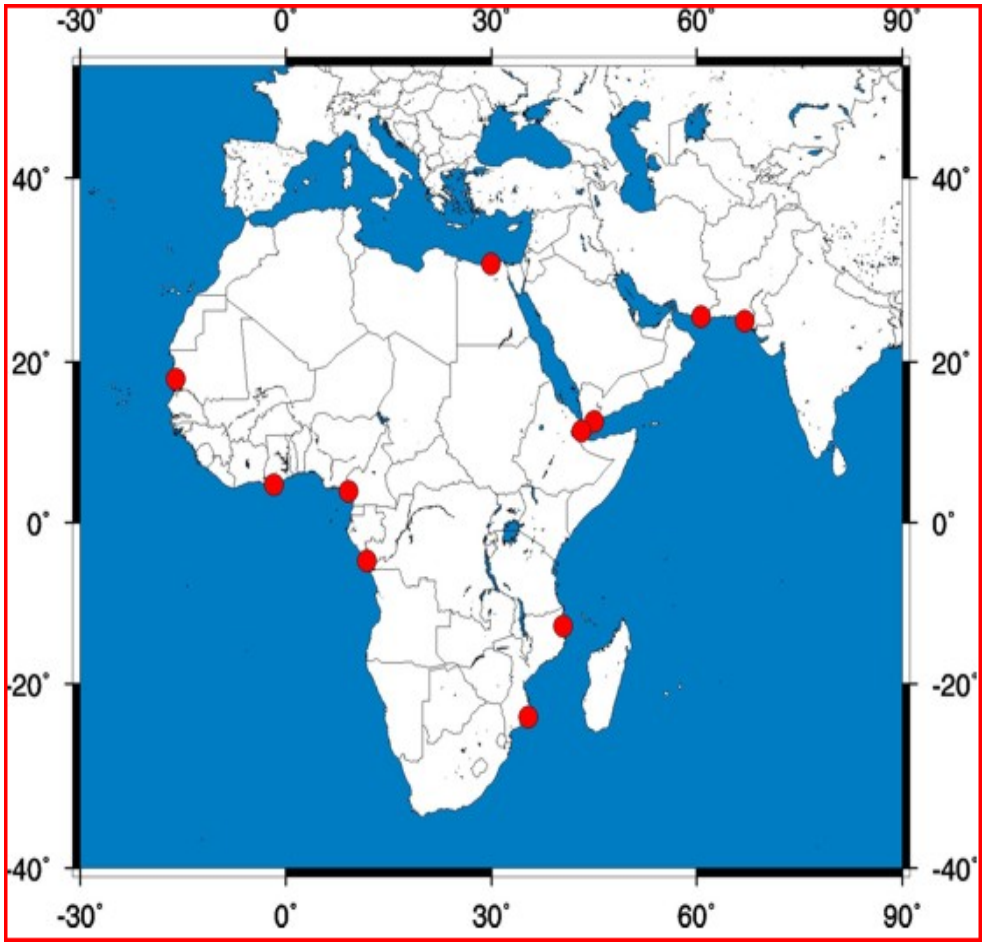

Figure 7. Distribution of sea level gauges for the Ocean Data and Information Network for Africa (ODINAFRICA) project.

Waves, currents, and bathymetry data for the study site were extracted, downloaded, and processed into formats compatible with the different modules of the numerical model. Different tools (such as Python, Scilab, Matlab, etc.) were experimented with in this stage of the project. Matlab 2013a was finally chosen and procured by Oceanography Department at Texas A&M University. It was installed on the different machines that were used during the project. This Matlab served as the base software for all data analyses and visualization. Several Matlab routines were written for post-processing of the numerical simulation output results.

The 30 arc second (≈927 meters) resolution bathymetric data were extracted from the TOPEX UCSD site in XYZ format (X for longitude, Y for latitude and Z for the water depth). Matlab codes were written to process them into matrices that can be read as input to both the SWAN and SHORECIRC curvilinear grids. Tidal surface elevation data were obtained from GLOSS and SIMORC. Routines were written to extract the dominant and representative thirteen tidal constituents: S_1, O_1, P_1, Q_1, J_1, T_1, K_1, M_2, N_2, S_2, R_2, L_2, and K_2. These tidal constituents (period, amplitude, and phase) were used to initialize the offshore boundary of the circulation model, SHORECIRC, along the southern boundary. In the northern boundary, river fluxes were specified at three grid points (estimates of river fluxes were obtained from published literature, Ewa-Oboho et al, 2009). Spatially uniform, time varying wind velocities from two neighboring stations were extracted from the NOAA NCEP archive. This wind was used to initialize both the wave and circulation models. Another important boundary data for the wave model was offshore wave conditions. After testing with three different spectral densities (PM, Gaussian, and JONSWAP), a JONSWAP spectral density was selected for both the swells and wind wave boundary condition specifications. Previous studies have shown that JONSWAP partitioned spectrum was most accurate in representing the wave conditions in the Gulf of Guinea

(Olagnon et al. 2004, Olagnon et al. 2013, Prevosto et al., 2013, Forristall et al. 2013, Ewans et al., 2013). Different parameters (significant wave height, SWH, mean period, T, mean direction, θ, directional spread, peakedness (gamma, γ)) were specified for multiple swells and wind sea conditions. Model sensitivity to the different forms of representation of boundary forcing is discussed in chapter 4. Swells arriving at the West African coasts have been identified to be mostly multi-peaked (Olagnon et al., 2004). Graphs of measured sea surface elevation, significant wave height and current magnitude are shown in figure 8.

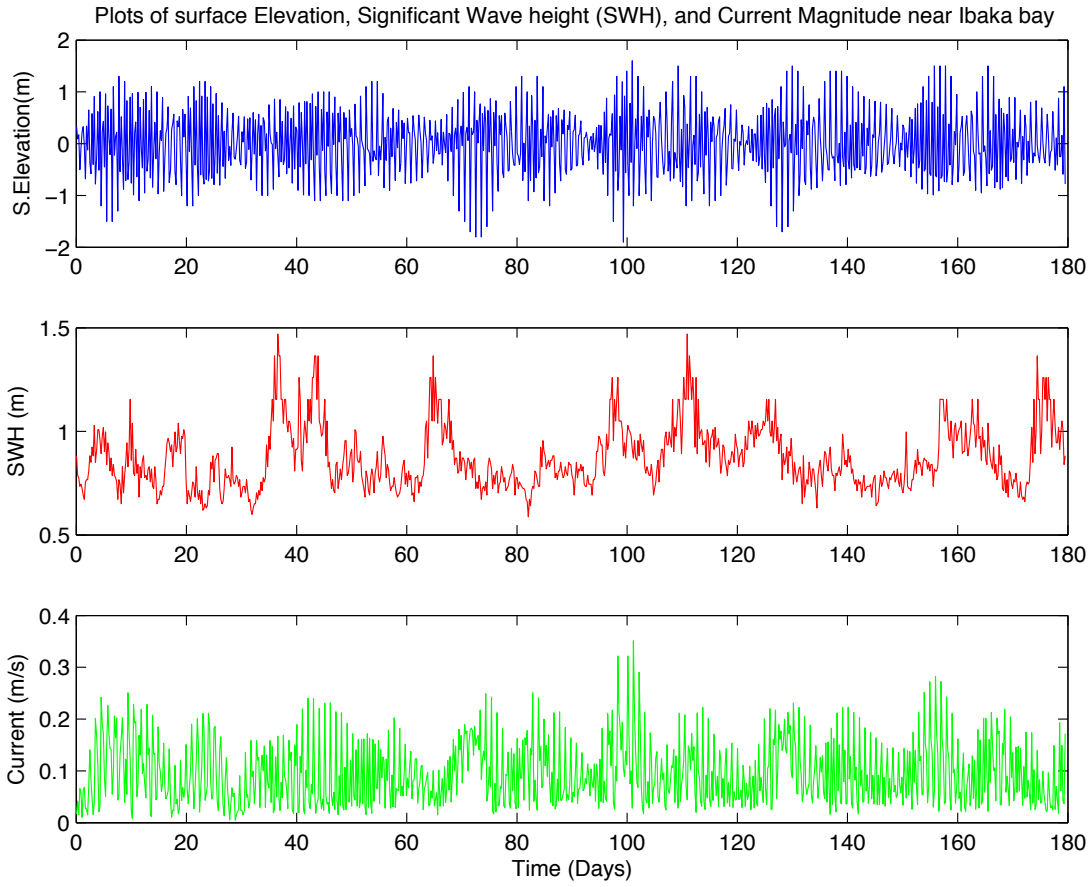

Figure 8. Time series graph of measured sea surface elevation, significant wave height, and current magnitude near Ibaka bay. (Courtesy: GLOSS and SIMORC)

Much effort was spent in getting the forcing and validating data because of scarcity of published literature for Ibaka bay. Thus, the numerical experiment was designed to minimize all known and anticipated sources of errors. A recent review of the accuracy of wave models using significant wave height as the metric by Ardhuin and Roland identified forcing fields (initial and boundary conditions) as the largest source of error (about 60%) in models (Ardhuin and Roland, 2013). This recent research finding has justified the huge time investment to obtain all available data within the Cross River Estuary and the environs to force and verify the numerical model. Ardhuin's review identified the following model sources of error, in diminishing order of importance: forcing fields (≈60%), parameterization of source terms (≈35%), and choice of numerical schemes (≈5%) (Ardhuin and Roland, 2013).

NUMERICAL MODELING

Nearshore Community Model – Total Variation Diminishing (NearCoM-TVD (Shi et al., 2012)) software was chosen as the base model for the numerical experiments. NearCoM-TVD consists of three different modules coupled together: wave module, circulation module and sediment module. The wave module is Simulating Waves Nearshore (SWAN), (Booij et al. 1999); the circulation module is the curvilinear SHORECIRC (Shi et al., 2003); and the sediment transport module adapted for this study is the Soulsby total sediment transport formulation (Soulsby 1997). A seabed change module for morphological changes computations is also included as a subroutine in the sediment module. The seabed change module contains a morphology factor, which serves to extend the time period of seabed change calculations in a periodic manner. The three modules are run in feedback mode (two-way wave-current interactions between the wave and circulation models are accounted for). NearCoM-TVD

simulations account for the effects of wave-current and other nonlinear interactions in the model. The wave module computes the gradient of radiation stresses and volume fluxes. The circulation module accepts the gradient of radiation stress (known as wave force) as one of its inputs and calculates the currents. The currents are fed back to the wave module. These interactions transform both the wave and current fields at each time step of the simulation. The importance of resolving wave-current interactions in hydrodynamic models was assessed elsewhere (Osuna and Wolf. 2005).

SHORECIRC (Van Dongeren et al., 1994; Svendsen et al., 2003; and Shi et al., 2007) is a quasi-three-dimensional (Q3D) circulation model, which solves the two-dimensional, depth integrated, wave averaged, horizontal momentum and continuity equations numerically and then incorporates the effects of wave-induced vertical variation of the horizontal currents. The equation for the vertical structure of this horizontal current is solved analytically in SHORECIRC, using a constant eddy viscosity and the assumption of polynomial distribution of along shore (u) and cross shore (v) velocity profiles. The full vertical structure equations and solutions can be found in the NearCoM-TVD documentation and users' manual (Shi et al., 2012). This process basically accounts for the effect of waves in the vertical structure of horizontal currents. This feature makes SHORECIRC more efficient (in terms of required computational resources) than other available three dimensional circulation models in non-stratified or well-mixed estuaries. SHORECIRC has been described as the preferred nearshore circulation model in well-mixed bays and estuaries (Svendsen et al., 2003 and Shi et al., 2011). Based on my study objectives and the available information I have gathered about the hydrodynamics of the study site, tidal mixing outweighs ocean stratification, hence NearCoM-TVD will accomplish my numerical objectives. Use of NearCoM-TVD will allow application of limited computational resources to conduct

much longer duration numerical model experiments than would have been possible if a fully three-dimensional numerical model were chosen for this research.

In order to minimize the error associated with offshore wave boundary conditions in the NearCoM-TVD domain, a nested computation approach was adopted. SWAN was run in a larger spatial domain (≈56 x 56 km or 0.5^{o}x0.5^{o}) as a standalone numerical simulation. The boundary data for the larger SWAN run was prescribed using parametric wave characteristics with a JONSWAP density spectrum. The bulk wave information (such as significant wave height, peak period, mean direction, and directional spread) was obtained from previous research reports in the Gulf of Guinea region such as ODINAFRICA publications. Since recent research findings by other investigators (e.g. Olagnon et al. 2013, Prevesto et al. 2013, Ewans et al. 2013, Forristall et al. 2013) have concluded that swells reaching the West African coasts from the Atlantic ocean are mostly multi-peaked, the wave system was partitioned to account for these multiple swell peaks. Thus, more than one JONSWAP spectral density (with appropriate parameters to represent swells and wind sea) was specified in each boundary location. This also ensured that appropriate shape parameters for the JONSWAP spectrum were specified for the multi-peaked swells and wind sea. All SWAN runs in this study use the third generation mode (3G). All wave models classified as 3G explicitly account for wave nonlinear interactions, and the shape of the wave spectral density evolves without constraints.

Computational grids for the simulations were generated with a FORTRAN program (for wave computations) and CoastGrid Matlab routines (for circulation simulations). CoastGrid is based on the adaptive grid generation method of Brackbill (Brackbill and Saltzman, 1982). SWAN and Curvilinear SHORECIRC used different curvilinear computational grids. The SWAN grid was generated with a FORTRAN program that was developed and implemented during this

project while the SHORECIRC computational grid was generated with the Matlab version of CoastGrid grid generation routines (Shi, 2013). Another Matlab code was written to transform the CoastGrid px2 (p is the length of mxn, where m is the number of grid points in the zeta (ζ) direction and n is the number of grid points in the eta (η) direction) output into a matrix format that could be read by the curvilinear SHORECIRC in the curvilinear grid. Figure 9 shows one of the CoastGrid-generated computational grids that was used in the simulations.

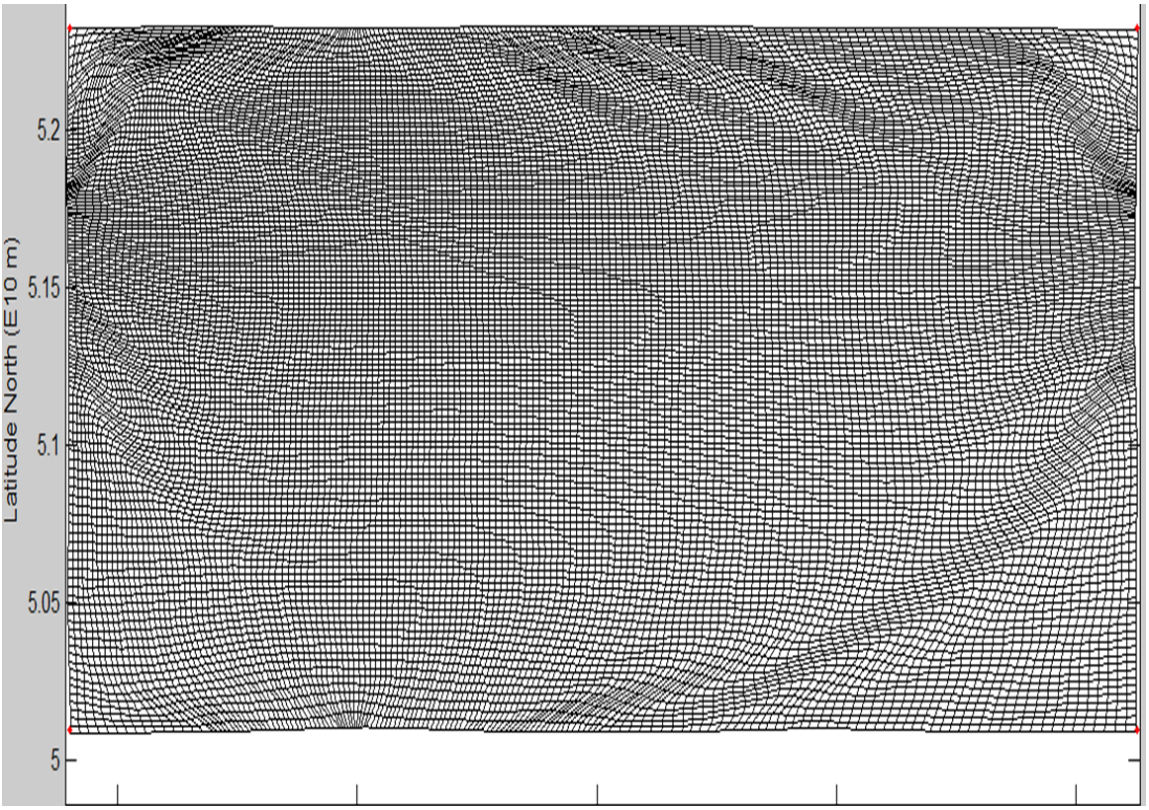

Figure 9. Curvilinear grid for NearCoM-TVD model. This grid was generated with CoastGrid matlab routines as described in the text.

The spatial extent of the nested NearCoM-TVD simulation domain is 22.265 km by 22.265 km (0.2^o x 0.2^o). Both curvilinear SWAN and SHORECIRC grids have 160 points in the

zeta, ζ, direction and 120 points in the eta, η, direction. The grids have the coarsest resolution of ≈100x150 meters in the offshore (southern) boundary of the simulation domain. The Ibaka bay coastal region and the dredged ship channel have the finest resolution of ≈20x25 meters in the zeta and eta directions respectively.

Several model sensitivity tests were run to evaluate the optimum computational grid resolution for the numerical experiments (optimum in this context is with respect to the tested cases). The major resource constraint that was considered in the choice of the optimum model grid resolution was the computational resource. Model output parameters used in this sensitivity evaluation were significant wave height (SWH), cross-shore and alongshore velocity components, and surface elevations. It was found that additional refinement of the computational grid beyond 160x120 points (ζxη directions) was a waste of the computational resources since the percentage improvement on the accuracy of output parameters was much lower (≈5% when the grid spacing was halved) compared to additional simulation time (≈800%) taken to complete each run. Simulation time is a direct measure of the SuperComputer central processing unit (CPU) Billing Units (BUs) consumed during simulations. Further refinement of grid spacing beyond 160x120 also increased the numerical diffusion of the processes simulated by the model. The next chapter (Chapter IV) is devoted to sensitivity analyses. Some results of what is highlighted in this paragraph and the next paragraph will be shown.

Sensitivity analyses were also carried out with other forcing functions. These helped to identify the major sources of error in wave predictions and then more efforts were channeled into getting the most accurate data available for those functions. These sensitivity analyses (discussed in the next chapter) were very helpful in determining the overall model uncertainties for the predicted processes in Ibaka (measured field data is scarce in Ibaka).

In some scenarios, the numerical model will be run with conditions comparable to conditions in which some analytical solutions exist (see Wang and Craig, 1993). Comparison of the computational results to the analytical solutions will provide an alternative means of evaluating the model. Once the model has been verified with acceptable confidence level, the model will be used, in hind cast mode, to study details of the different components of the processes affecting the hydrodynamics and morphodynamics of the bay. Due to paucity of data, Wang and Craig had reduced a complicated coastal ocean model to a simple analytic model and studied tidal circulation in the Hey River Estuary, Australia (Wang and Craig, 1993).

The wave module, SWAN, is a spectral or phase-averaged wave model that solves the wave action balance equation (Booij et al., 1999).

$$\partial N/\partial t + \partial c_x N/\partial x + \partial c_y N/\partial y + \partial c_\sigma N/\partial \sigma + \partial c_\theta N/\partial \theta = S/\sigma \quad \ldots\ldots\ldots\ldots\ldots\ldots\ldots\ldots\ldots\ldots \quad (2)$$

where the wave action density is $N=N(\sigma,\theta)=E(\sigma,\theta)/\sigma$ (σ is the wave frequency relative to the current and θ is the direction angle), E is the wave energy density(which is not a conserved quantity in the presence of currents whereas N is conserved in the presence of currents), c_σ is the propagation speed in frequency space (Doppler shifting), c_x and c_y are respective x- and y-components of the group velocity of the wave and S is the source term representing the generation, dissipation, wave-wave interaction and wave-current interaction.

Both SWAN 40.91 (Booij et al, 2012) and NearCoM-TVD have been ported, compiled and linked on the Texas A&M University Supercomputer for the numerical experiments. SWAN (being a spectral model: spectral models do not have phase coherence of the waves) cannot explicitly handle diffraction around obstacles and breakwaters. Phase resolving models,

such as Boussinesq or mild-slope equation type models can be applied to shallower depth along the coast if surf zone details are required (Nwogu, 1993). An alternative formulation of Shallow water wave propagation model that attempts to intertwine the functionalities of the phase resolving and spectral models was described by Liu (Liu, 1994). However, Liu's model cannot be applied efficiently to larger coastal domains.

Required inputs to SWAN are boundary spectra, bathymetry or water depth, and wind. Boundary wave spectra input to the NearCoM SWAN 40.51AB (wave-hydrodynamic coupled model that accounts for effects of wave-current interactions) will be provided by the stand alone SWAN 40.91 model output taken at the boundary points of the nested NearCoM domain. Model sensitivity to these input parameters will be examined.

Wave action density (calculated by SWAN) is simply the wave energy density per unit relative frequency, σ, (wave action density is conserved in the presence of currents whereas wave energy density is not conserved when currents are present). Jonsson (1998) gave a physical interpretation of wave action flux. The SWAN model is capable of predicting wave parameters, such as, significant wave height, set-up, wave direction, wave period, and radiation stress. It is most suited for modeling short-crested waves in nearshore regions. The model has been used extensively (and verified) for modeling waves in many parts of the world since it was released in 1999 (Wolf et al., 2000; Lin et al., 2002; Moeini and Etemad-Shahidi, 2009). However, since the source terms of the model were empirically derived (with wider ranges of free parameters), some verification is necessary when using the model in a new project site.

Since my study attempts to test the hypothesis that wave forcing is a major factor in changing circulation patterns in Ibaka bay, the influence of the open ocean waves in the Gulf of Guinea need to be properly specified on the NearCoM computational domain boundaries. For

accurate wave information at the domain boundaries, SWAN 40.91 will be run (as a standalone model) in a larger domain (longitudes 0^{o}E to 12^{o}E and latitudes 1^{o}S to 7^{o}N) in the Gulf of Guinea to get the required waves information for boundary forcing of the nested NearCoM-TVD model. SWAN 40.91 will be forced by wind data extracted from the National Centers for Environmental Predictions (NCEP) and MyOcean archives. The nesting technique is portrayed in Figure 10. In figure 10 below, SWAN grid for transforming the deep-water wave field to the nearshore wave field is indicated by the "Larger SWAN domain". The curvilinear computational grid is the yellow region called the "Nested domain".

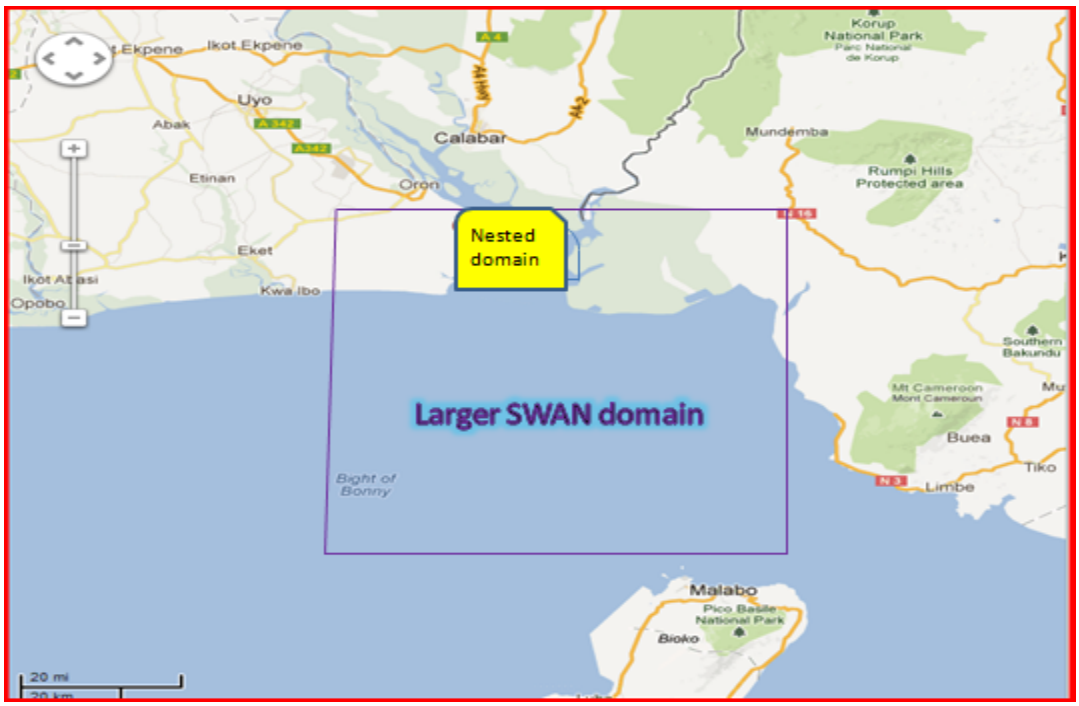

Figure 10. A sketch of the nesting technique applied in the numerical experiment.

Wave boundary conditions for NearCoM-TVD were obtained from large area SWAN run. Two different methods were used to apply the boundary conditions. First, the outer

boundaries of the nested NearCoM-TVD computational grid was made rectangular, and then the nestout command was invoked in the output command of the nesting computation (nesting run refers to the larger domain SWAN run while nested simulation refers to the combined waves and circulation NearCoM-TVD runs) to get the spectral output for the entire nested boundaries. Boundnest command was used in the SWAN input file of the NearCoM-TVD model to apply the boundary conditions. The second approach was to take the spectral output at different points along non-rectangular NearCoM-TVD boundaries using the commands points and specout. These commands are described in the SWAN user manual. The second approach provided more flexibility on the design of the computational grid – the curvilinear grid could follow the coastal terrains exactly. The only downside of the second method was that the number of interpolation of the boundary input parameters increased. Comparisons of significant wave height output of these two methods indicated that the wave transformation in the interior of the domain were similar. I chose the second method to specify the wave boundary conditions in this study.

The inputs to NearCoM-TVD circulation model, SHORECIRC, were wind, wave, river flux, and tides. A constant wind in space, but varying in time, was specified using a typical seasonal average wind value from the Nigerian Institute of Oceanographic and Marine Research (NIOMR) database for the Niger Delta Region in Nigeria. The time varying wind was formatted in three columns for the following components: eastward-westward component, northward-southward component, and average direction. The wave spectrum was obtained from the larger SWAN run and applied to NearCoM-TVD as offshore boundary condition. Most parts of the model lateral boundaries were land; hence waves were not specified on the lateral boundaries. The river flux entered the domain from the northern boundary and was specified

using typical values from a local measuring station (Antia E., personal communication). The tides entered the model as tidal constituent parameters specified by their periods, amplitudes, and phases. Sea surface elevation data were obtained from the Global Sea Level Observing System (GLOSS). Tides were extracted from the sea surface elevation data and analyzed to get the required harmonics. The tidal harmonics analyses utilized the MATLAB version of DiMarco's cyc_opt code (DiMarco, 2012 Class lectures) which uses the method of cyclic descent as given in Bloomfield, 1972. Thirteen tidal constituents were extracted and applied at the offshore boundary to force NearCoM-TVD model. Fortran codes were written to process the tidal constituents and river flux data into input file formats compatible with NearCoM-TVD curvilinear grids.

The sediment transport/seabed module used the same curvilinear grid as SHORECIRC. Two sediment modules were selected for the numerical experiments. These were Soulsby's total load sediment transport model (Soulsby, 1997) and Kobayashi's suspended load and bed load sediment transport model (Shi et al, 2012). After testing with different initial and boundary conditions, and sediment characteristics common in the region, it was found that Soulsby's formula was more robust and better suited for the experiments. In this formulation, the total sediment load (both bed load and suspended sediment) is computed in one swoop (jointly) in contrast to Kobayashi's technique, where bed load and suspended load are computed separately in different subroutines. The gross and net sediment transport are calculated and then the instantaneous seabed changes are evaluated. The interested reader is referred to "Dynamics of marine sands: A manual for practical applications" (Soulsby, 1997) for detailed derivation of the model equations. The inputs to the sediment module are hydrodynamic quantities obtained from SHORECIRC and the median sediment grain size. This sediment

predictive model has been used extensively in different coastal domains around the world (Soulsby and Clarke, 2005; Balson and Collins, 2007; Michael and Balson, 2007; Grunnet et al., 2008; Sutherland and Obhrai, 2009 etc.) to achieve good agreement with data. The model equations have been verified in a wide range of simulation conditions. However, being a semi-empirically derived model, the model needs to be verified in any given coastal domain it is applied. This is due to large ranges of free parameters (tuning coefficients) inherent in the model. The optimum or default coefficients might not give the best output result in some region; hence the modeler has to choose the parameters based on the conditions of his model domain.

The major input data to the sediment module were the sediment grain size distribution (d_{10}, d_{50} and d_{90}), the bed roughness, bed wave orbital velocity, and bed shear stress. The sediment characteristics were specified based on in-situ measurement and previous published documents analyses. Wave orbital velocity and bed shear stress for the sediment transport module were obtained directly from the coupled wave and circulation modules.

Due to limited computational resources available for running the coupled model for longer time periods (a few years' time scale), a morphology factor was incorporated into the seabed level change module. The morphology factor extended the time period of the seabed evolution by the specified factor. For instance, if the actual simulation time is six months and a morphology factor of four is specified in the input file, then the resulting morphological changes will represent a two-year period. The underlying assumption in applying a morphology factor is that the processes causing the sediment transport in that region will have a periodic time period similar to the actual duration of the simulation. Unfortunately, there is no long tem record of sediment transport or morphological changes in Ibaka bay to guide an objective determination

of a morphology factor. Nevertheless, the morphology factor was carefully chosen to ensure that the accuracy of the model output was not significantly compromised. The morphology factor chosen for this experiment ranged between 4 and 10 (depending on the model resolution and duration of each run). The bed slope change was updated at every time step of the sediment transport calculations. This implies that the sediment module outputs fed back directly to the circulation model.

The most efficient and economical channel design is shown in Figure 11. The locations of the different stations used for the time series and statistical analyses are also indicated in the figure. Stations 1 and 2 are on the left and right flanks of the channel respectively while station 3 is in the center (deepest part) of the channel. These three stations were used to analyze the erosion and accretion of the ship channel. Station 4 is dedicated for analysis of the impacts of the ship channel on Ibaka beach and Tom Shot Island. Stations 5 and 6 are located on Ibaka bay. These two stations (5 and 6) are near the locations where the ship turning basin and other major port infrastructures will be built. The proposed 4-kilometer quay will pass through station 6 and joins Ibaka shoreline to the left of this station. Stations 7 and 8 are at the middle of the study area (they are located east of the dredged channel). Stations 9 and 10 are located in the northeast part of the study domain. These last two stations will be used to examine processes much further away from the influence of the ship channel.

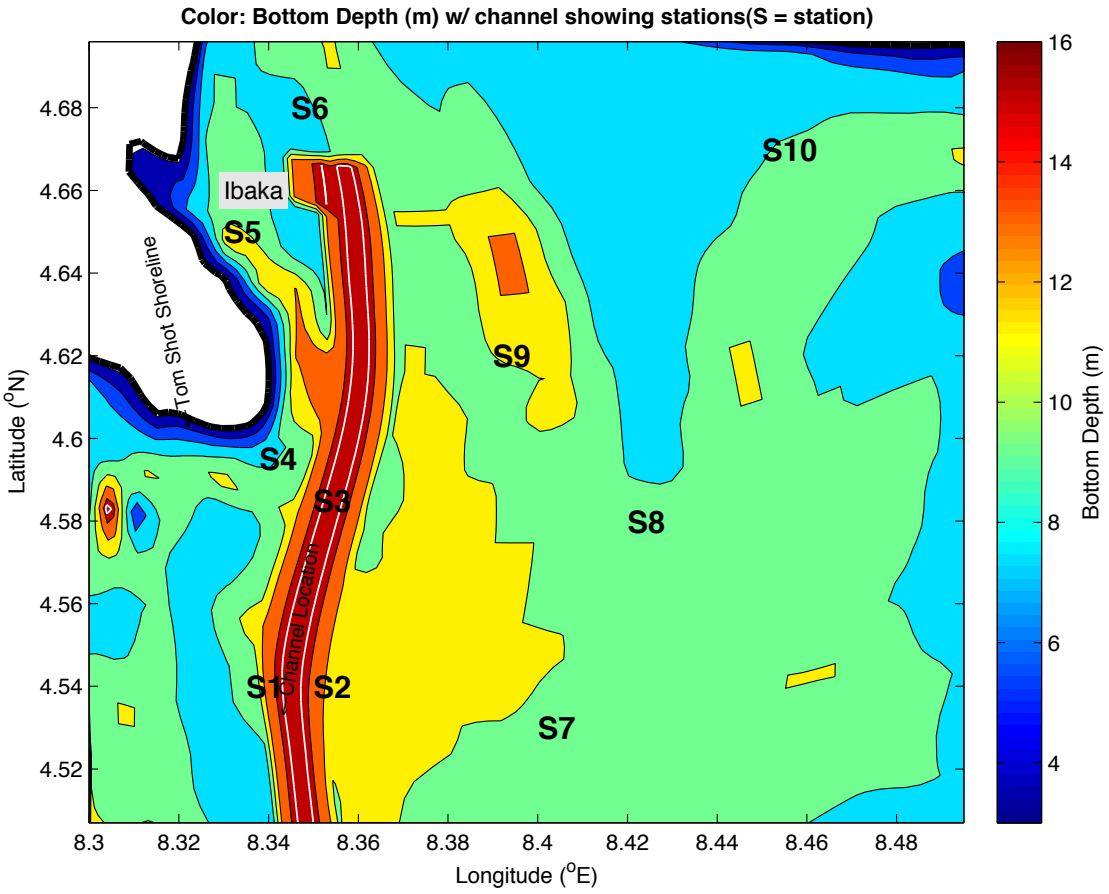

Figure 11. Ibaka depth contour map showing the ten stations used for data analyses. Stations are designated S followed by the station number. White contour line indicates the main ship channel.

Runge-Kutta third-order adaptive time stepping scheme was chosen in the model configuration. The sediment module time step was made smaller than the wave and circulation modules time step to ensure that the sediment module was called at least once in every wave and current update. The flow chart for the numerical experiment is shown in figure 12 below.

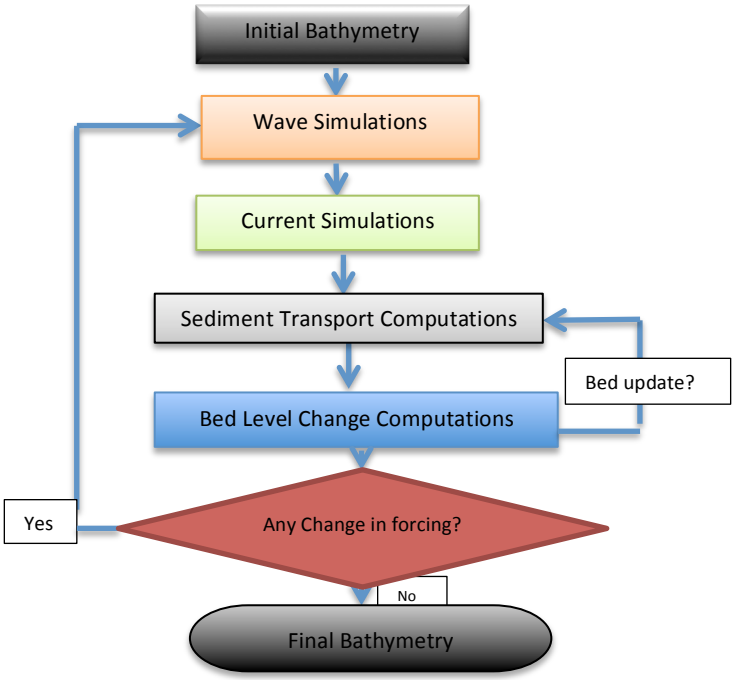

Figure 12. Flowchart for the numerical modeling processes. The bed update was found to be small at each time step, thus it did not change the wave and current significantly. It was not necessary to restart the entire simulation processes when the bed was updated within a time step (as long as the morphology factor was within the range used in these numerical experiments).

An attempt was also made to modify some sections of the base model and then compared the results with available data and other previous work, especially some past field experimental reports within the spatial extent of my modeling domain. The first candidate for this modification was the sub-grid scale process such as the lateral dispersion in the hydrodynamic module. An alternative reasonable assumption was made to relate the parameterized term with the mean flow or another well resolved variable in the system. The newly formulated equation was appropriately discretized (using either the same numerical method or another compatible technique) and ported into the model to replace the existing sub-grid scale process. Some aspects of this new sub-grid scale modeling followed similar work done in Ocean

Modeling for Beginners and Advanced Ocean Modeling (Kämpf, 2009). Model improvements based on this modification was quantified using the relevant statistical techniques. The sub-grid space varying eddy viscosity did not show significant improvement in the model. Rather, it increased model simulation time substantially. The reason for this minor improvement after a Smargorinsky type of eddy formulation was included could be ascribed to the fact that NearCoM-TVD has a good lateral mixing built-in mechanism. This mechanism is called lateral dispersion in NearCoM-TVD.

CHAPTER IV

MODEL SENSITIVITY ANALYSES

In this chapter, the robustness of NearCoM-TVD model to forecast shallow water processes in Ibaka bay was tested. A general approach adopted in conducting model sensitivity studies is to vary only one input parameter at a time and observe the response of the system. By conducting this kind of study, the modeler understands the relative uncertainty each inaccurate model source term introduces to the overall model output errors. Our focus in this section is on the errors associated with the major forcing functions and grid resolutions. The major forcing functions (offshore waves, wind, currents, and bathymetry or water depth) will be isolated and perturbed (by varying degrees) to observe their impacts on selected model response variables (significant wave height, north-south velocity component, current magnitudes, and seabed level changes). This analysis is vital when assessing the errors in hind cast models as well as evaluating the reliability of model predictions.

Due to the dearth of data in Ibaka bay and its environs, the available input data will be perturbed with random fluctuations using MATLAB **randn** function generator as shown in equation 3 below. Statistical methods (such as mean, standard deviation, Analysis of Variance (ANOVA), and multiple comparison) will be applied to the time series of the model output response (such as significant wave heights (SWH or H_s)) to evaluate the significance of model errors due to variation of these input parameters. Those input functions with significant impacts, when they are perturbed, on model output will serve as a guide to estimate the errors in the overall model output.

$$X' = X + \sigma.*\text{randn}(m,n) \quad \ldots\ldots\ldots\ldots\ldots\ldots\ldots\ldots\ldots\ldots\ldots\ldots\ldots\ldots\ldots\ldots\ldots\ldots \quad (3)$$

where X' is the new pseudorandom matrix or array, X is the original input data matrix or array, σ is the specified standard deviation (e.g. 0.1, 0.5, 1, 3, or 5), and m,n are the original data matrix or array dimensions.

In previous related studies, Plant and his colleagues found that resolution of some near shore bathymetries highly influenced the accuracy of wave and flow predictions (Plant et al., 2009). They found that uniform refinement of bathymetry for both the wave and flow models did not result in identical improvements on both model outputs. They recommended non-uniform smoothing of bathymetry for the various components (wave, flow, and sediment modules) of a near shore-coupled model.

Manian et al. had carried out further work in optimum bathymetric smoothing and developed an optimized bathymetric sampling procedure using Genetic Algorithm techniques (Manian et al, 2012). Their technique used the sensitivity of spatially averaged significant wave height model prediction to different bathymetric resolution to determine the optimum bathymetric resolution for a specific simulation objective. Their study aimed at providing experimental scientists with a reliable tool they can use to design optimum tracks for near shore bathymetric sampling. Their formulation was limited to specific wave events and cannot be applied in a general wave climate with reasonable confidence. Their paper contained some suggestions for improvement of the model for wider applications.

We started the sensitivity analysis with the computational grid resolution. The initial NearCoM-TVD curvilinear grid resolution was halved (offshore resolution reduced from ≈400 m to 200 m) and other parameters were kept constant. Three model output parameters (significant wave height, current speed, and seabed level change) from the two computational grid resolutions were compared. This analysis was done for a one-year simulation period. There

was approximately 20% improvement in the model outputs (relative to data analyzed from SIMORC archive), but this improvement was at the expense of the scarce computational resources (computational time increased eight folds). The grids were further refined such that the offshore grid spacing was approximately 100 m and another set of simulations were carried out. The slight improvement (≈ 5 %) on model output was not commensurate with the huge additional computational resource required for simulations at this grid resolution. Figure 13 shows time series of model sensitivity due to grid resolutions for three parameters (SWH or H_s, current magnitude, and seabed level change).

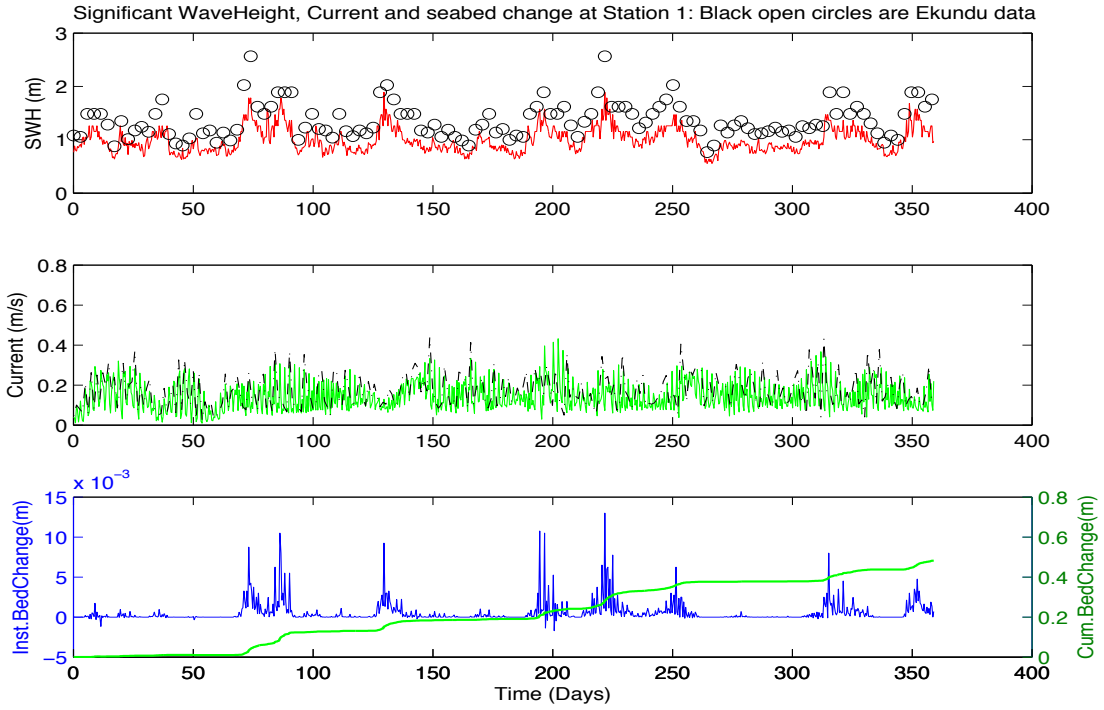

Figure 13. Grid refinement plots for determination of optimum grid spacing. Black open circles and the black dash-dot line are data from SIMORC archive. SWH stands for significant wave height. This plot is for the 200 m optimum resolution discussed in the text. A morphology factor of four was specified for this simulation.

Also shown in figure 13 above are the significant wave height (SWH) data (black open circles) and current data (dash-dot line) from SIMORC data analyses.

Next, the input forcing functions and the bathymetry resolutions were varied (one function at a time) and run on each of the three different computational grid resolutions. The results, in figure 14, show that the sediment processes are sensitive to variations in offshore wave height (for offshore significant wave height > 1.0 m) but they exhibited less sensitivity to other forcing functions. When offshore significant wave height is below 1.0 meter, there is no seabed level change. These variations in different input forcing functions validated the earlier result that offshore grid spacing of 200 m was optimum resolution for these numerical experiments. Thus, the resolution with about 200 m spacing at the offshore boundary and approximately 50 m near shore was chosen as the optimum computational grid resolution for the entire experiments.

With this spatial resolution, SWAN integrates in 3 minutes time step with an accuracy of at least 99% in all wet grid cells. The circulation module, SHORECIRC uses adaptive time stepping scheme, although guided in some way by the wave model time step. The sediment module uses a smaller time step than the wave time step to ensure that it is called at least once during every wave update interval. This model configuration allowed up to a one-year duration run to be carried out within a day (24 hours) on the TAMU Super Computing facility with the parallel eight cores assigned to this project.

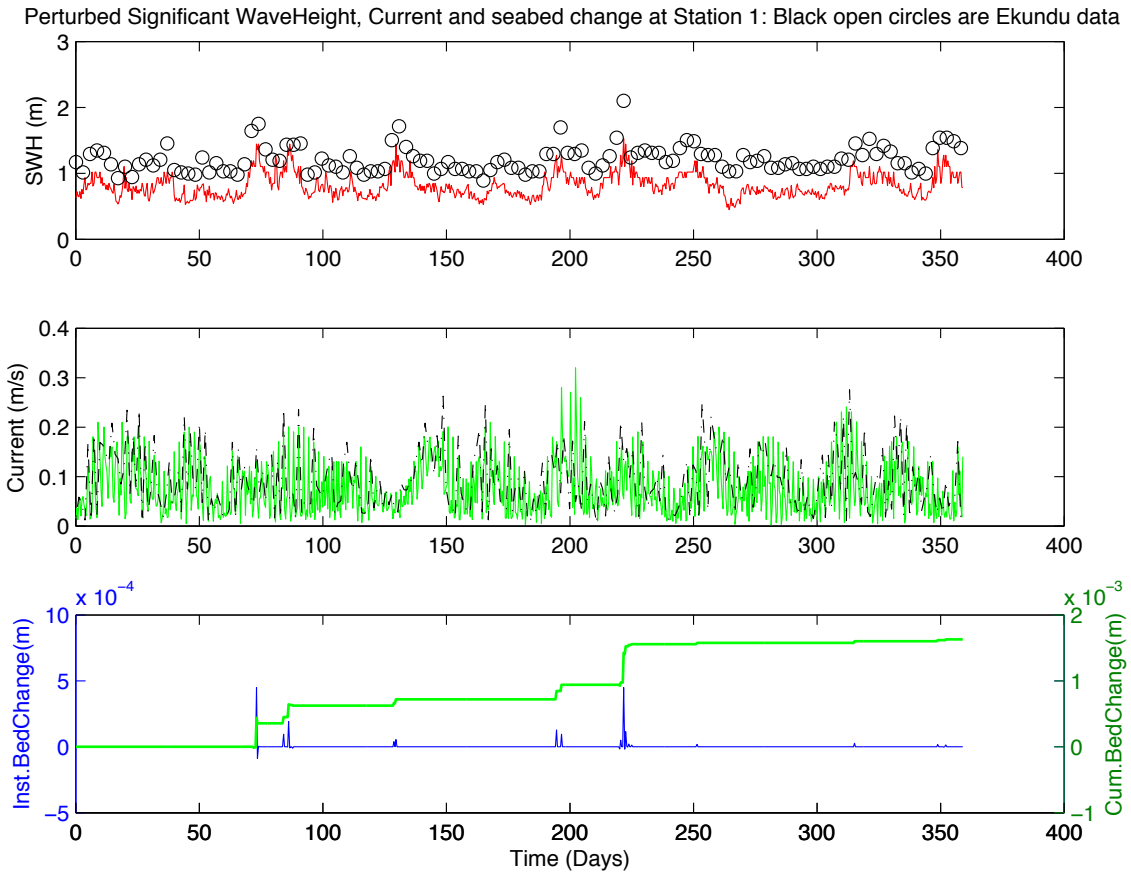

Figure 14. Sensitivity of sediment processes due to variations in offshore wave height. The significant wave height in this graph is reduced (compare with figure 13) by a factor of 0.8. This resulted in a seabed level change (reduction) of three orders of magnitude during the one-year simulation period. A morphology factor of four was specified for this simulation.

This aspect of the study gives guidance on which physical parameter perturbations have the greatest effect on model response. The knowledge gained in this analysis will help in proper planning, time and resource management while conducting this study. As a result, more effort was spent in getting the most accurate physical forcing data for the most sensitive input function, the offshore significant wave height. Also, the curvilinear computational grid was further refined in locations with comparative large errors during this analysis. This analysis will also guide efficient future field measurement campaigns in the bay. Efforts will be concentrated

on sampling data (at higher resolutions) at locations that exhibited high sensitivity to that particular input function. More resources will be committed to procure sophisticated and more accurate and precise instruments to measure parameters that have been identified in this analysis as the most sensitive to model response. These will help in further development and improved utility of this coupled model for Ibaka and other bays with similar characteristics.

CHAPTER V

RESULTS

The objective of this chapter is to show model results and also compare those results with available data. The next chapter will be devoted to the discussion of these results. Time series and maps of wave parameters (such as significant wave height (SWH), wave orbital velocities, mean wave periods, and wave force or the gradient of radiation stress), circulation output parameters (such as along shore and cross shore velocities, water surface elevation, and mean current magnitude), and sediment output variables (e.g. rate of sediment transport and seabed level changes) will be displayed. Critical bed sheer stress will be calculated using the relevant model output parameters and fluid properties (see equation 4 below). Since the main theme of this dissertation centers around determining the most economical (without violating basic environmental laws) ship channel design for Ibaka deep seaport; there is need to understand the critical bed shear stress and the main processes governing the exceedance of this critical stress level in the bay. It is common knowledge that bed shear stress determines the mobilization of bottom sediments into the water column. After mobilization, the sediment could be transported either as suspended sediment load or bed sediment load. The minimum stress required for this mobilization is called critical bottom stress, τ_b. Bottom shear stress is usually parameterized in sediment models as a quadratic function of the depth-averaged velocity, U.

$$\tau_b = \rho C_d U^2 \quad \ldots\ldots\ldots\ldots\ldots\ldots\ldots\ldots\ldots\ldots\ldots\ldots\ldots\ldots\ldots\ldots\ldots\ldots \quad (4)$$

where C_d is the dimensionless drag coefficient that can be variable or constant with typical values within the range of $1 – 4 \times 10^{-3}$, ρ is the water density.

One intriguing result I have found is the relationship between wave energy (represented by significant wave height in this chapter) and sediment transport in the study area. Sediment transport will not occur if the offshore significant wave height (a measure of the wave action) does not exceed a certain threshold value. Several numerical tests carried out during this study revealed that significant wave heights must exceed 1.0 meter in the model domain before the resulting orbital velocities can mobilize seabed sediments into motion as shown in figures 15,17,19,21, and 23 for five different locations (Stations 1,2,3,6,and 10). Figures 16,18,20,22,and 24 show the corresponding stations' wave transformation due to wave-current interactions and the cumulative seabed level changes over the entire simulation period (A morphology factor of four was specified for this run, thus the cumulative seabed level change is for a duration of four times the time period shown in the graphs). Opposing currents amplify the wave height (hence more wave action to initiate sediment transport for a given significant wave height, especially near the threshold value) while following currents tend to reduce the wave action. The effect of wave-current interactions in the model output results is most noticeable when the offshore significant wave heights are slightly below the 1.0-meter threshold value. The strength and direction of current interactions with the waves determine the initiation of sediment transport in the study area for significant wave heights within the range 0.9 – 1.0 meter.

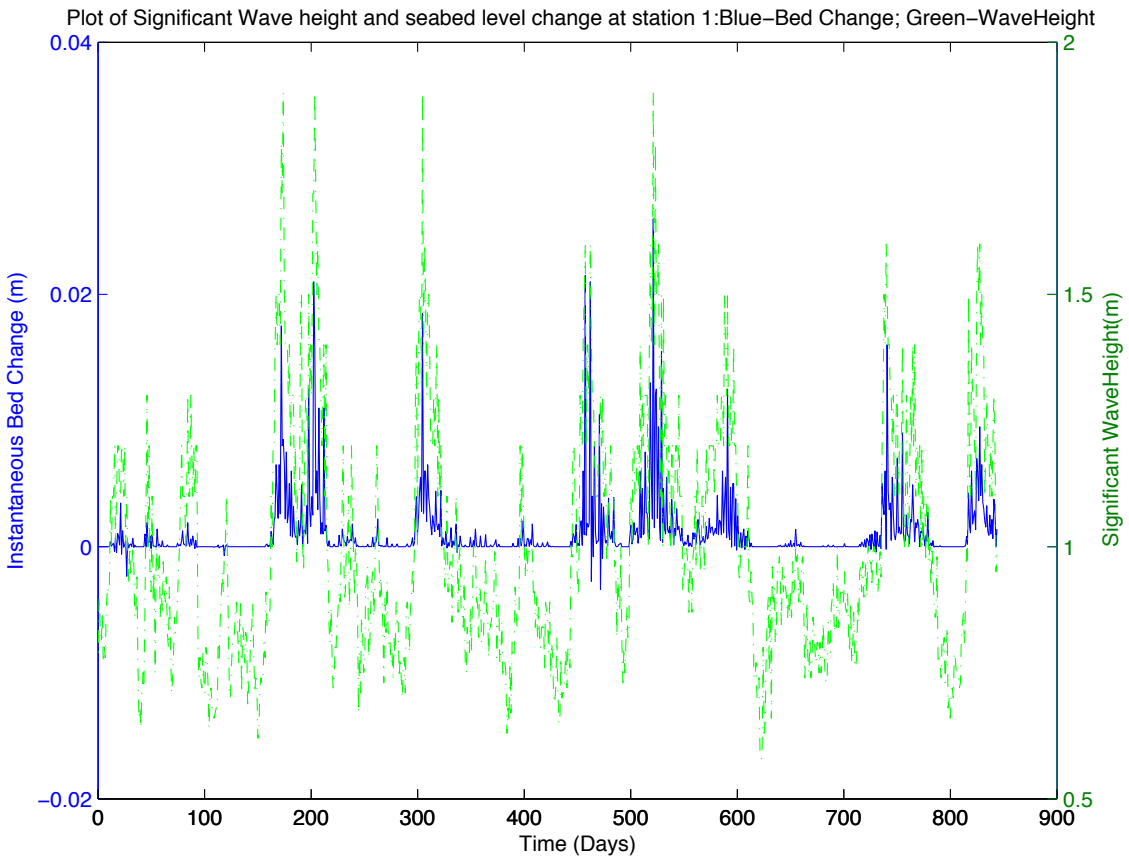

Figure 15. Variations of offshore wave height effects on seabed changes in Ibaka bay at station 1. Seabed sediments are mobilized into motion when the significant wave height exceeds 1.0 meter. The resulting sediment fluxes either erode (negative seabed level change values) or accrete (positive seabed level change values) the seabed.

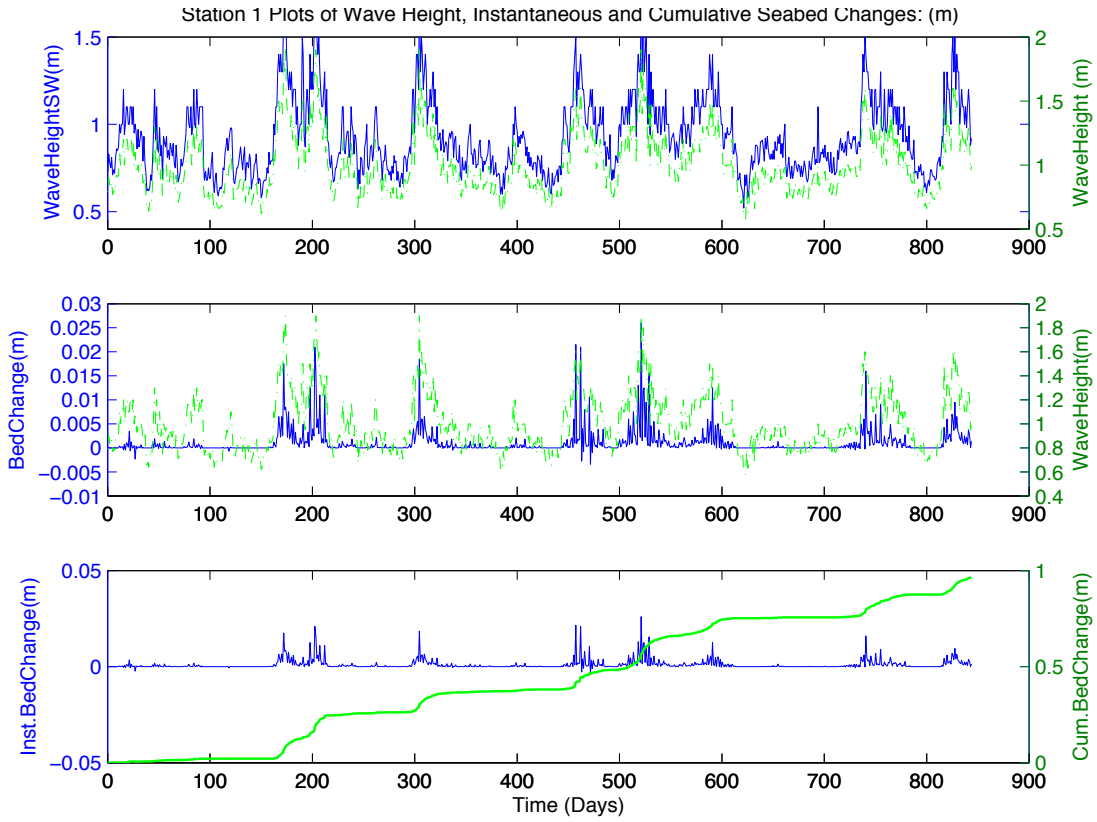

Figure 16. Effects of significant wave height on instantaneous and cumulative seabed level changes at station 1. The top panel indicates the effect of wave-current interactions on the significant wave height (Blue color is for SWAN output significant wave height which has no current feedback while the green line shows NearCoM-TVD output significant wave height). Middle panel shows the instantaneous seabed level changes (blue line) with the significant wave height overlaid (green line). Bottom panel shows the cumulative seabed change with the dash-dot green line (A morphology factor of 4 was specified for this simulation, thus the time duration for the cumulative seabed level change is ≈9 years).

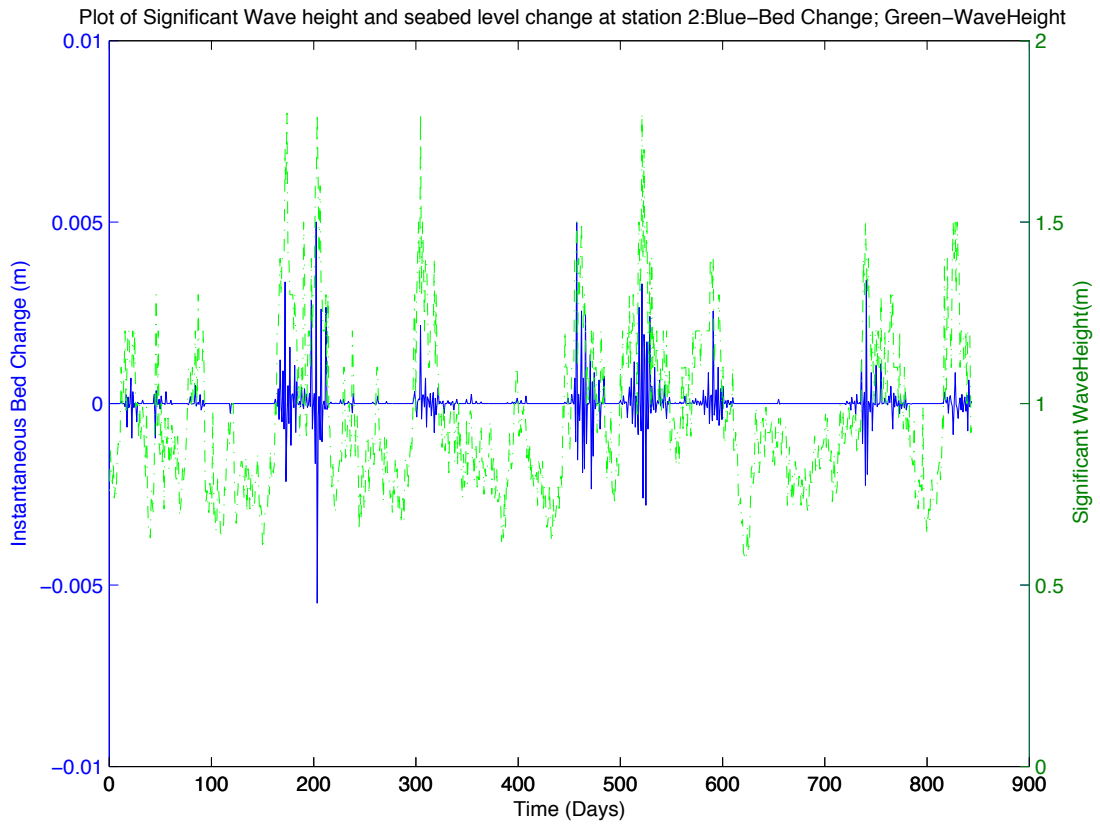

Figure 17. Variations of offshore wave height effects on seabed changes in Ibaka bay at station 2. Seabed sediments are mobilized into motion when the wave height exceeds 1.0 meter. The resulting sediment fluxes either erode (negative seabed level change values) or accrete (positive seabed level change values) the seabed.

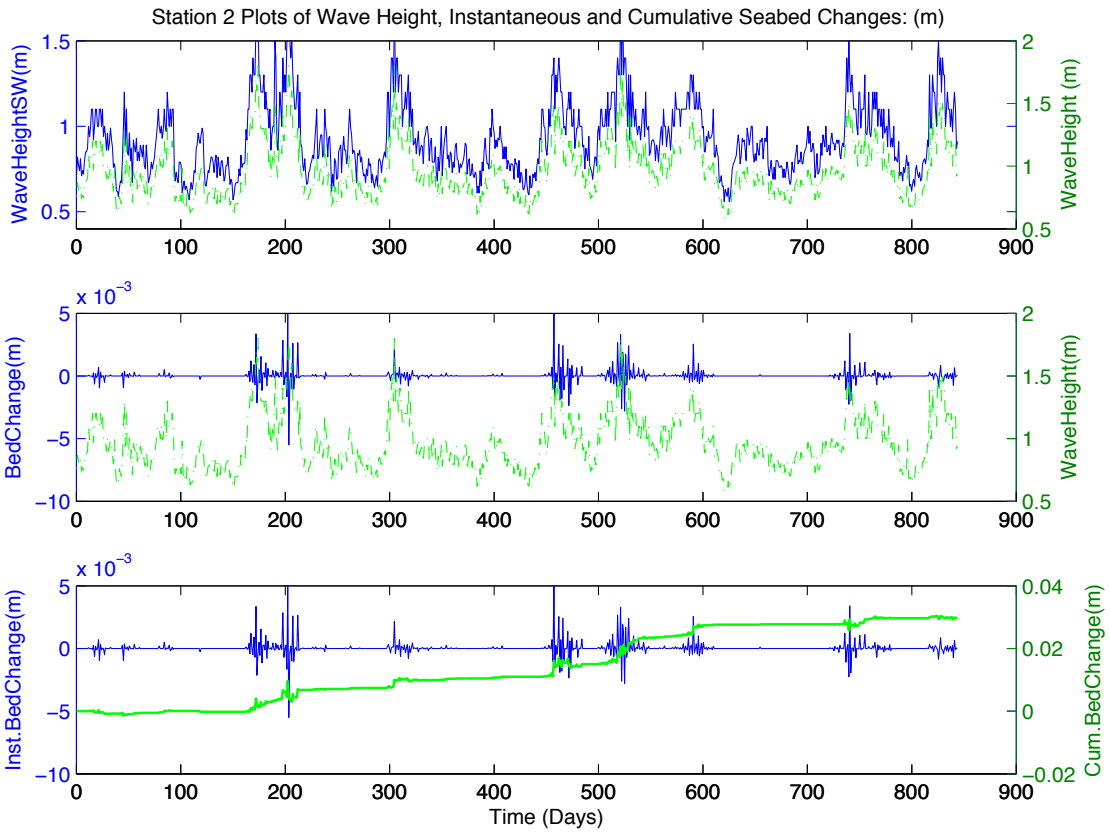

Figure 18. Effects of significant wave height on instantaneous and cumulative seabed level changes at station 2. The top panel indicates the effect of wave-current interactions on the significant wave height (Blue color is for SWAN output significant wave height which has no current feedback while the green line shows NearCoM-TVD output significant wave height). Middle panel shows the instantaneous seabed level changes (blue line) with the significant wave height overlaid (green line). Bottom panel shows the cumulative seabed change with the dash-dot green line (A morphology factor of 4 was specified for this simulation, thus the time duration for the cumulative seabed level change is ≈9 years).

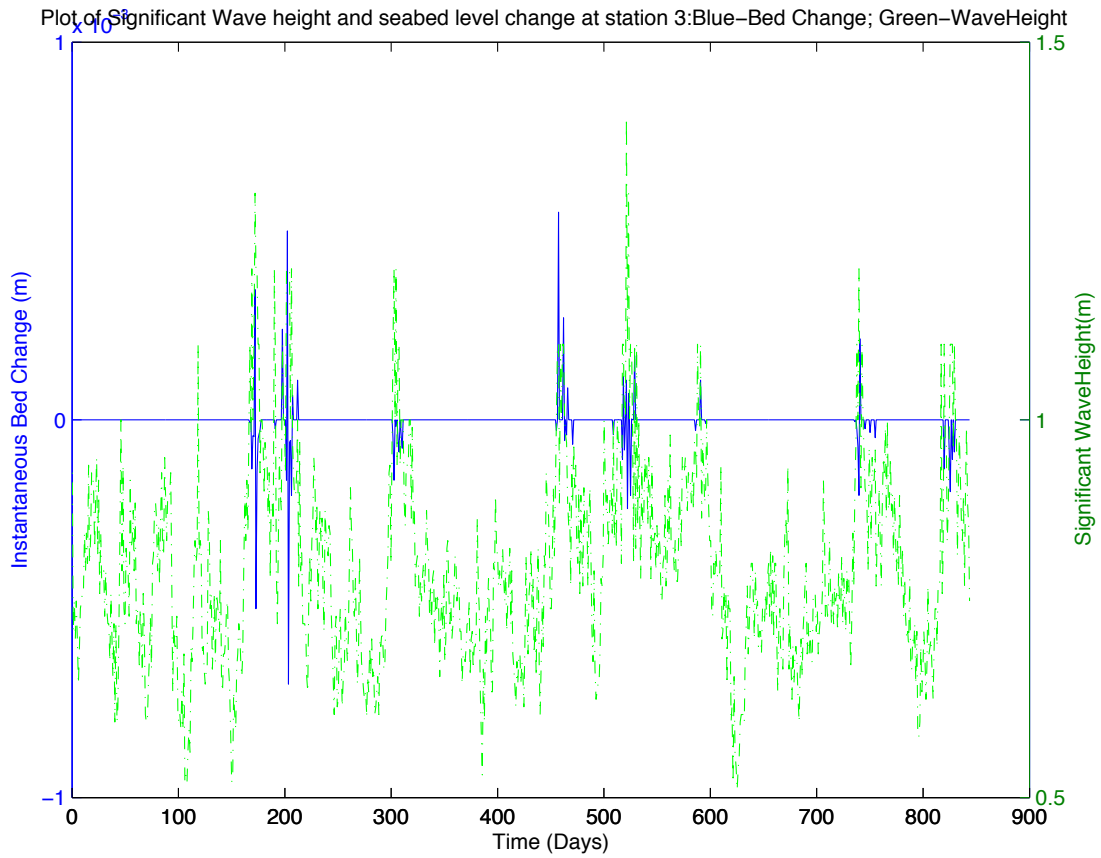

Figure 19. Variations of offshore wave height effects on seabed changes in Ibaka bay at station 3. Seabed sediments are mobilized into motion when the wave height exceeds 1.0 m. meter. The resulting sediment fluxes either erode (negative seabed level change values) or accrete (positive seabed level change values) the seabed.

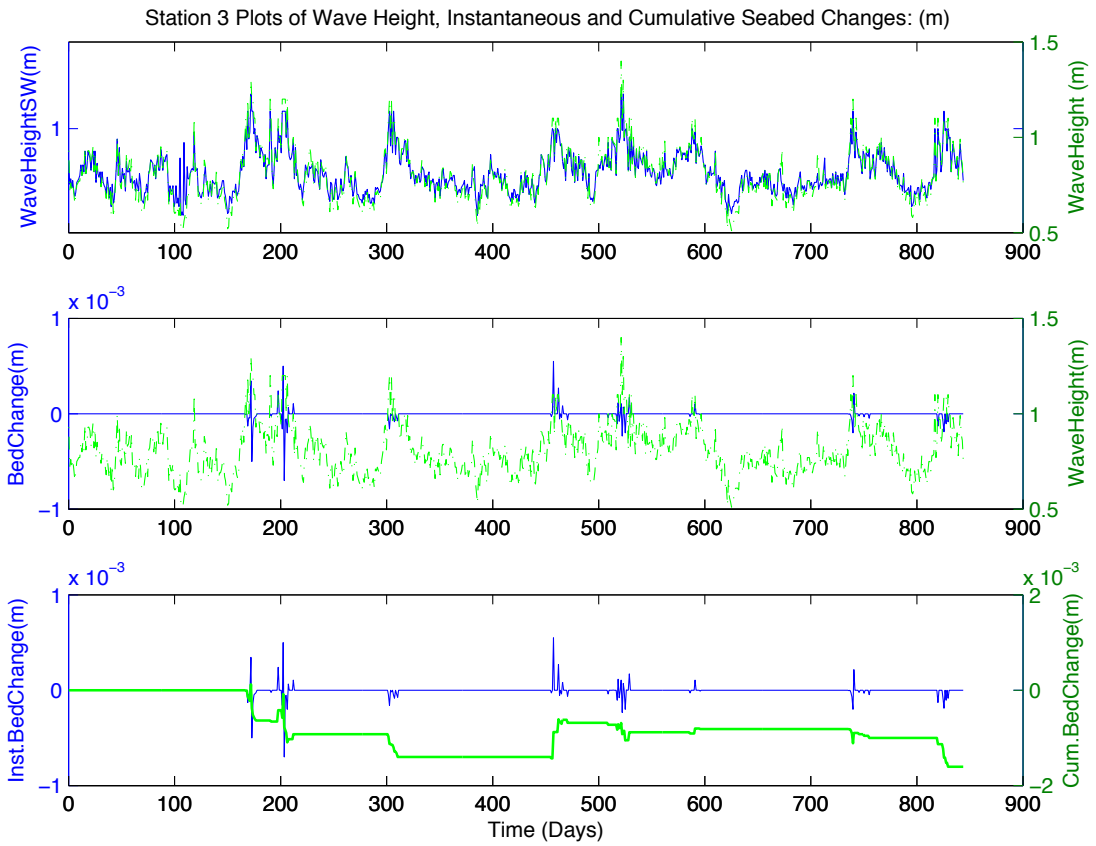

Figure 20. Effects of significant wave height on instantaneous and cumulative seabed level changes at station 3. The top panel indicates the effect of wave-current interactions on the significant wave height (Blue color is for SWAN output significant wave height which has no current feedback while the green line shows NearCoM-TVD output significant wave height). Middle panel shows the instantaneous seabed level changes (blue line) with the significant wave height overlaid (green line). Bottom panel shows the cumulative seabed change with the dash-dot green line (A morphology factor of 4 was specified for this simulation, thus the time duration for the cumulative seabed level change is ≈9 years).

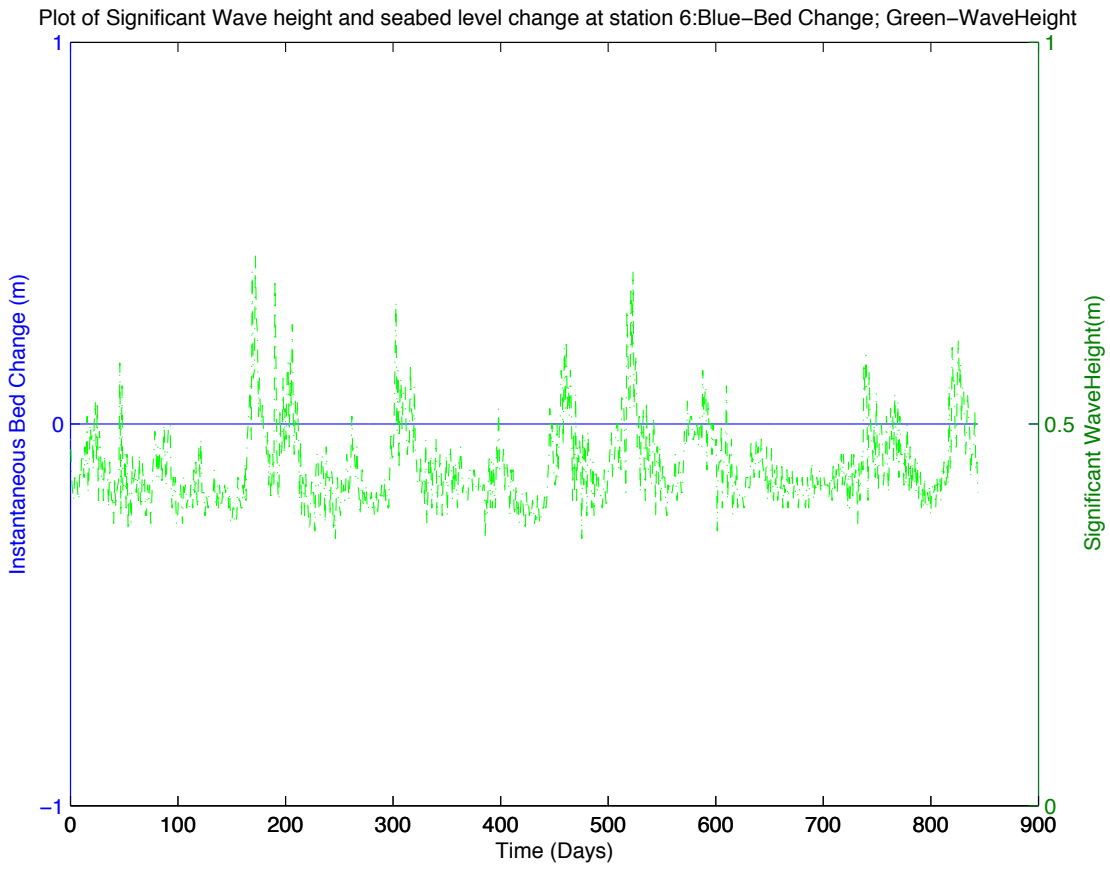

Figure 21. Variations of offshore wave height effects on seabed changes in Ibaka bay at station 6. Seabed sediments are mobilized into motion when the wave height exceeds 1.0 m. At this location, there is no seabed level change because the significant wave heights are below 1.0 m due to wave dissipation as the wave propagates towards the north end of the study area. Station 6 is the closest station to Ibaka harbor.

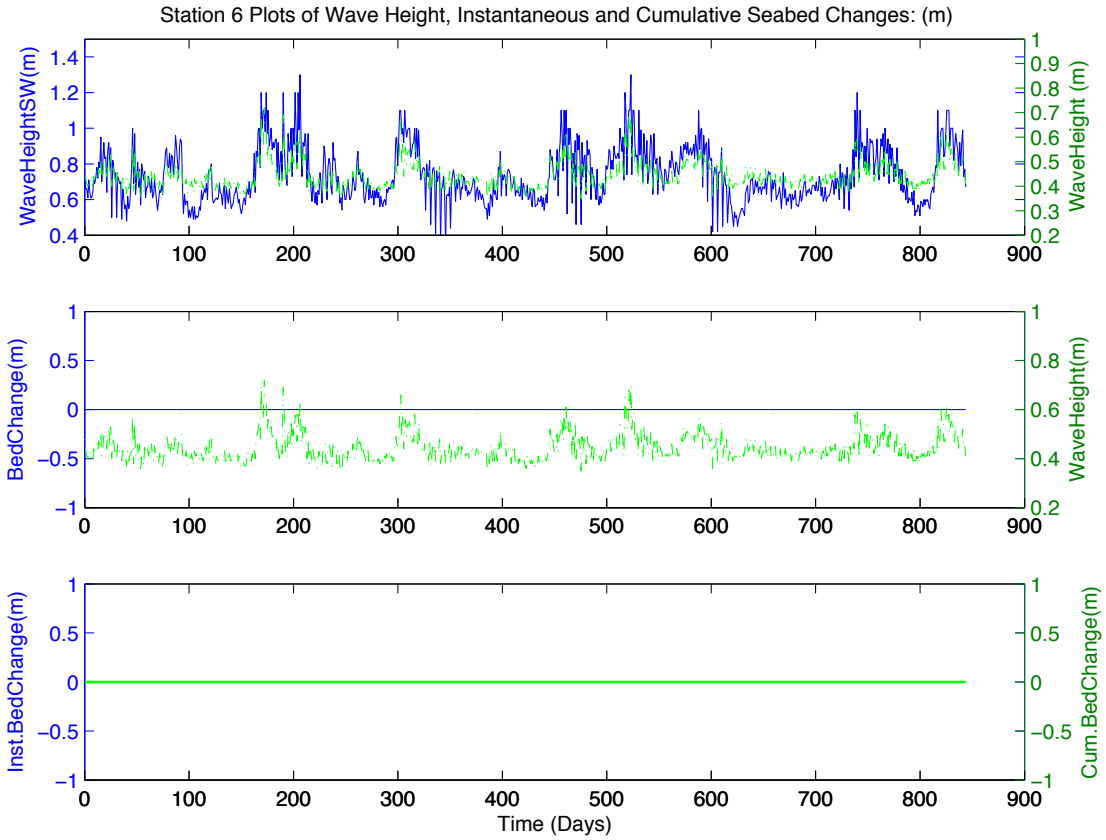

Figure 22. Effects of significant wave height on instantaneous and cumulative seabed level changes at station 6. The top panel indicates the effect of wave-current interactions on the significant wave height (Blue color is for SWAN output significant wave height which has no current feedback while the green line shows NearCoM-TVD output significant wave height). Middle panel shows the instantaneous seabed level changes (blue line) with the significant wave height overlaid (green line). Bottom panel shows the cumulative seabed change with the dash-dot green line (A morphology factor of 4 was specified for this simulation, thus the time duration for the cumulative seabed level change is ≈9 years).

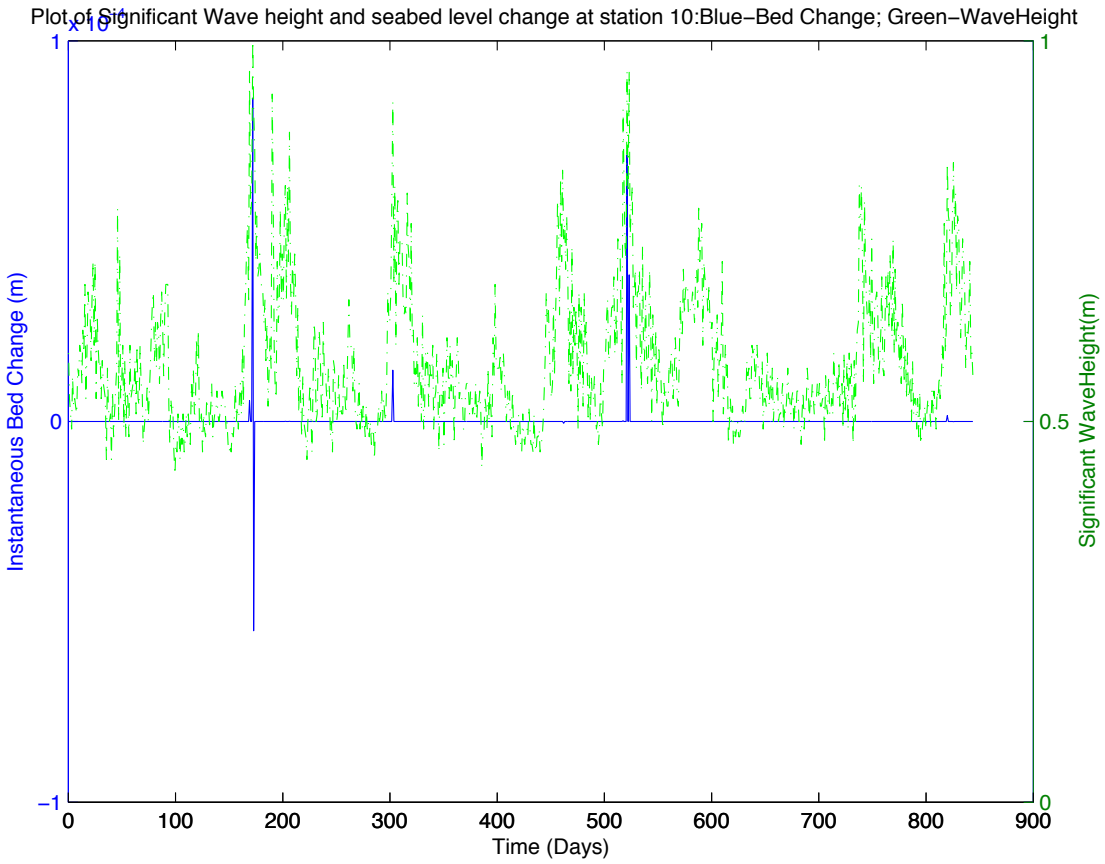

Figure 23. Variations of offshore wave height effects on seabed changes in Ibaka bay at station 10. Seabed sediments are mobilized into motion when the wave height is about 1.0 meter. The resulting sediment fluxes either erode (negative seabed level change values) or accrete (positive seabed level change values) the seabed.

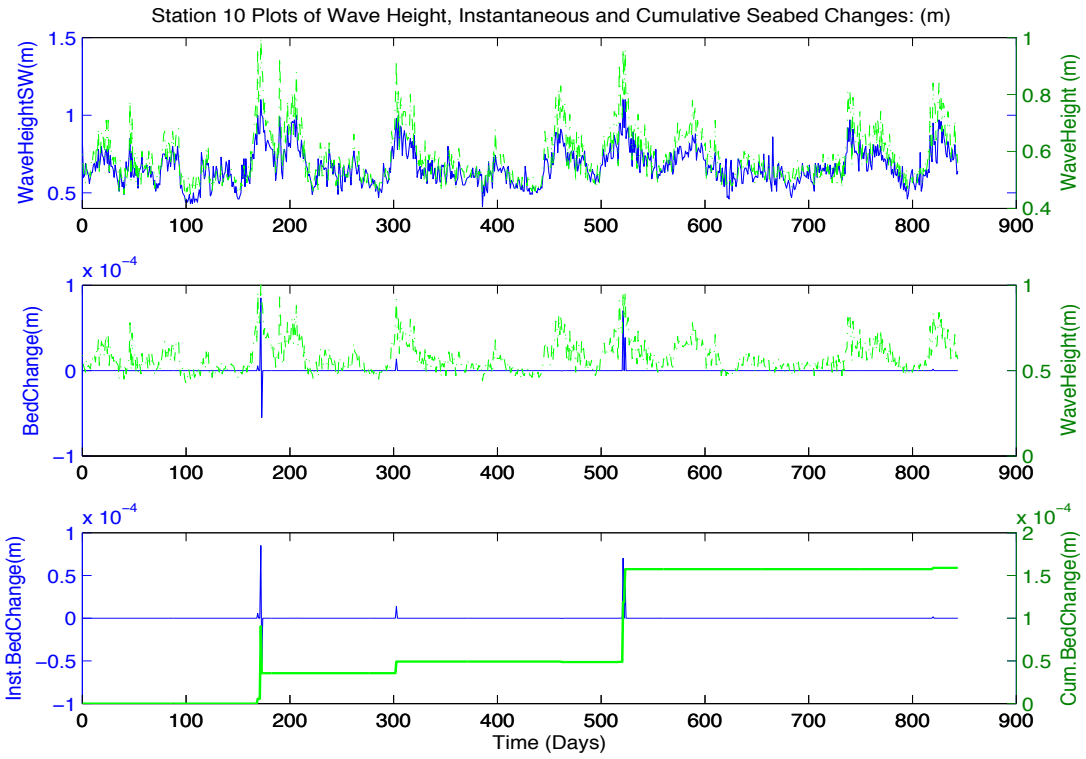

Figure 24. Effects of significant wave height on instantaneous and cumulative seabed level changes at station 10. The top panel indicates the effect of wave-current interactions on the significant wave height (Blue color is for SWAN output significant wave height which has no current feedback while the green line shows NearCoM-TVD output significant wave height). Middle panel shows the instantaneous seabed level changes (blue line) with the significant wave height overlaid (green line). Bottom panel shows the cumulative seabed change with the dash-dot green line (A morphology factor of 4 was specified for this simulation, thus the time duration for the cumulative seabed level change is ≈9 years).

Based on the offshore wave height threshold value for sediment transport in the study location, it was anticipated that storm events could cause a lot of damages to port infrastructures in Ibaka bay. Such anticipated damages could include regular filling of the ship channels, destruction of anchors and other mooring lines, fatigue impacts on the quay, and temporary suspension of operations in the seaport. However, historical analyses of available storm data indicate that over 90% of recorded storms in Cross River Estuary come from the

South-South-West direction (210^{o} using the nautical convention) (Olagnon, et al. 2004). Tom Shot Island is strategically positioned to shield Ibaka bay from such storms. Also, the continental shelf extent (≈120 km) in the south-south region of Nigeria aids in breaking high waves that propagates from the South Atlantic Ocean towards the estuary. The bathymetric features of the study area also constrain the maximum wave heights that can reach the northern side of the domain. Bathymetric contour map is shown in figure 25.

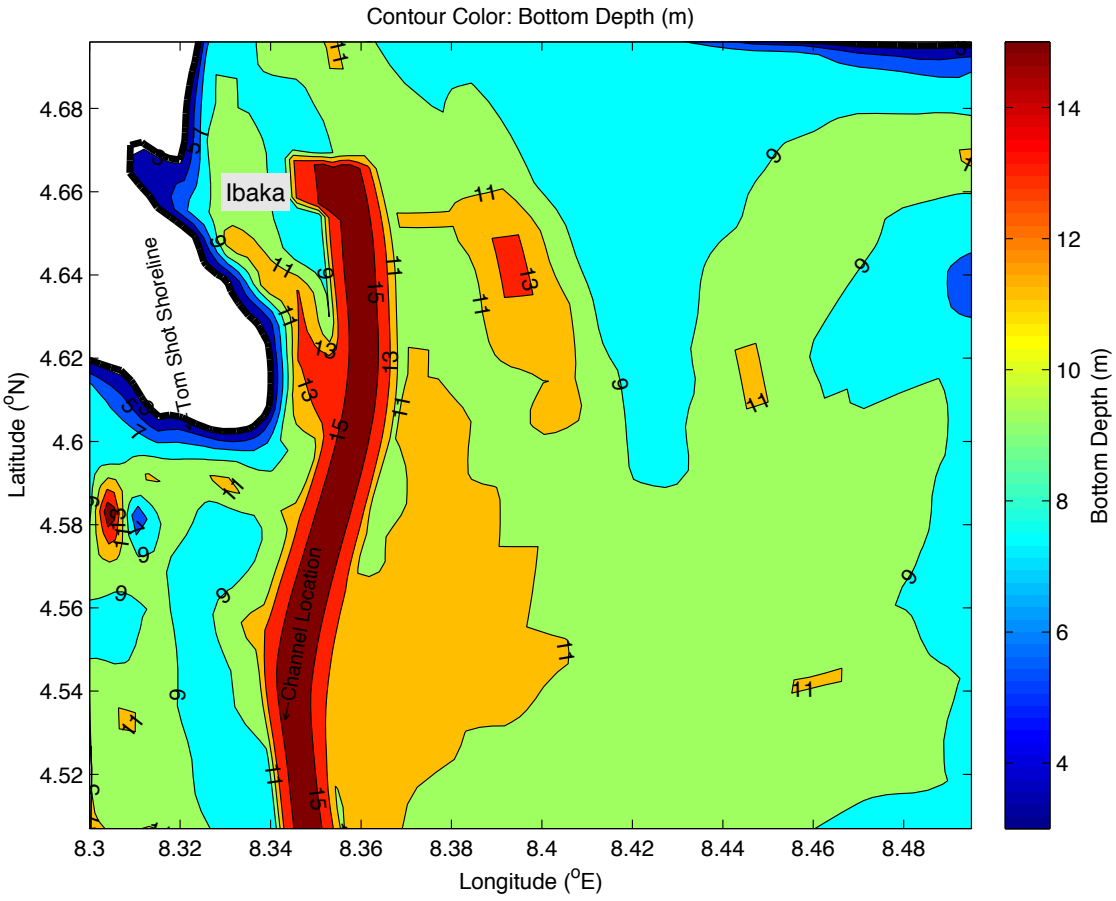

Figure 25. Bathymetric contours of study area with respect to the local mean sea level. The ship channel is dredged to about 15 m.

Figures 26 to 28 show these maximum wave height limitations as the wave propagates from the offshore south boundary towards Ibaka bay. The deepest part of the dredged channel in these figures is 15 meters that can accommodate vessels up to about 150,000 DWT. Each of these figures is for a different wave height scenario.

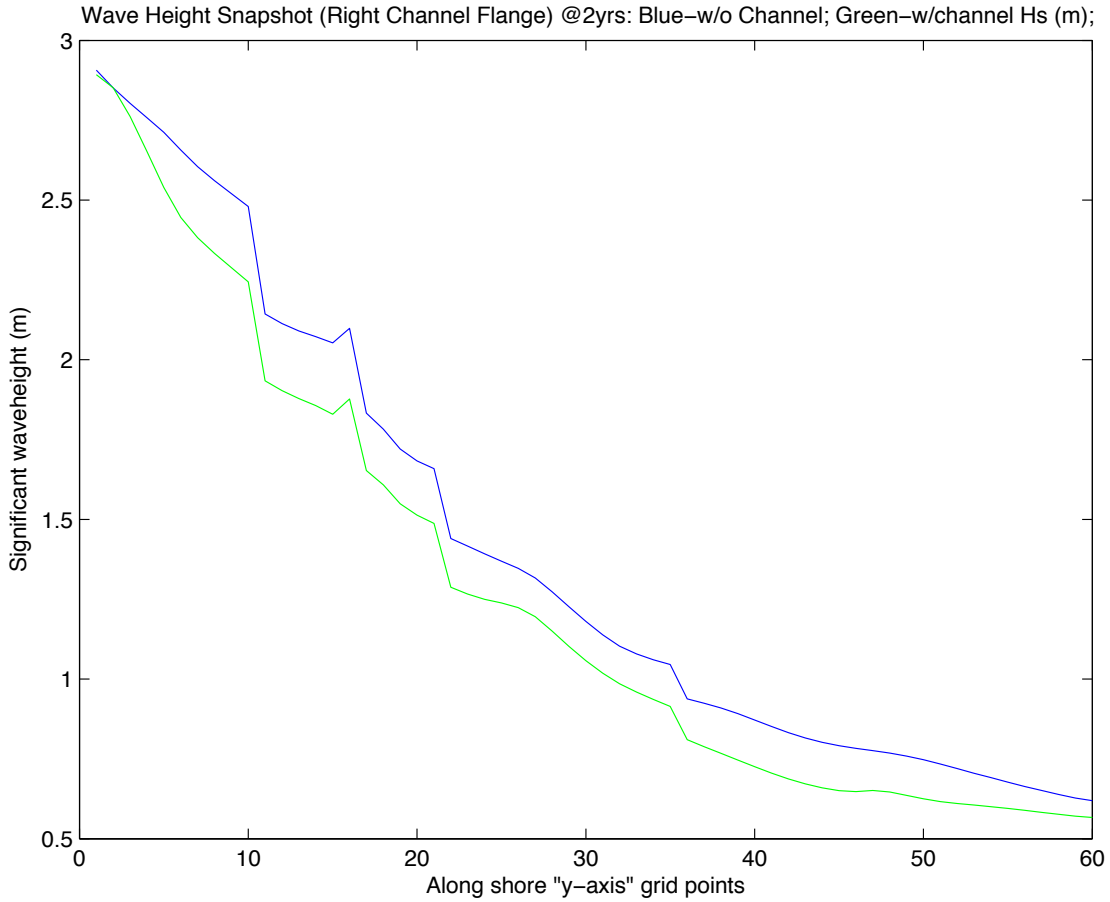

Figure 26. About 3 m high swells coming from offshore into the study area are attenuated below 1.0 m before it reaches Ibaka bay. The geometry and bathymetric features of the bay dissipate the wave action (through depth-limited breaking, bottom friction and white-capping) such that no wave height above 1.0 m reaches Ibaka bay. Ibaka bay is situated between y-axis grid point 45 and 55. Flange in the title refers to the sloping flank of the channel. W/o channel means without channel while w/channel means simulation with the dredged ship channel.

The three representative offshore significant wave heights (shown in these figures) were chosen based on analyses of time series records of measured significant wave heights in the region. The end result of these combined processes is that Ibaka sediment processes are somewhat immune from offshore wave height variability. The graphs in figures 26 to 28 also demonstrate that the dredged ship channel reduces the wave action as the wave propagates towards the shore. Flange in the title of figure 26 refers to sloping flank of the channel.

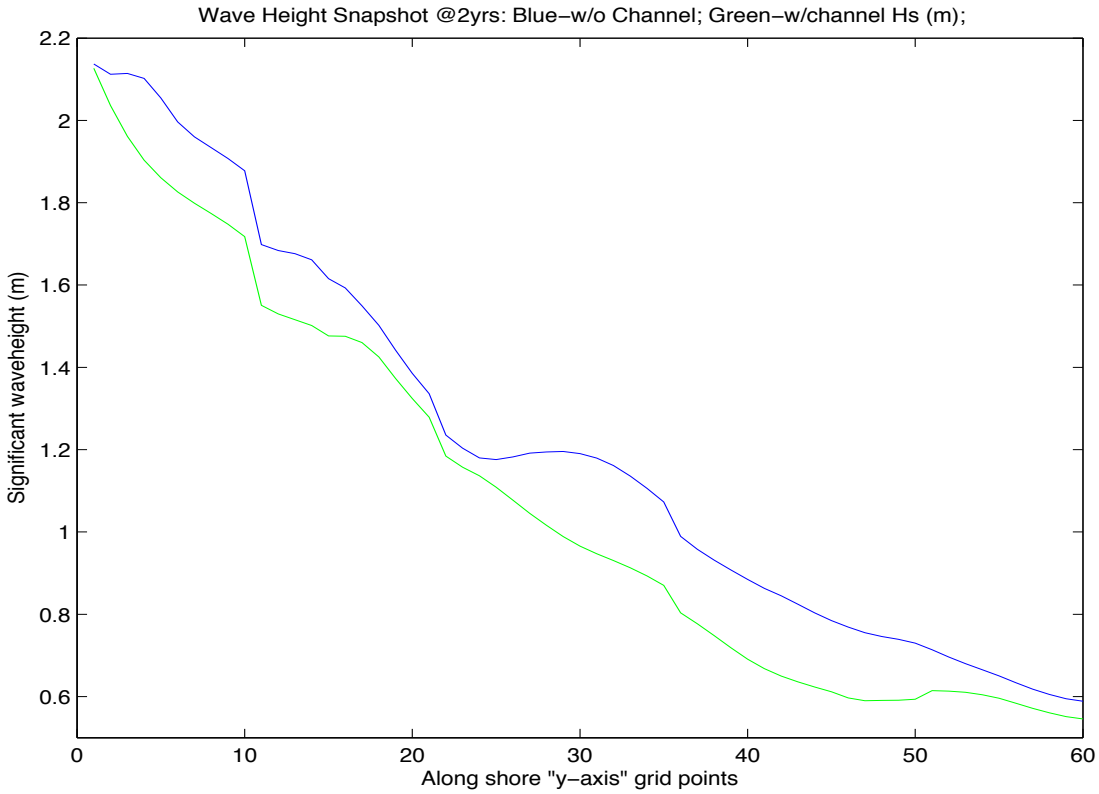

Figure 27. About 2.2 m high swells coming from offshore into the study area are attenuated below 1.0 m before it reaches Ibaka bay. The geometry and bathymetric features of the bay dissipate the wave action (through depth-limited breaking, bottom friction and white-capping) such that no wave height above 1.0 m reaches Ibaka bay. Ibaka bay is situated between y-axis grid point 45 and 55. W/o channel means without channel while w/channel means simulation with the dredged ship channel.

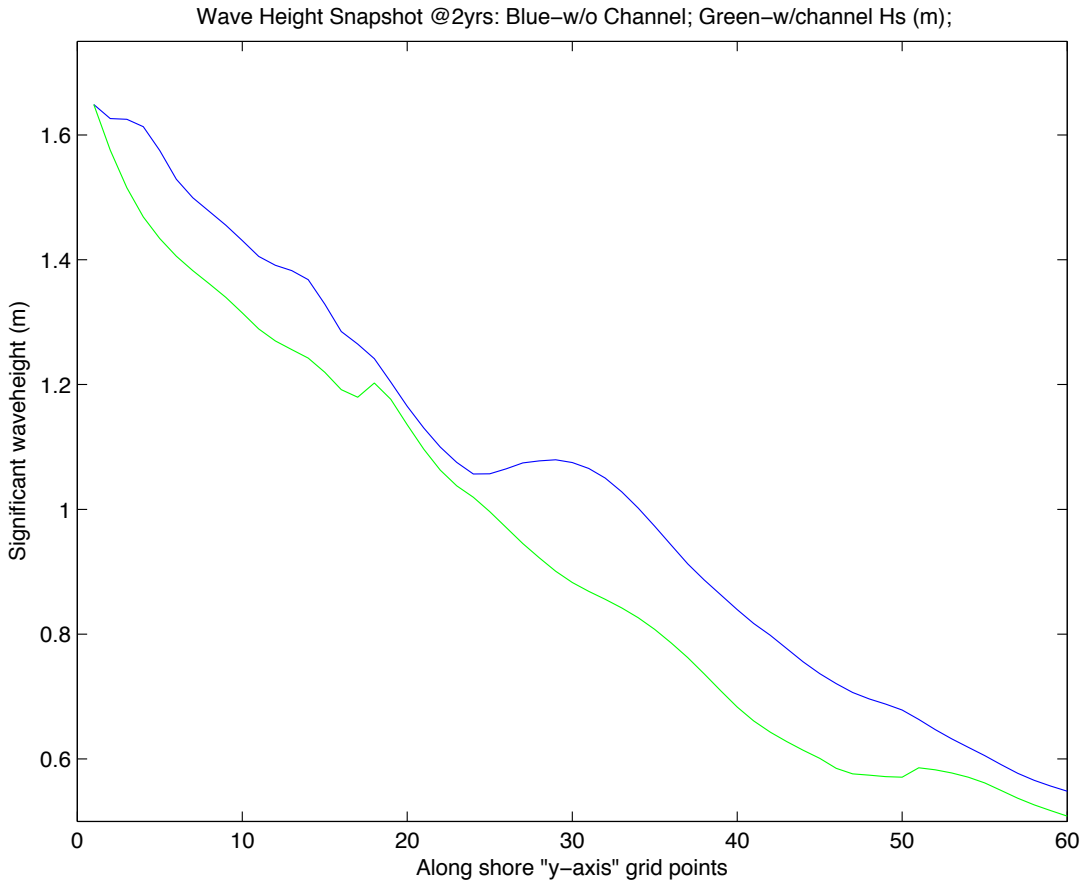

Figure 28. About 1.6 m high swells coming from offshore into the study area are attenuated below 1.0 m before it reaches Ibaka bay. The geometry and bathymetric features of the bay dissipate the wave action (through depth-limited breaking, bottom friction and white-capping) such that no wave height above 1.0 m reaches Ibaka bay. Ibaka bay is situated between y-axis grid point 45 and 55. W/o channel means without channel while w/channel means simulation with the dredged ship channel.

Nevertheless, if the main objective of this project to provide a safe harbor for high tonnage vessels (>200,000 DWT) is to be realized, we have to quantify the impacts of changing wave heights on sediment transport and bed morphological changes on the approaching ship channel when the channel is dredged further to accommodate vessels heavier than 200,000

DWT. This implies that the near offshore boundary of this study area has to be dredged to the required depth of about 18 meters (this draft is partly dependent on the design ship chosen). A contour map of the initial bathymetry of this domain in figure 3 above showed that there are some subsurface seamounts near the offshore boundaries. It is pertinent to investigate the relative contribution of these seamounts (which will be removed as a result of dredging to deepen the channel to desired depth to accommodate >200,000 DWT vessels) to the attenuation of the rarely (but probably) occurring storm waves directed towards Ibaka bay. Accurate quantification of the effects of this high wave energy (estimated to have a return period of five years, Olagnon et al., 2004) will provide reliable data for economic analysis of the benefits of this project to the state and other stakeholders.

In addition to the estimate of significant wave height of the storm wave, accurate knowledge of the duration of such storms will provide adequate data for quantitative analyses of its impacts on sediment transport in the study area. Measured and archived data on the duration of unusually high storm waves in Ibaka bay or the Cross River Estuary is lacking in the literature. The investigation of the impacts of storm duration on sediment processes will rely heavily on the coupled numerical model since it had been validated and verified to model and predict circulation and sediment processes in the study area with a high model skill (> 0.7). To minimize wild guesses on the maximum possible duration of irregular storm surges in Cross River Estuary, I have incorporated the estimate of time duration I obtained during my interactions with some experienced fishermen in Ibaka during the December 2012 field experiments. Figure 29 shows the significant wave height transformation after the channel was further deepened. The significant wave height attenuation in this figure is similar to the ones obtained from the previous graphs when the channel was only dredged to contain relatively

lighter vessels. Thus, the main concern for future deepening of the ship channel should be the dredging cost.

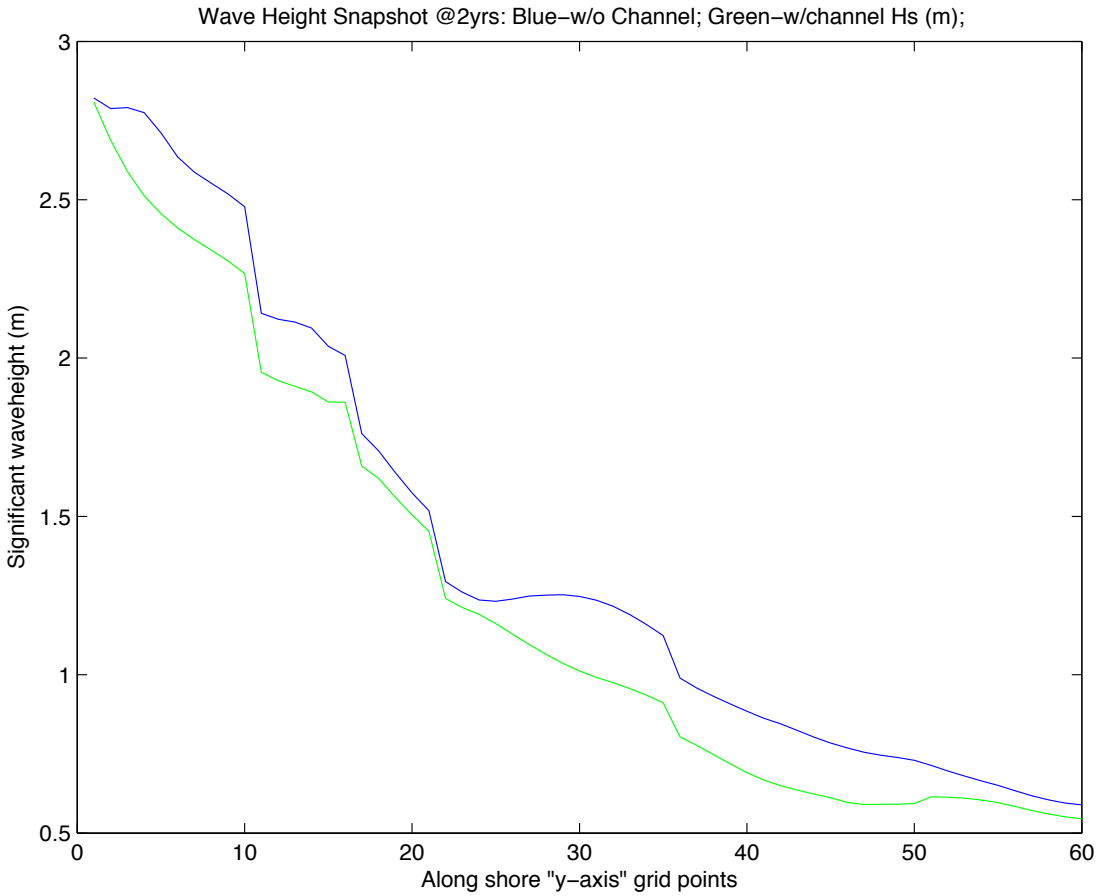

Figure 29. About 3 m high swells coming from offshore into the study area are attenuated below 1.0 m before it reaches Ibaka bay when the approach channel is further deepened to 18 m. The geometry and bathymetric features of the bay dissipate the wave action (through depth-limited breaking, bottom friction and white-capping) such that no wave height above 1.0 m reaches Ibaka bay. Ibaka bay is situated between y-axis grid point 45 and 55. W/o channel means without channel while w/channel means simulation with the dredged ship channel.

Attention will now be given to effects of changing wave heights on the bed shear stress (or drag force per unit area) in the study domain. Gardner discussed how intermittent focusing

of internal energy resulted in periodic re-suspension of particulate matter in Baltimore canyon (Gardner, 1989b). Based on the analysis of his experimental data, Gardner showed that, during late winter and early spring, re-focusing of internal tidal energy generated bed shear stress that exceeded a certain threshold value for suspension of particulate matter in the water column. Assuming a constant drag coefficient, $C_d = 1.4 \times 10^{-3}$, Gardner's estimates indicated that an equivalent free stream velocity of about 0.28 – 0.32 ms^{-1} (friction velocity, u*= 0.011 – 0.012 ms^{-1}) was required to trigger sediment suspension, of medium to coarse-grained sand (d_{50}: 0.25 to 1.00 mm), in Baltimore canyon. He opined that the identified process of sediment transport could inhibit filling of the submarine canyon during interglacial times.

Brooks followed Gardner's approach in his work at Kennebec River of central Maine and obtained results that were consistent with Gardner's critical values of friction velocity, u* for initiation of sediment suspension (Brooks, 2014). Brooks further found that a lower critical stress (≈0.11 Pa or 0.11 Nm^{-2}, equivalently, u*≈ 0.01 ms^{-1}) was enough to suspend sediment in Sasanoa River. Further analysis revealed that Sasanoa River was dominated by fine sediments; $d_{50} < 63$ µm. Brooks used these results to explain why some locations of his study domain had exposed bed rocks.

Most of the areas in my study region have sediment in the medium grain size ($d_{50} \approx$ 0.27 mm) category. Gardner (1989b) showed that the velocity profile for a hydrodynamically smooth flow could be computed in two ways based on available measurements. These formulations are important to this study because they relate the free stream velocities with the critical shear stresses to initiate sediment transport. If there are measured velocities within the logarithmic law region (locations near the seabed where the logarithmic law or law of the wall is valid), then velocity profile is calculated using:

$$u/u^* = 2.5 \ln(u^* z/v) \quad \ldots\ldots\ldots\ldots\ldots\ldots\ldots\ldots\ldots\ldots\ldots\ldots \quad (5)$$

where u* is the friction velocity, u is the mean free-stream velocity, z is depth above the sea floor, and v is the kinematic viscosity. If the velocity measurements occur in locations above the logarithmic law region, then quadratic stress law could be applied to get the critical bed shear stress as given below:

$$u^2 = u^{*2}/C_d \quad \ldots\ldots\ldots\ldots\ldots\ldots\ldots\ldots\ldots\ldots\ldots\ldots\ldots\ldots \quad (6)$$

where C_d is the drag coefficient ($\approx 1.4 \times 10^{-3}$ in smooth flow).

Since there were no velocity measurements in the logarithmic layer for Ibaka bay, the second formula (equation 6) will be used to estimate the critical bed shear stress using the mean free stream velocity obtained from the circulation model and TOTAL current meter measurements. Table 1 in Gardner (1989b) showed that the differences in erosion velocity calculated with the two formulas, for selected sediment grain sizes, were within 10%. The quadratic law consistently yielded a slightly higher free stream velocity than the logarithmic law for given grain size.

Using the formula in equation 6 and the study site sediment characteristics, it was estimated that a free stream velocity of 25.1 cm/s was needed to initiate sediment transport in most locations of the study area. We now make some plots to see if model output, based on the input sediment characteristics and flow regime in our study site, followed this empirical estimate. Figures 30 to 32 relate wave height, currents, and bed level change at stations 1, 2,

and 8 respectively. It is seen that the model does not perfectly reproduce the empirical estimates obtained using equation 6. This might be due to different processes contributing to the mean free stream flow rather than predominantly tidal currents that drove the mean flow in the region this formula was developed. Another factor that could be examined is the current direction. Since the wave and current interact in the model, the directionality of the current components might be an important parameter in determining initiation of sediment transport at some locations.

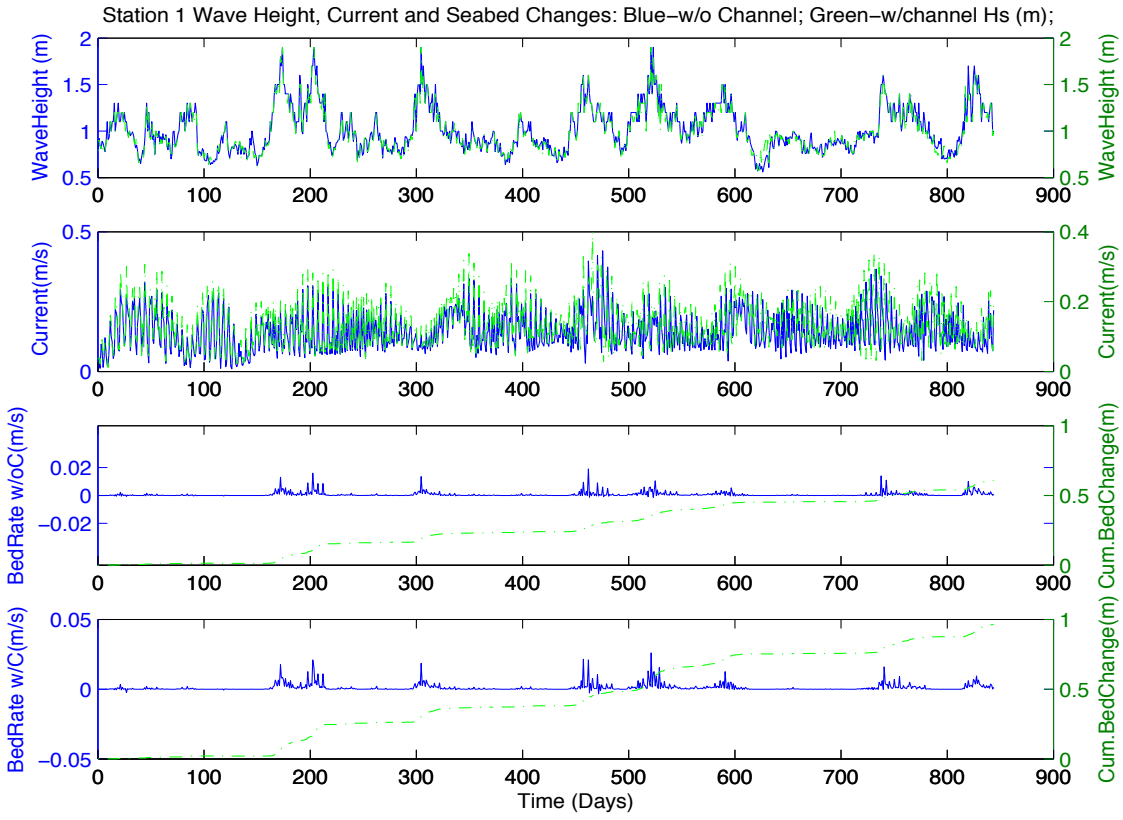

Figure 30. Graph showing the effects of variations of wave heights and currents on seabed changes at Station 1. w/oC stands for model run without the ship channel while w/C is for model run with the channel dredged. Green dash-dot lines in the bottom panels represents the cumulative seabed change over the simulation period. A morphology factor of four was specified for the sediment module. Note the scale changes on the axes at the different stations.

Also, the sediment characteristics in the particular locations where these outputs were taken should be analyzed closely. Specification of an average sediment size (d_{50}) for the model might not be sufficient to evaluate the relationship between the mean free stream and friction velocities. More in-situ measurements are needed to draw a definitive conclusion on the threshold mean free stream velocity that stirs sediment into motion in this study area.

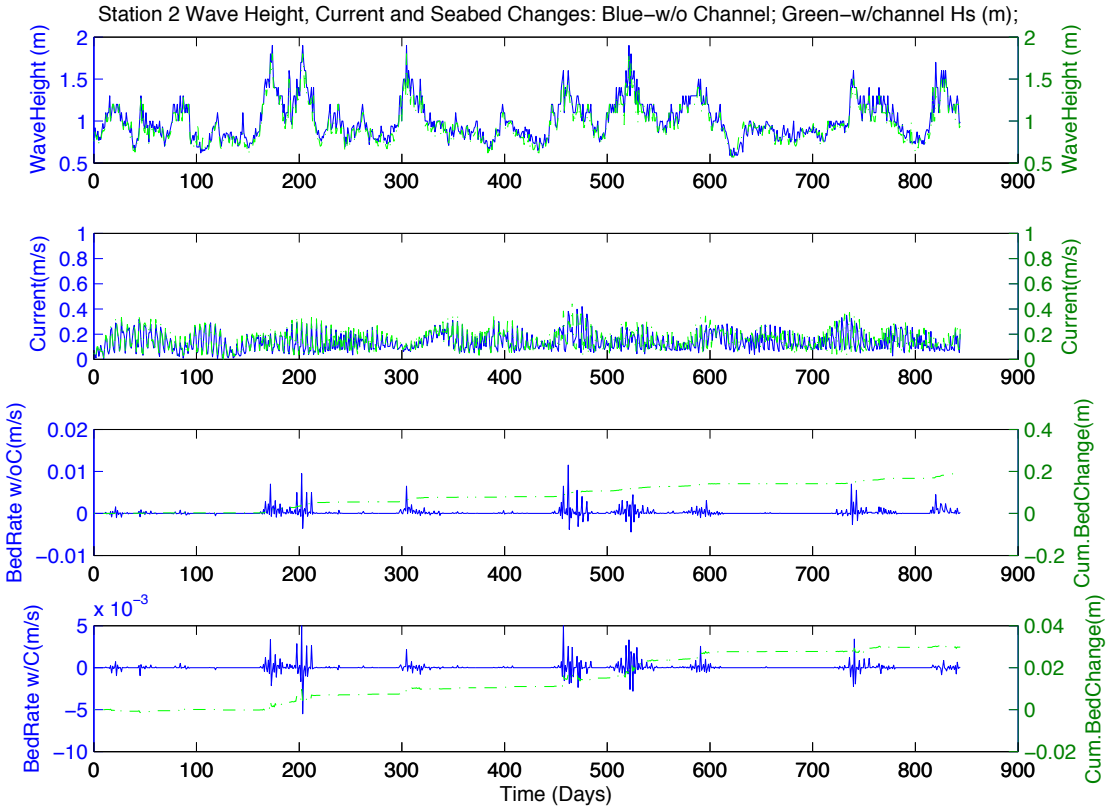

Figure 31. Graph showing the effects of variations of wave heights and currents on seabed changes at Station 2. w/oC stands for model run without the ship channel while w/C is for model run with the channel dredged. Green dash-dot lines in the bottom panels represents the cumulative seabed change over the simulation period. A morphology factor of four was specified for the sediment module. Note the scale changes on the axes at the different stations.

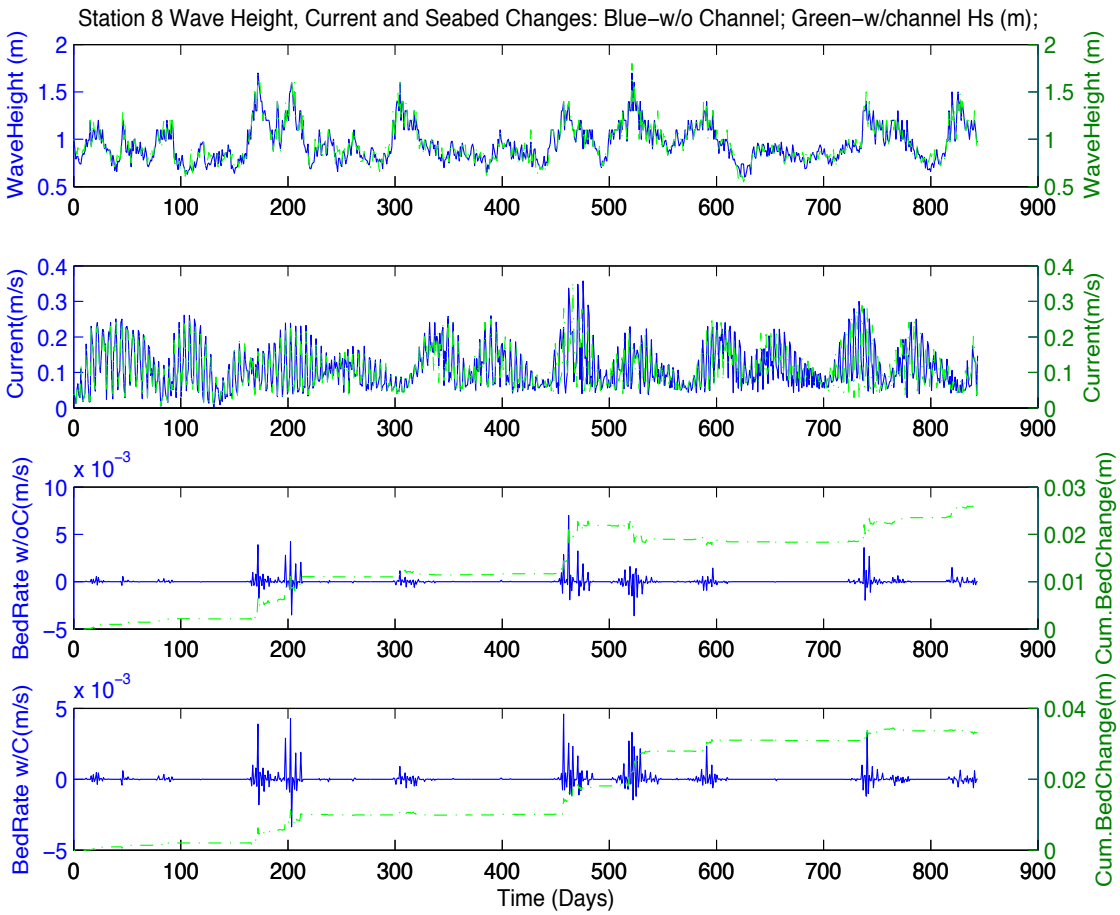

Figure 32. Graph showing the effects of variations of wave heights and currents on seabed changes at Station 8. w/oC stands for model run without the ship channel while w/C is for model run with the channel dredged. Green dash-dot lines in the bottom panels represents the cumulative seabed change over the simulation period. A morphology factor of four was specified for the sediment module. Note the scale changes on the axes at the different stations.

The estimated erosion velocities are however correlated with the magnitude of the offshore significant wave height entering the study domain. The model result shows that mean free stream velocities of 25 cm/s are obtained whenever the offshore significant wave height exceeds 1.0 m. Figure 33 illustrates the correlation between offshore significant wave height and erosion velocity in the study area. The coefficient of determination, r^2, for these two variables was

0.76. The figure illustrates that a positive correlation exists between the two variables. To get a better understanding of what causes this pattern, we need to look at the parameters that were used to compute the free stream velocity. One parameter to consider is the drag coefficient. The drag coefficient was parameterized as a function of water depth in the model equation. In shallow water, the wave height is limited by water depth. Thus, it is not a surprise to observe this pattern, especially as it is also a direct variation. Our main focus here is the effects of these processes on the sediment transport and bed morphological changes in the channel and bay.

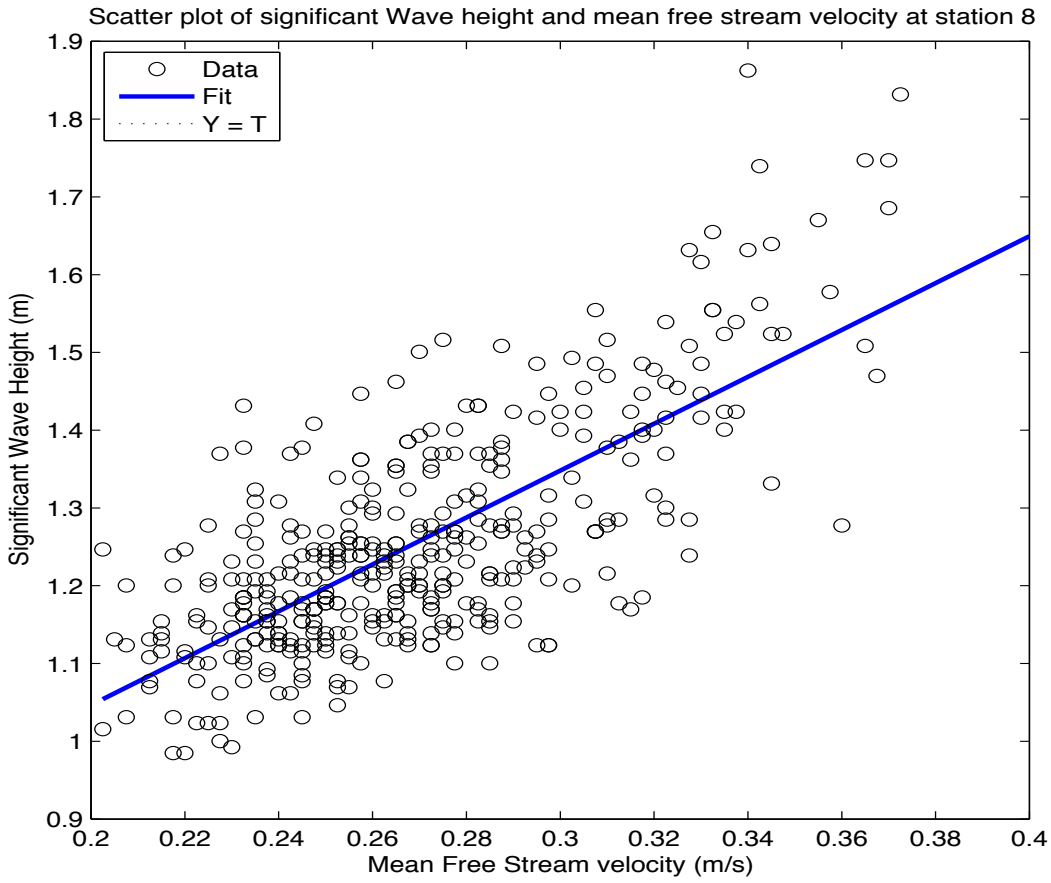

Figure 33. Scatter plot of offshore significant wave height and mean free stream velocity at station 8. Both output variables were from a one-year model run. The blue line is a regression line. Y = T is a dotted line fit underlain in the main blue line fit.

Figure 34 compares the correlation of the significant wave height with the mean free stream velocity for station 7. The trend line of the scatter diagram in figure 34 is similar to that of figure 33.

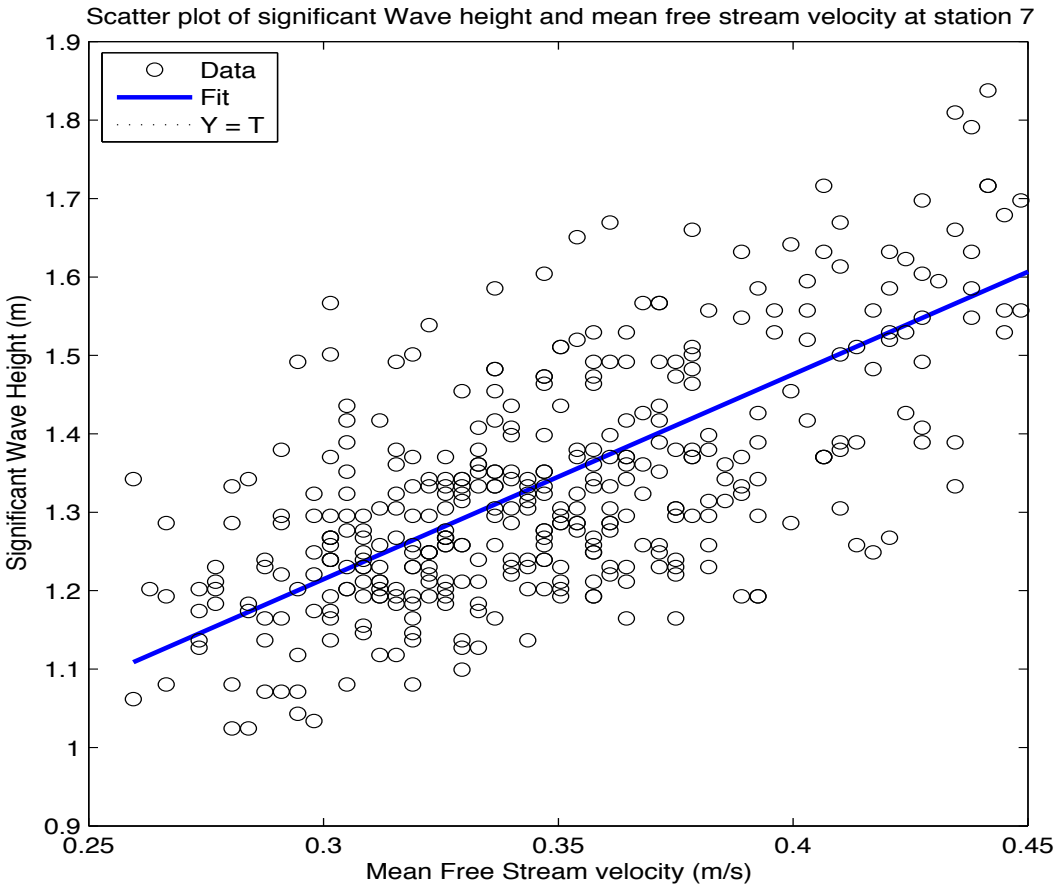

Figure 34. Scatter plot of offshore significant wave height and mean free stream velocity at station 7. Both output variables were from a one-year model run. The blue line is a regression line. Y = T is a dotted line fit underlain in the main blue line fit.

The scatter plot of these two variables for station 1 is also shown in figure 35.

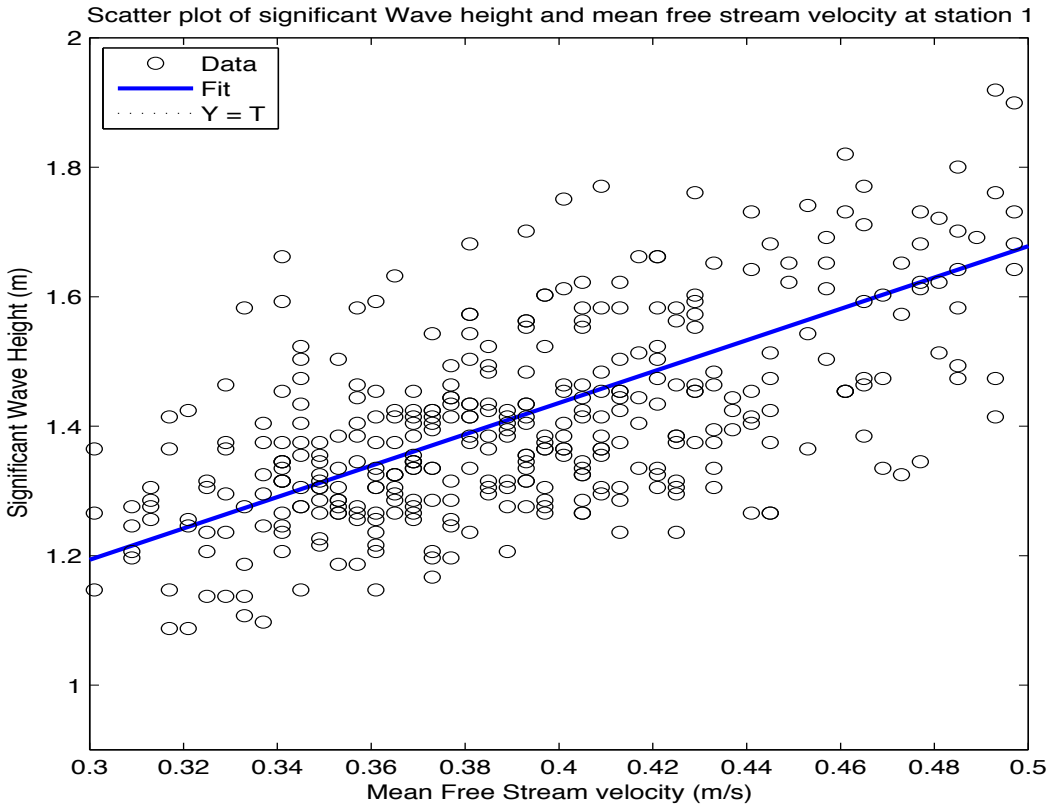

Figure 35. Scatter plot of offshore significant wave height and mean free stream velocity at station 1. Both output variables were from a one-year model run. The blue line is a regression line. Y = T is a dotted line fit underlain in the main blue line fit.

Figure 36 shows the mean slope of all ten stations and their error bars for the comparison of significant wave height versus mean free stream velocities. The figure indicates that stations 4, 5, and 6 mean slopes are significantly different from stations 7, 8, and 9 mean slopes. Stations 4, 5, and 6 are located near Ibaka bay while stations 7, 8, and 9 are further away from Ibaka bay in the study domain.

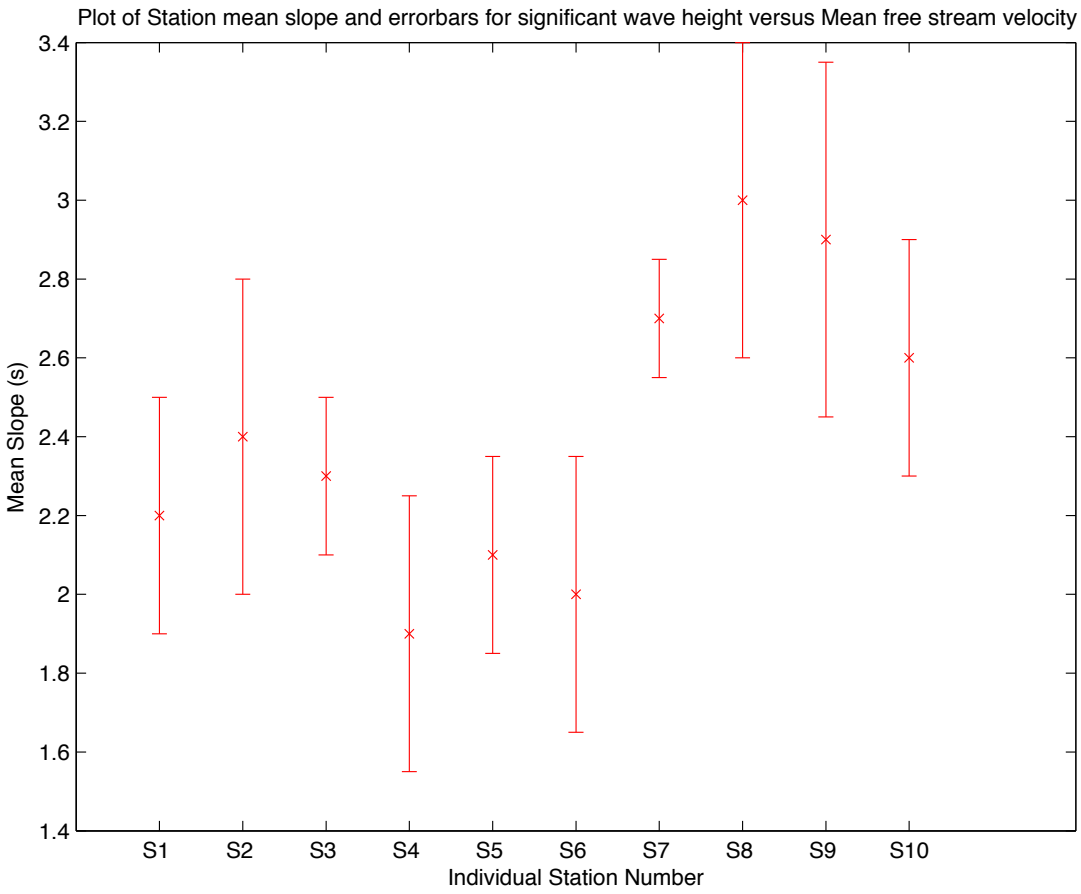

Figure 36. Graph of each individual station mean slope with error bars for comparison of significant wave height versus mean free stream velocity. S in the x-axis stands for station.

Figure 37 illustrates the correlation between significant wave height and seabed level change over a period of one year at station 1. There is a strong positive correlation (r = 0.73) between significant wave heights greater than 1.0 m and the seabed changes. A look at this scatter diagram indicates that there is more than a single dominant process that accounts for the observed variation. The two visible processes are likely due to the seasonal (dry and rainy seasons) variations in the forcing functions (as shown in the next chapter). Also, a residual plot (not shown here) of the data indicated a bimodal distribution.

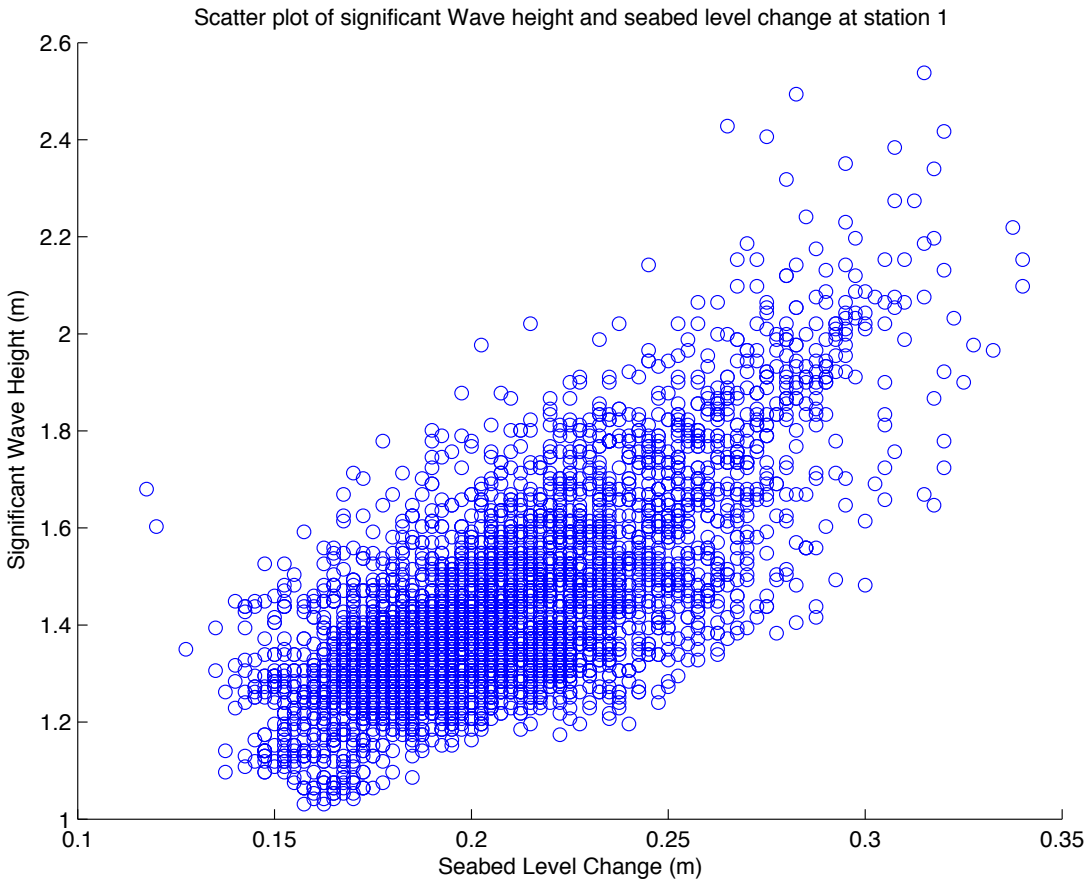

Figure 37. Scatter plot showing the correlation between significant wave height and seabed level change at station 1. Both outputs plotted here were from a one-year simulation run.

Other stations (not shown) had similar scatter diagrams for the significant wave height versus seabed level change comparison as that of station 1. The stations mean slopes were slightly different from one another but the error bars overlapped similar to figure 36 above.

CHAPTER VI

DISCUSSIONS

This chapter is devoted to discuss some results presented in the previous chapters and the major findings of this dissertation. First, we will present graphical evidence of why NearCoM-TVD (with some modifications to the original codes) could be used to predict circulation and sediment processes in Ibaka bay and the Cross River Estuary, with some level of confidence. Secondly, we will dwell on the sediment processes: its general importance and how sediment processes investigations have contributed to actualizing the objectives of this study. More specifically, what new knowledge has this investigation brought to the shipping and scientific community? We will discuss sediment processes on the second part of our discussions as they relate to the following four areas: Environmental dredging, Navigation dredging, Coast/Shoreline protection, and sediment management and re-use.

To achieve the first goal, we have configured and run the model at time periods when data was sampled with current meters, RDI ADCP, wave staff, tide gauges, and anemometer near Ibaka bay. The measured time series were split into segments for this investigation. The first segment was used to initialize the model, while following segments served as calibration and model verification data. The two main data archives utilized for this part of the study were SIMORC and GLOSS. SIMORC contained quality controlled wave and current data while GLOSS has sea surface elevation data. SIMORC data used for this study were collected by TOTAL between April 2004 and February 2008 at Ekundu, Cameroon (Longitude 8.4182 E and Latitude 4.2735 N) in 24 meters water depth by subsurface moored current meters. There were some gaps in the time series data. These gaps were filled with appropriate interpolation techniques

available in Matlab. The physical oceanographic data sampled were wave height and period statistics as well as horizontal velocity and current direction in the water column. Figure 3 showed the bathymetric contours and the location of the sampling instruments (annotated as Ekundu). Figures 38 and 39 show the raw current speed, current direction, significant wave height and mean wave period sampled every 10 minutes for half a year in Ekundu. These data were used to initialize and validate the wave and circulation models. Data for 2004 are plotted in figure 38 while 2005 data are plotted in figure 39.

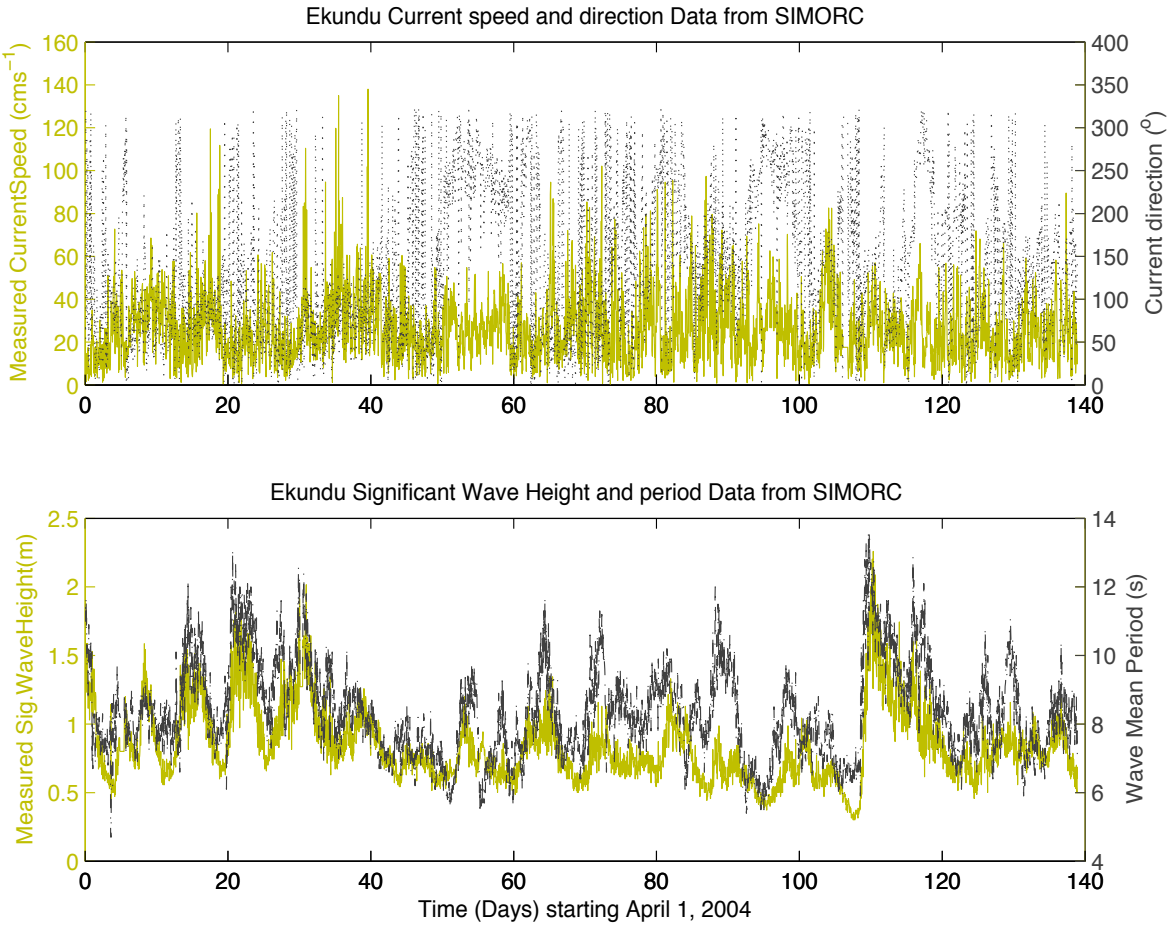

Figure 38. Raw current speed, current direction, significant wave height, and mean wave period sampled in Ekundu near Ibaka bay by TOTAL (courtesy: SIMORC)

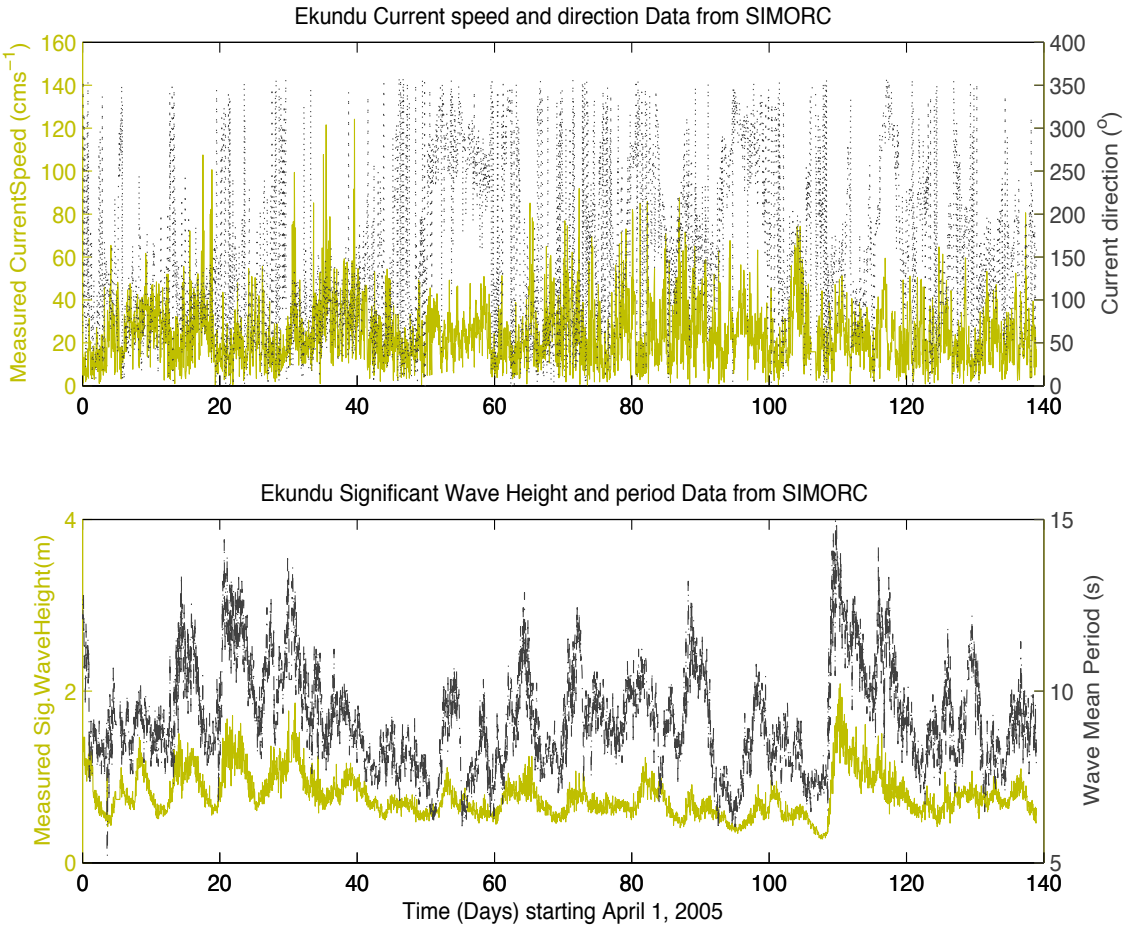

Figure 39. Ekundu current magnitude, current direction, significant wave height, and mean wave period data used for model verification.

Figure 40 shows model comparison with measured data in Ekundu. The measured significant wave height showed a very good agreement with model output. The coefficient of determination, r^2 was 0.91. The current speed was also modeled fairly well by the circulation model with r^2 of 0.87. Both the wave period and mean current direction (not shown) were verified with r^2 of 0.82 and 0.79 respectively. The available data was used to initialize and run

the model for different seasons of the year. The model reproduced the measured data quite well, without seasonal bias.

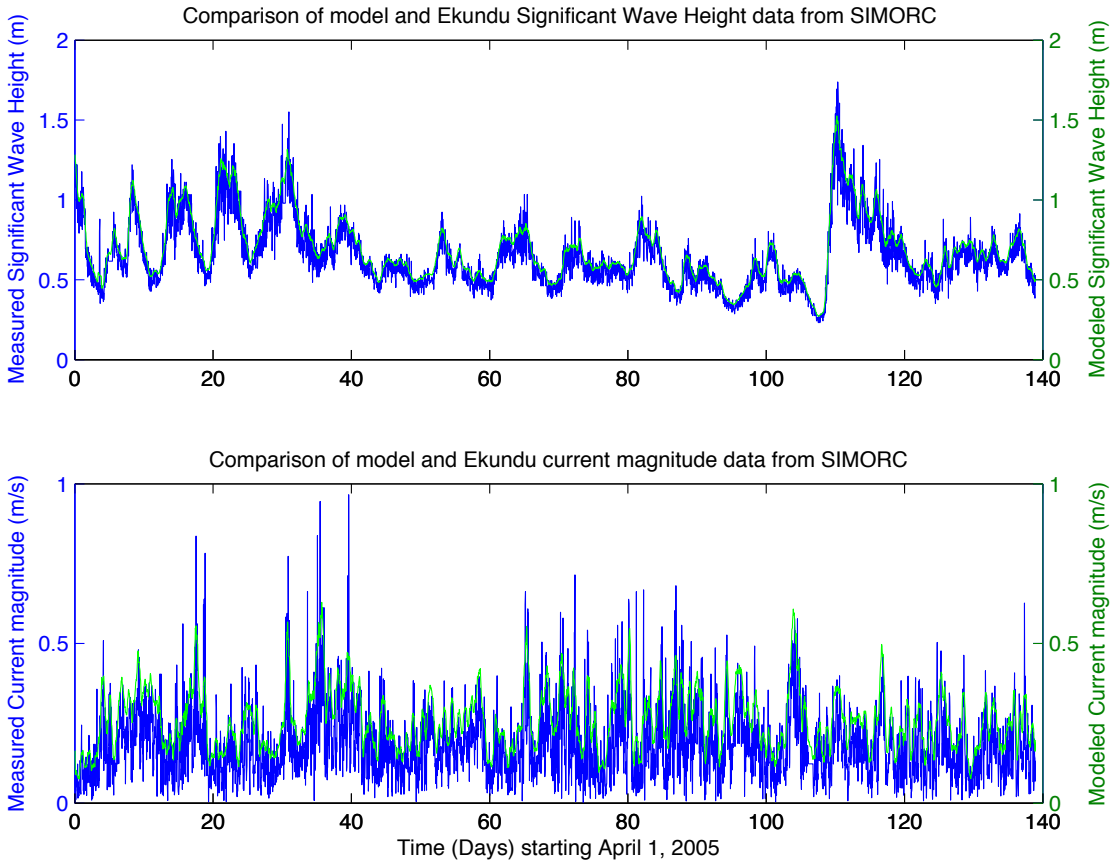

Figure 40. Modeled significant wave height, current speed, and Ekundu data comparison. Blue lines are the data while green lines are model output. Upper figure is the significant wave height; lower figure is the current magnitude. Model output is taken at a distance of 2 km North of the measurement station.

A larger curvilinear grid was designed to cover this station and model output taken out at a distance of 2 km north of the data sampling station. The data and the model output were plotted on the same graph axes for comparison as shown in figure 40 above for Ekundu for a

three-and-half-month period starting in April 1, 2005. Based on this high model skill (about 0.86 using wave height and current speed as the metrics), Ekundu data were used to initialize the coupled wave-circulation-sediment model and run for a one-year period, and then output were taken at five selected stations and plotted in figures 41 to 45 below. These five stations were spread over the entire study region. These five stations in the study region could account for about 90 % of variance in parameters of interest. The black dash dot lines are SIMORC data.

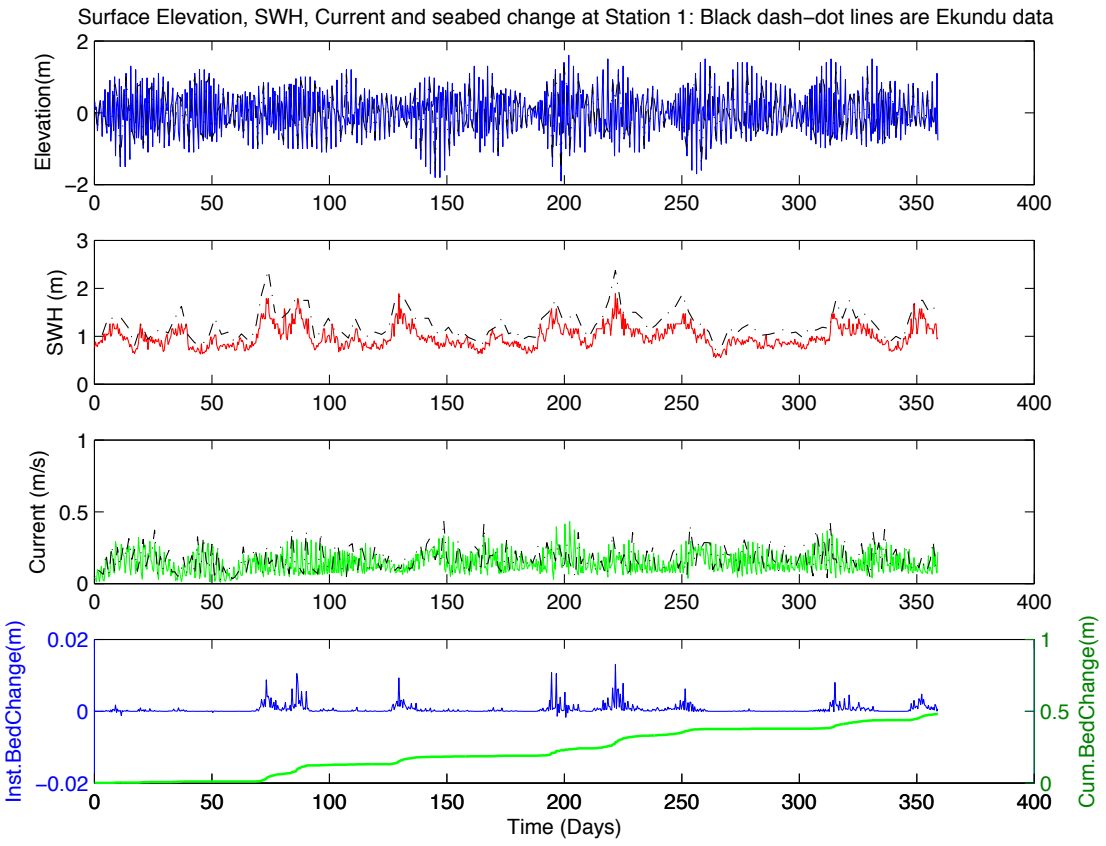

Figure 41. Comparison of SIMORC measured data and model output for station 1. A one-year (starting January 1, 2006) bed level change (≈0.5 m) is also shown. SWH stands for significant wave height. The black dash-dot line is Ekundu data from SIMORC archive. A morphology factor of four was specified for these simulations. Note the scale changes on the graph for the different stations.

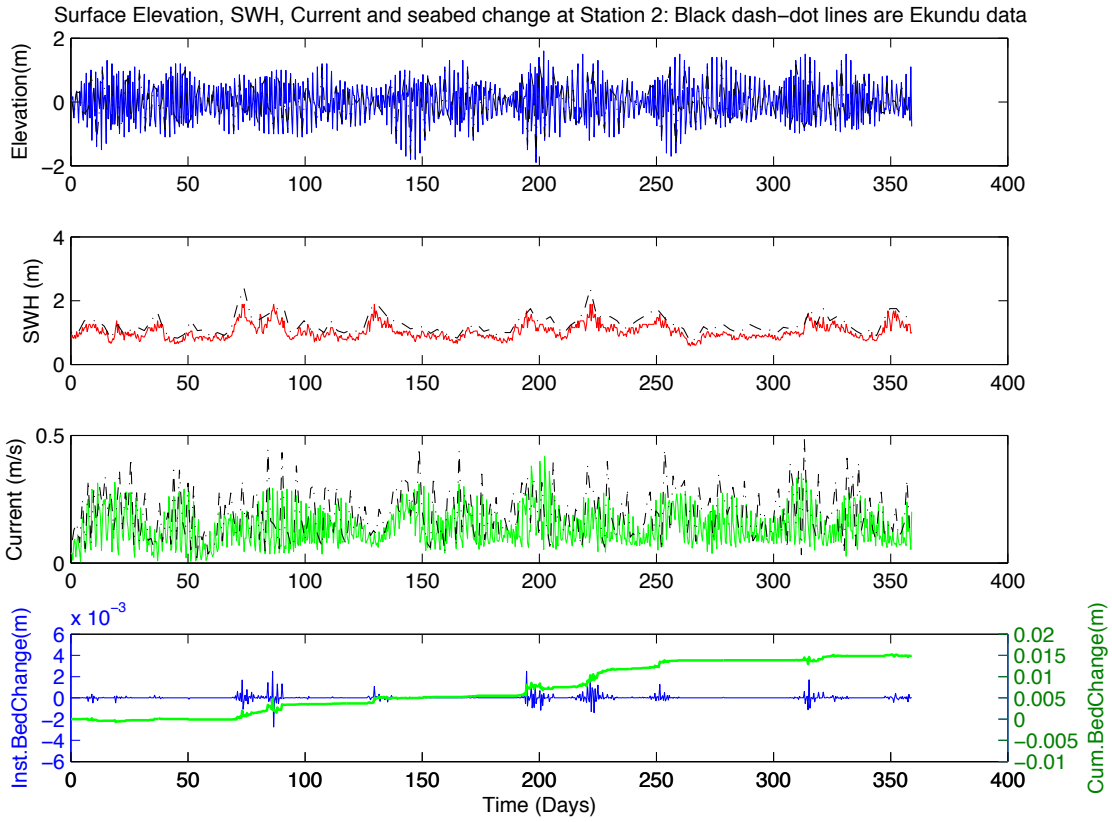

Figure 42. Comparison of SIMORC measured data and model output for station 2. A one-year (starting January 1, 2006) bed level change (≈0.015 m) is also shown. SWH stands for significant wave height. The black dash-dot line is Ekundu data from SIMORC archive. A morphology factor of four was specified for these simulations. Note the scale changes on the graph for the different stations.

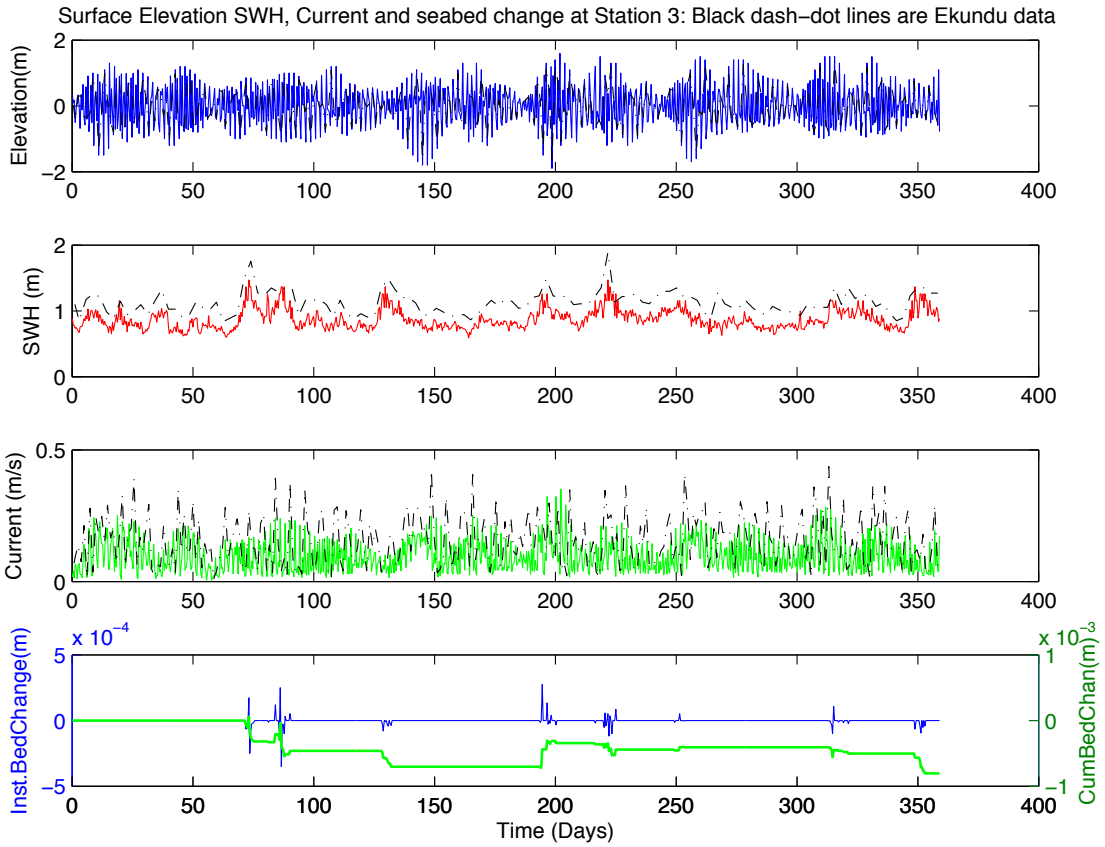

Figure 43. Comparison of SIMORC measured data and model output for station 3. A one-year (starting January 1, 2006) bed level change (≈ -0.001 m) is also shown. The black dash-dot line is Ekundu data from SIMORC archive. A morphology factor of four was specified for these simulations. Note the scale changes on the graph for the different stations.

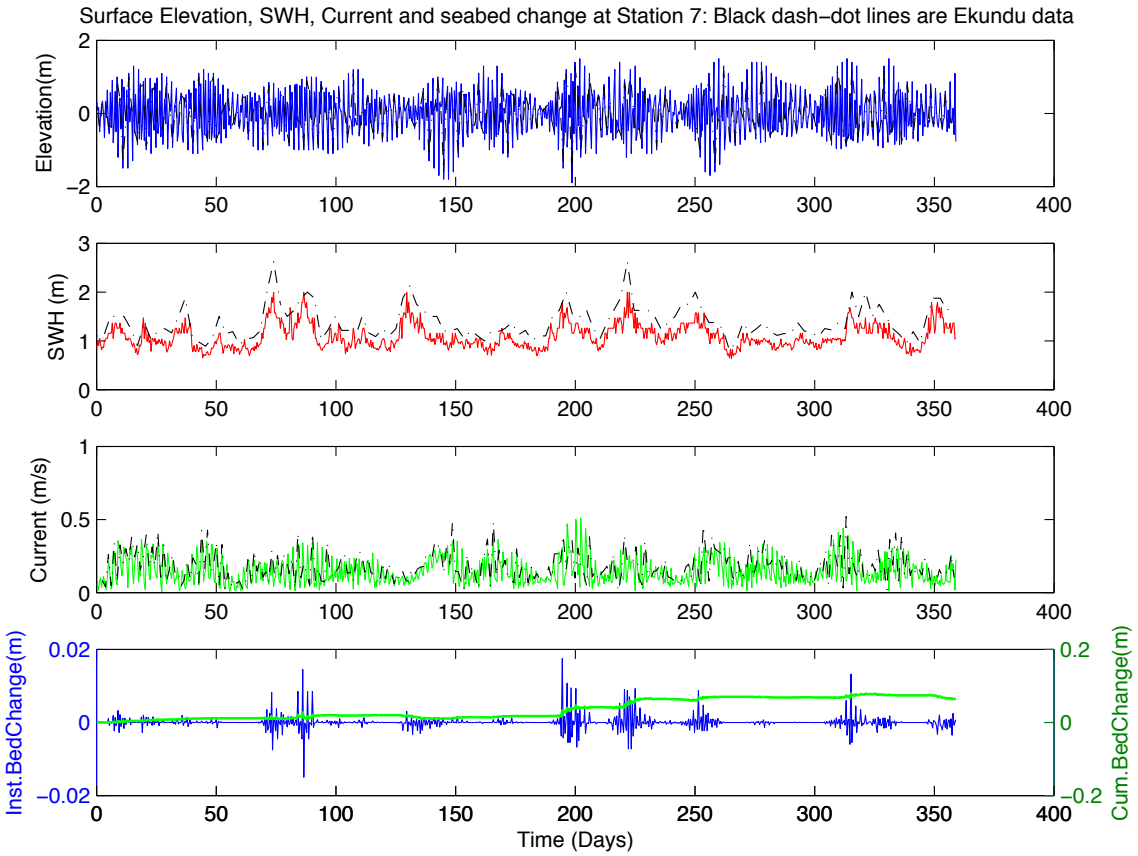

Figure 44. Comparison of SIMORC measured data and model output for station 7. A one-year (starting January 1, 2006) bed level change (≈0.2 m) is also shown. The black dash-dot line is Ekundu data from SIMORC archive. A morphology factor of four was specified for these simulations. Note the scale changes on the graph for the different stations.

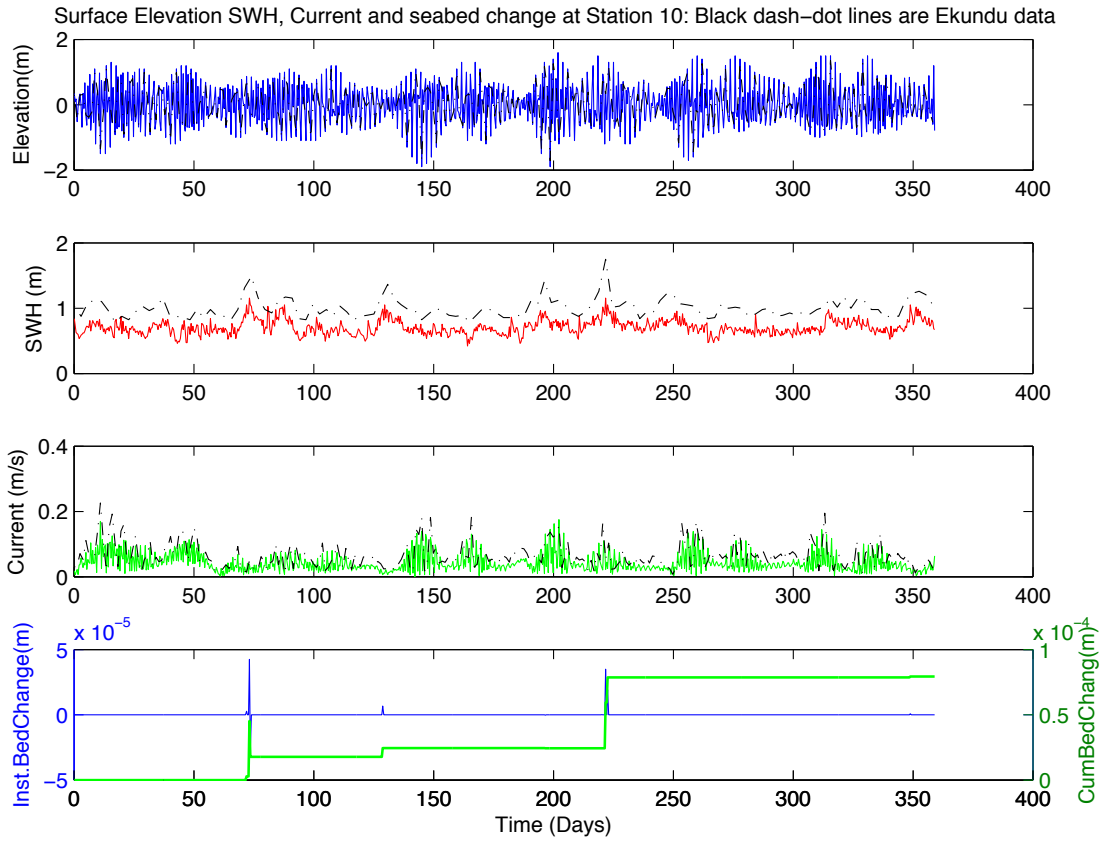

Figure 45. Comparison of SIMORC measured data and model output for station 10. A one-year (starting January 1, 2006) bed level change (≈0.0003 m) is also shown. The black dash-dot line is Ekundu data from SIMORC archive. A morphology factor of four was specified for these simulations. Note the scale changes on the graph for the different stations.

Using data from Ekundu (a data sampling station near Ibaka bay), we examined the seasonal variations of wave heights. The four-year wave data (April 2004 to February 2008) were split into quarterly segments (January to March, April to June, July to September, and October to December). Mean and standard deviation of these quarterly segments of the significant wave height data were found as plotted in figure 46 below. Based on our earlier findings (wave height > 1.0 meter required to initiate sediment transport in most areas of the

study domain), it can be inferred from figure 46 that most sediment transport and seabed changes in Ibaka bay occur during the rainy season (April to October).

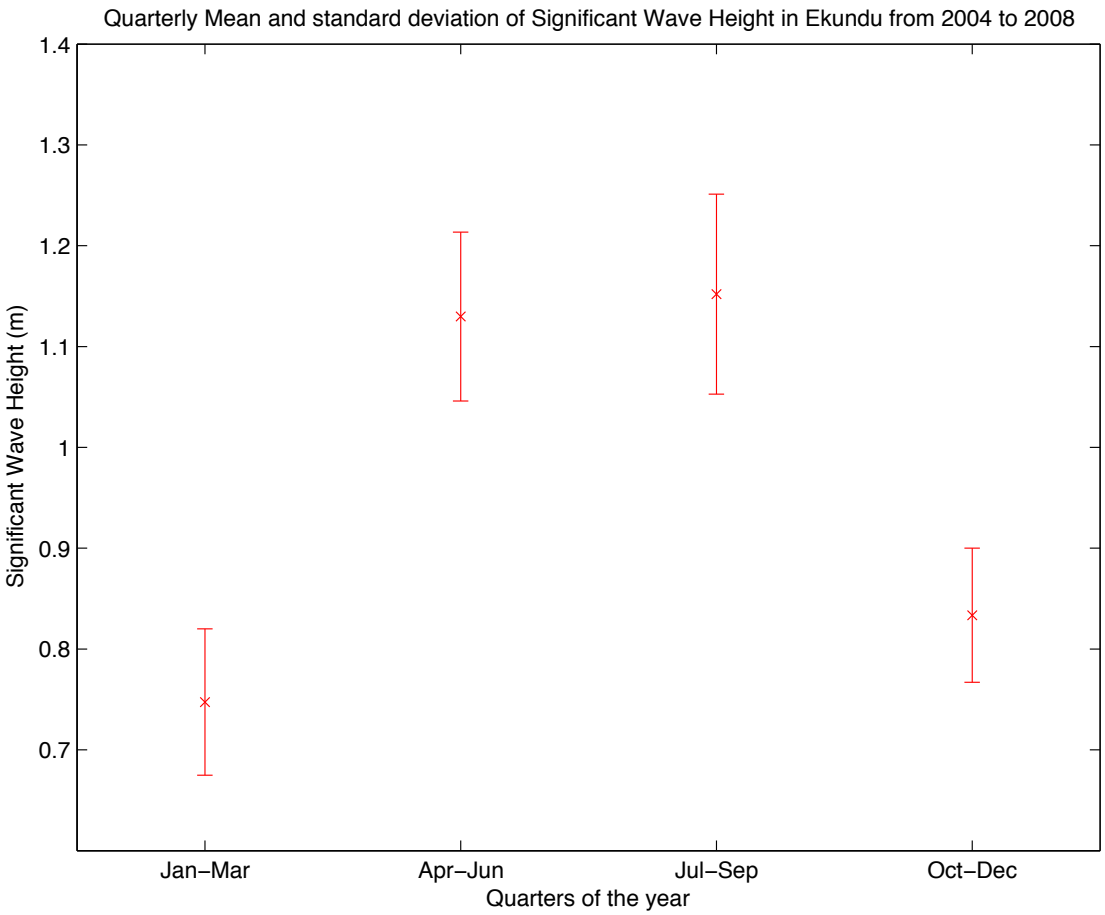

Figure 46. Quarterly mean and standard deviation of Significant wave height in Ekundu near Ibaka for 2004 to 2008. (Courtesy: TOTAL and SIMORC). Error bars indicate two standard deviations

The error bars in figure 46 show that January to March significant wave heights are very different from the wave heights arriving the bay during the rainy season. The red stars indicate the mean values while the bars indicate two standard deviations (equivalent to 95% confidence

interval). A typical wave height of 0.75 meters arrives the bay during the dry season (November to March) while a typical wave height of 1.05 meters is found during the rainy season. Although we have found that wave-current interactions sometimes increases significant wave heights if the current and wave oppose each other, such modification never exceeded 15% of the wave height in this study. Even with a more conservative 20% significant wave height increase due to wave-current interactions and other non-linear interactions, the dry season wave heights will never reach 1.0 m high. Thus, NearCoM-TVD model could be run for the rainy season alone, with an appropriate morphology factor, to estimate long-term sediment processes with a high confidence. This result will be very useful when we try to estimate maintenance dredging time windows for the bay. A similar analysis was done for the measured current as shown in figure 47. The dry season could not generate the calculated mean free stream velocity of 25.1 cm/s for initiation of sediment transport. The rainy season currents exceeded this threshold value most of the time. The four-year average value for the rainy season current magnitude in Ekundu is 28 cm/s while the typical value for the dry season current is 20 cm/s.

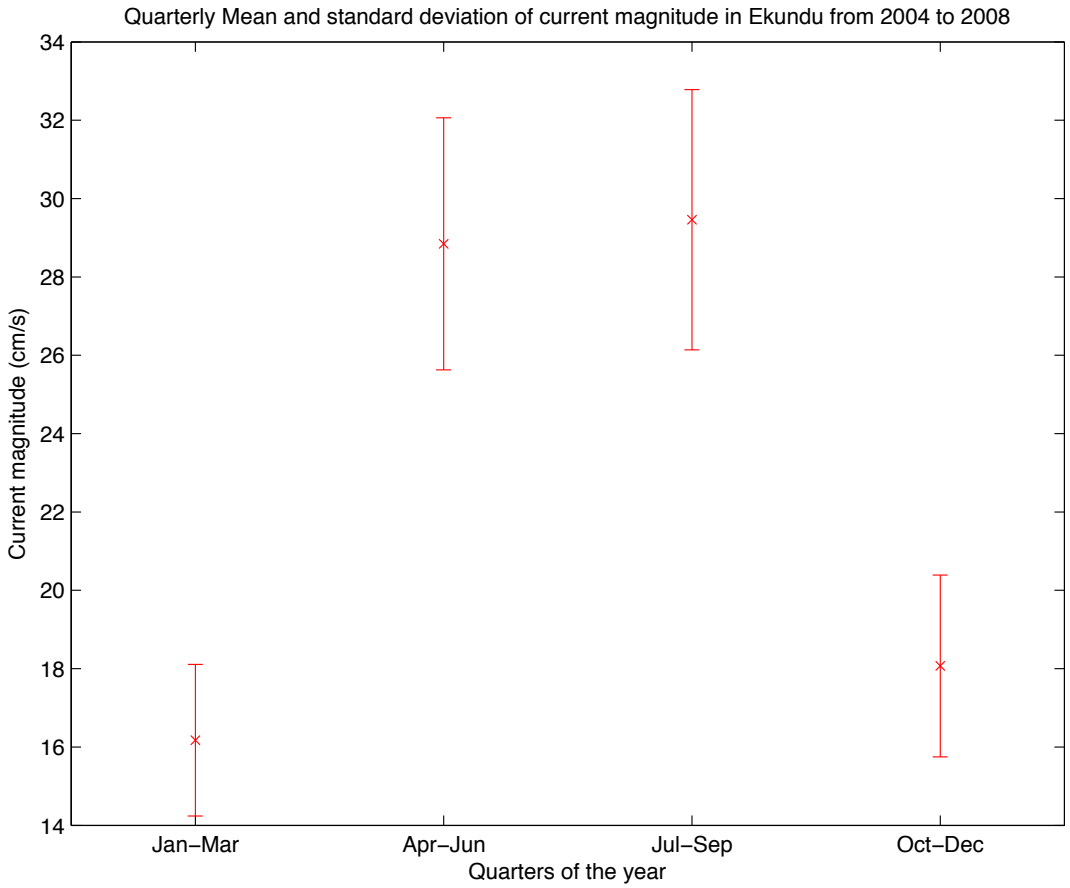

Figure 47. Quarterly mean and standard deviation of current magnitude in Ekundu near Ibaka for 2004 to 2008. (Courtesy: TOTAL and SIMORC). Error bars indicate two standard deviations.

In order to verify if the model could faithfully simulate this seasonal variations in significant wave heights and current speeds, we initialized the model and run for the four-year period (2004 to 2008). The model output results at station 1 were averaged quarterly and plotted along with the data as shown in figure 48 for the significant wave height. Ekundu data is represented with red line and star while blue line and diamond depict station 1 model output. A similar result was obtained for the current speed at station 1 and shown in Figure 49.

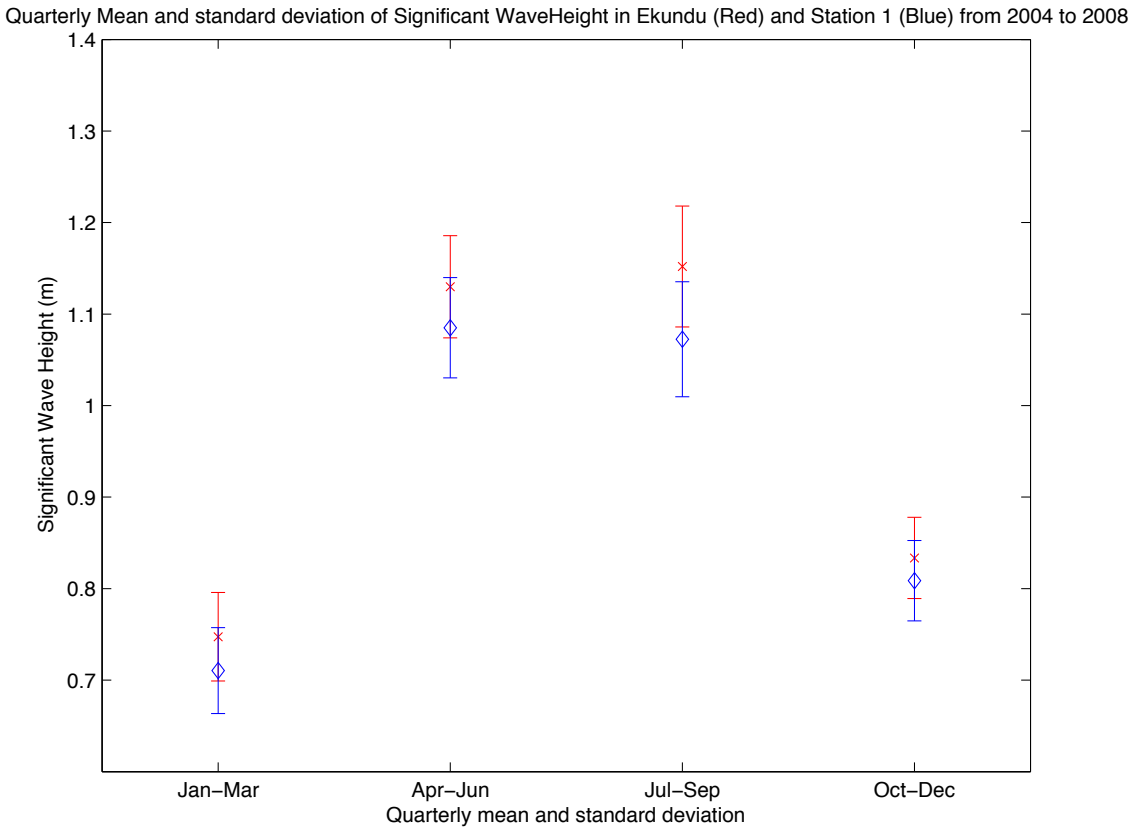

Figure 48. Comparison of quarterly mean and standard deviation of significant wave height in Ekundu (Red with star) and Station 1 model output (Blue diamond). The averaging is for the four-year period (2004-2008) when the data were collected by TOTAL. Error bars indicate two standard deviations.

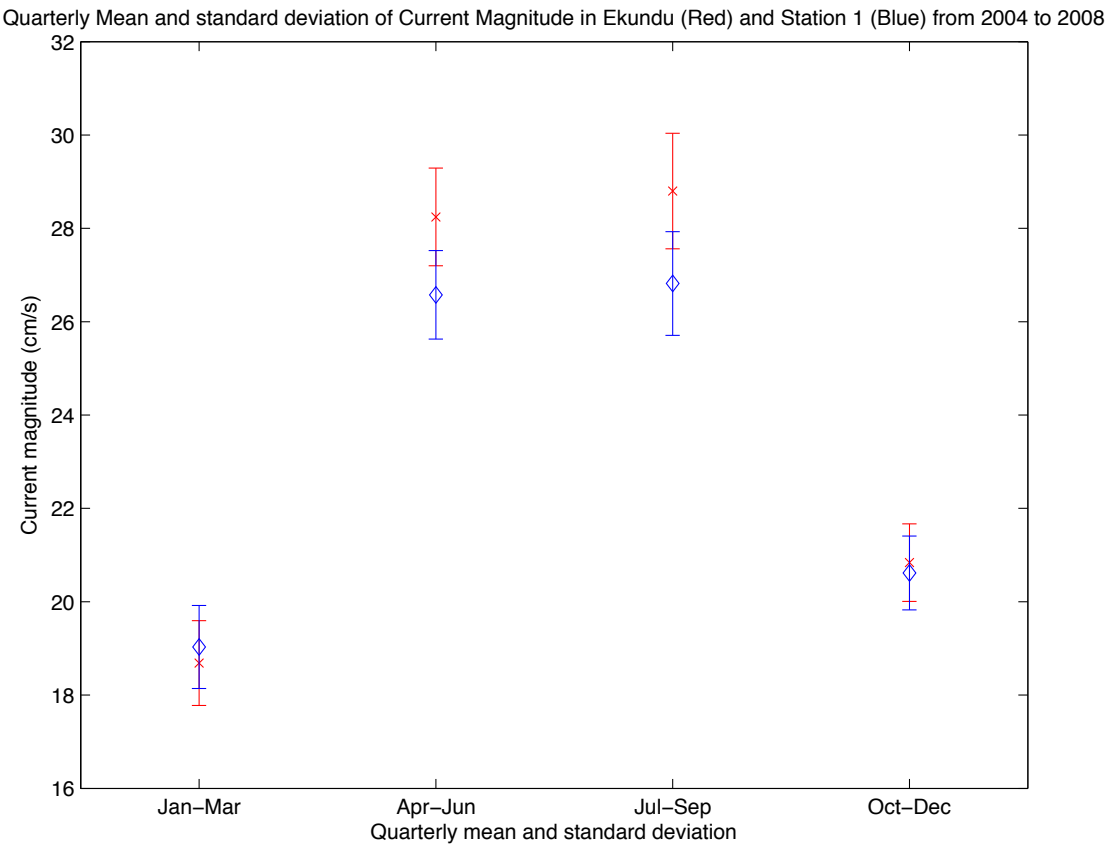

Figure 49. Comparison of quarterly mean and standard deviation of current in Ekundu (Red with star) and Station 1 model output (Blue with diamond). The averaging is for the four-year period (2004-2008) when the data were collected by TOTAL. Error bars indicate two standard deviations.

To further investigate if these quarterly averaged significant wave heights are significantly different from one another, Analysis of Variance (ANOVA) was run on the data. The statistical results using ANOVA2 function in Matlab are presented in Tables 1 and 2 for the measured and modeled data respectively. Anova2 evaluates the null hypothesis that columns, rows, and interaction effects of the given data are all the same. Here, the columns are the different quarters of the year; the rows are the sampled data for each quarter. The results, as

indicated in the Prob>F columns (p-values = 0), show that at least one quarterly mean of both the measured and modeled data is significantly different in a statistical sense. A small p-value (close to zero) is strong evidence against the null hypothesis. This analysis uses the default alpha value of 0.05 which is acceptable in most engineering applications. The choice of alpha value guides the rejection or failure to reject the null hypothesis.

Table 1. Analysis of Variance (ANOVA) for Ekundu wave height quarterly averaged data. (Columns indicate the four different quarters of the year while rows are data points within each quarter). The ANOVA table is a direct MATLAB output table.

ANOVA Table

Source	SS	df	MS	F	Prob>F
Columns	1.06881e+06	3	356269.5	2005.31	0
Rows	2.04636e+06	12959	157.9	0.89	1
Error	6.90702e+06	38877	177.7		
Total	1.00222e+07	51839			

Table 2. Analysis of Variance (ANOVA) for station 1 modeled significant wave height quarterly averaged output. (Columns indicate the four different quarters of the year while rows are data points within each quarter). The ANOVA table is a direct MATLAB output table.

ANOVA Table

Source	SS	df	MS	F	Prob>F
Columns	1.05351e+06	3	351168.8	1615.31	0
Rows	2.49737e+06	12959	192.7	0.89	1
Error	8.45189e+06	38877	217.4		
Total	1.20028e+07	51839			

In the ANOVA tables, the first column (Source) indicates the source of variability (The sources in this analysis are quarterly data segments (Columns) and the number of data points in each quarter (Rows)). The second column (SS) is the sum of squares due to each source. The third column is the degrees of freedom (df). The fourth column is the mean squares (MS) calculated as the ratio of SS to df. The fifth column indicates the F statistics (F). The last column is the calculated p-value.

Since the main goal of this study is to examine what happens at the seabed over some specified period of time, it is pertinent to also run ANOVA for the quarterly seabed level change output from the model. The result for the quarterly seabed level change at station 1 is shown in table 3 below. Again, we obtain zero p-value for the columns. This indicates that at least one of the quarterly bed level changes is significantly different from the rest in a statistical sense.

Table 3. Analysis of Variance (ANOVA) for station 1 modeled seabed level change quarterly averaged output. (Columns indicate the four different quarters of the year while rows are data points within each quarter). The ANOVA table is a direct MATLAB output table.

ANOVA Table

Source	SS	df	MS	F	Prob>F
Columns	7.99418e-14	4	1.99854e-14	156.1	0
Rows	1.11557e-12	8733	1.27741e-16	1	0.5514
Error	4.47228e-12	34932	1.28028e-16		
Total	5.66779e-12	43669			

A similar statistically significant result was found for the wave force (gradient of radiation stress) output from the model. The quarterly variance of the output of wave force is shown in table 4 below.

Table 4. Analysis of Variance (ANOVA) for station 1 modeled wave force quarterly averaged output. (Columns indicate the four different quarters of the year while rows are data points within each quarter). The ANOVA table is a direct MATLAB output table.

ANOVA Table

Source	SS	df	MS	F	Prob>F
Columns	350.34	4	87.5849	8599.13	0
Rows	2321.67	8733	0.2659	26.1	0
Error	355.79	34932	0.0102		
Total	3027.81	43669			

At this point, all we can infer from the ANOVA test is that at least one of the quarterly data is significantly different from the others. We cannot tell which of the quarterly data are different or same. We perform a further statistical test to determine which pairs of these quarterly data are significantly different. The Matlab multi comparison function (multcompare) was employed in the following tests. The input to multcompare function is the statistics structure of the data generated during ANOVA test. Figure 50 illustrates the multi comparison statistical analysis conducted on the measured current speed in Ekundu. The Matlab graphical user interface that was used to generate these graphs makes provision for clicking each of the tested groups of data to see if they are significantly different from others. The default plotting color is red for all the group means. The color changes to blue for any of the quarterly group that was clicked.

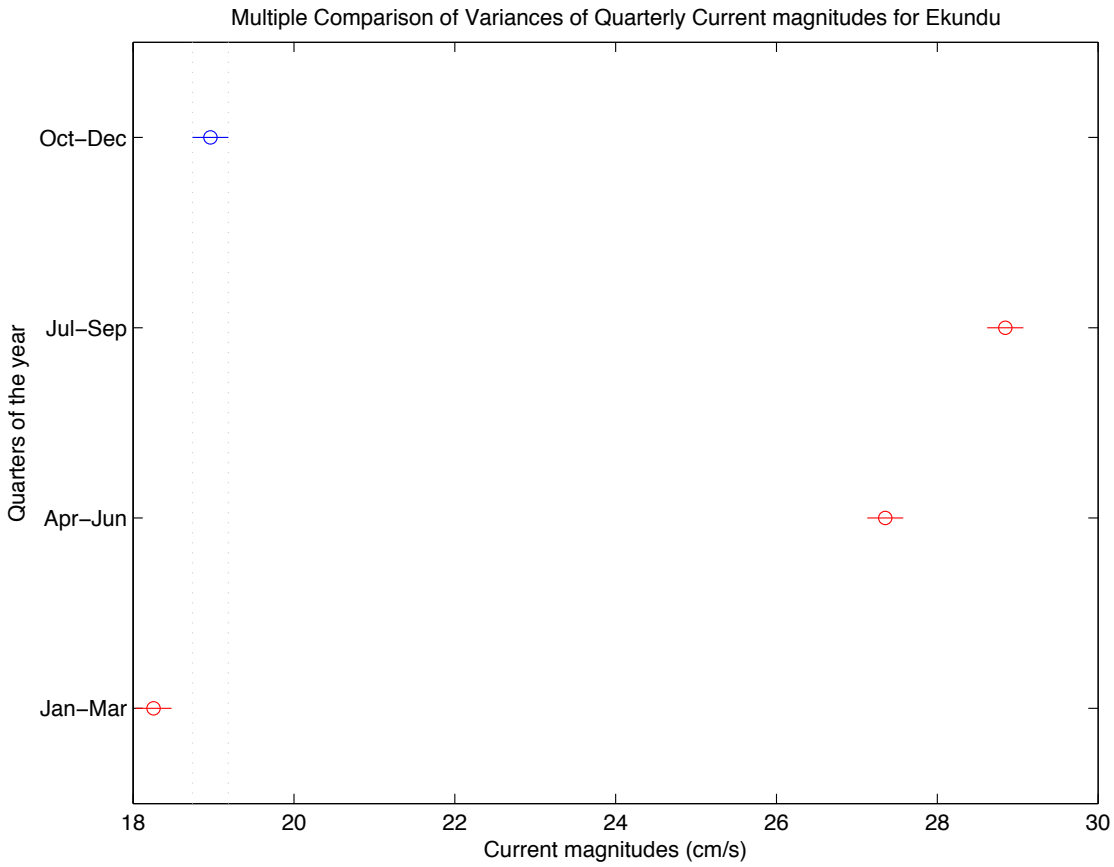

Figure 50. Multiple comparison tests for the means of the quarterly current magnitude data sampled in Ekundu between 2004 and 2008. Y-axis is the four quarters of the year while x-axis shows current values. Quarters 1 and 4 (January to March and October to December) represent the dry season while quarters 2 and 3 (April to September) represent the rainy season. The blue color represents the particular quarter of the year that was compared at the time the output was taken out of MATLAB. Dash lines show two standard deviations from the mean of the quarter compared with others at this time.

Figure 51 illustrates a similar multi-comparison test as in figure 50 for the modeled current magnitude at station 1.

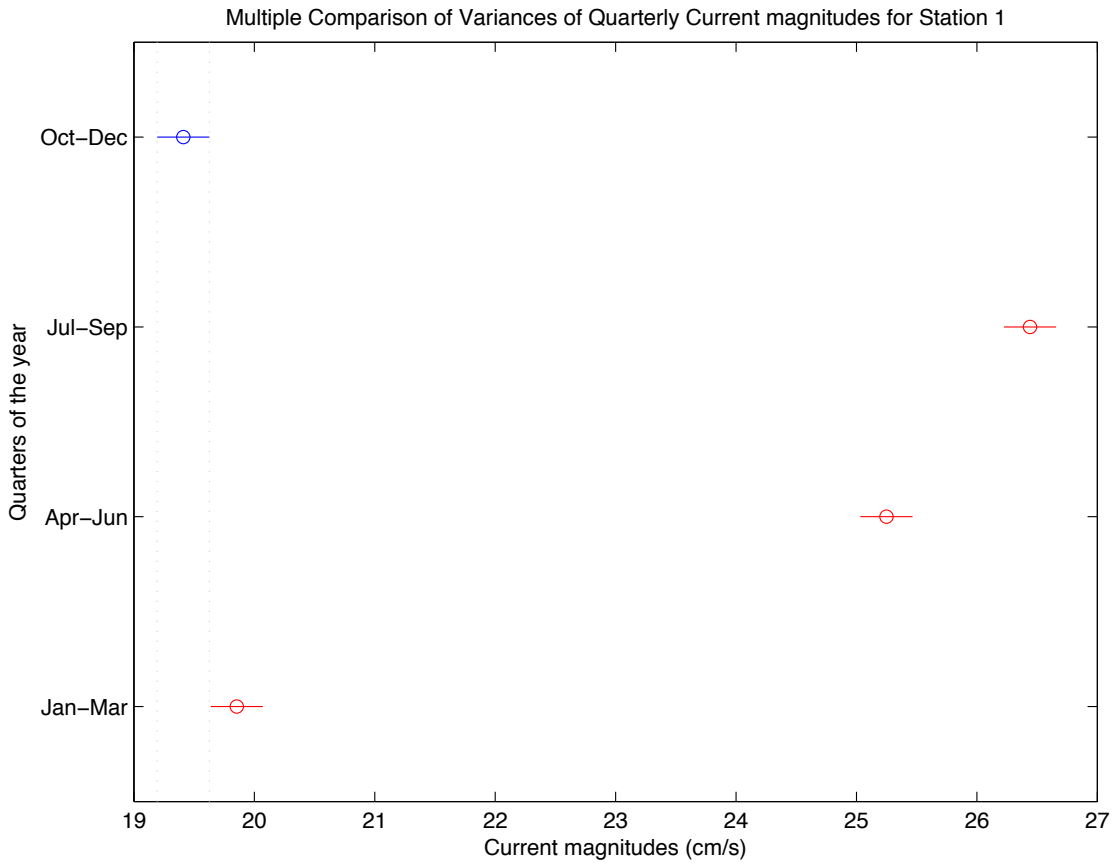

Figure 51. Multiple comparison tests for the means of the quarterly modeled current magnitudes for Station 1 between 2004 and 2008. Y-axis is the four quarters of the year while åx-axis shows current values. Quarters 1 and 4 (January to March and October to December) represent the dry season while quarters 2 and 3 (April to September) represent the rainy season. The blue color represents the particular quarter of the year that was compared at the time the output was taken out of MATLAB. Dash lines show two standard deviations from the mean of the quarter compared with others at this time.

The multcompare function graph in figures 50 and 51 above show each quarterly group mean represented by a circular symbol and horizontal line interval around the symbol. This graph confirms that the quarterly means are all significantly different since none of their intervals overlap. Similar results were found for the quarterly significant wave heights as shown in figures 52 and 53 below for Ekundu data and station 1 model output respectively.

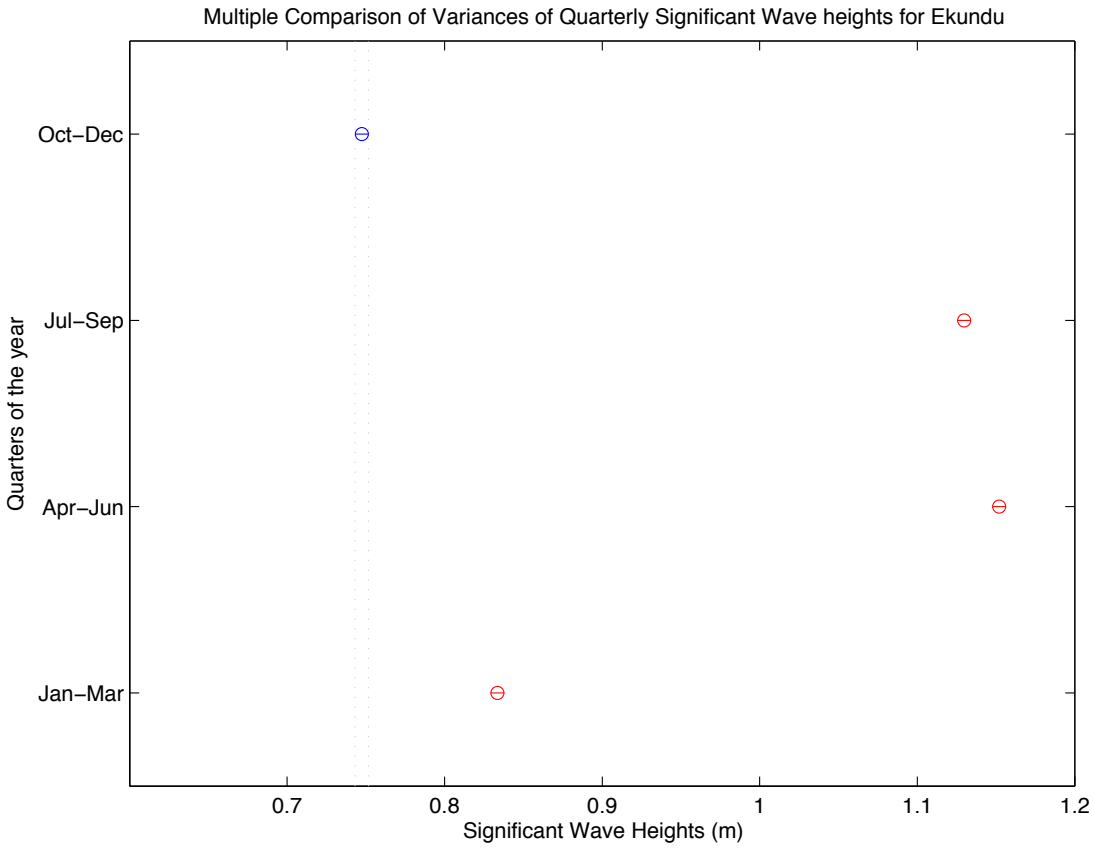

Figure 52. Multiple comparison tests for the means of the quarterly significant wave height data sampled in Ekundu between 2004 and 2008. Y-axis is the four quarters of the year while x-axis shows significant wave height values. Quarters 1 and 4 (January to March and October to December) represent the dry season while quarters 2 and 3 (April to September) represent the rainy season. The blue color represents the particular quarter of the year that was compared at the time the output was taken out of MATLAB. Dash lines show two standard deviations from the mean of the quarter compared with others at this time.

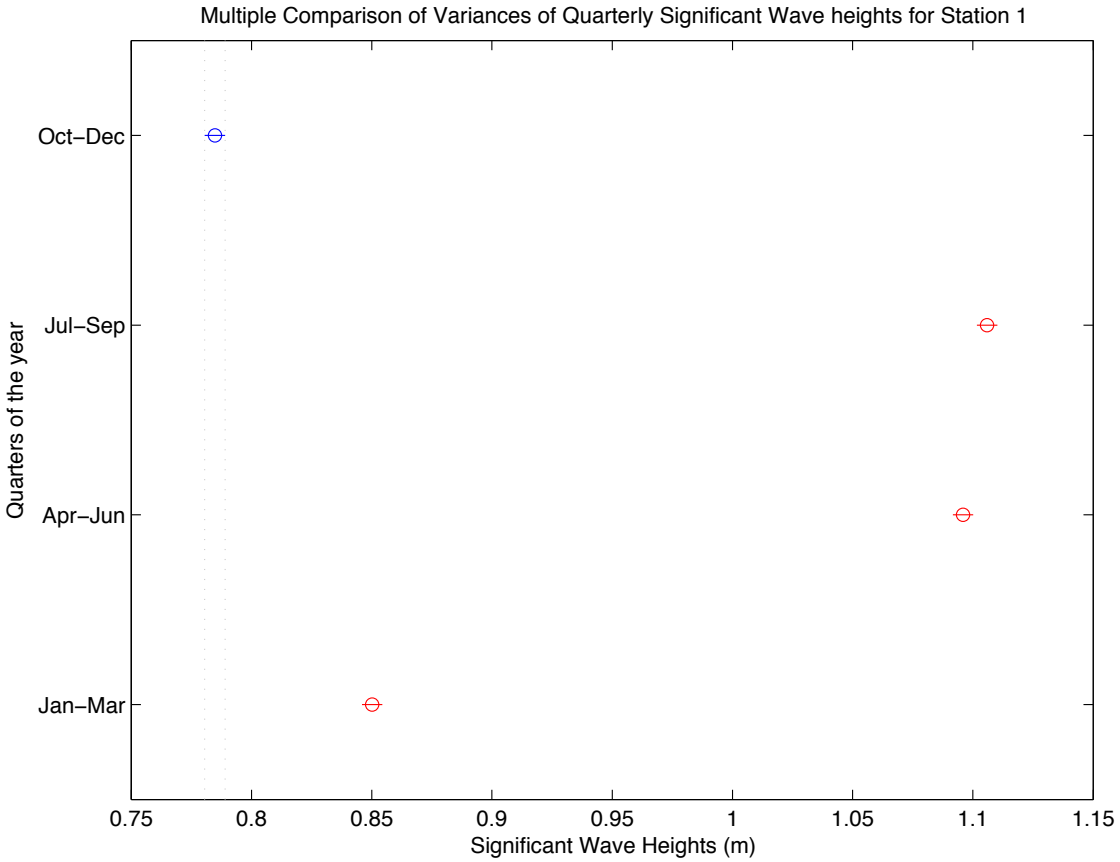

Figure 53. Multiple comparison tests for the means of the quarterly modeled significant wave height at station 1 between 2004 and 2008. Y-axis is the four quarters of the year while x-axis shows significant wave height values. Quarters 1 and 4 (January to March and October to December) represent the dry season while quarters 2 and 3 (April to September) represent the rainy season. The blue color represents the particular quarter of the year that was compared at the time the output was taken out of MATLAB. Dash lines show two standard deviations from the mean of the quarter compared with others at this time.

Before we end the discussion on ANOVA and multi comparison functions, we want to show statistically that the stations we took output from the model have different variations of the major parameters of interest in this study. Figure 54 illustrates the variance of model significant wave height from the five odd numbered stations. This multi comparison test result shows that each individual station's significant wave height is significantly different from the

other stations. Similar test results (not shown) were obtained for the current speed of the odd-numbered stations and also major model output variables for the even-numbered stations.

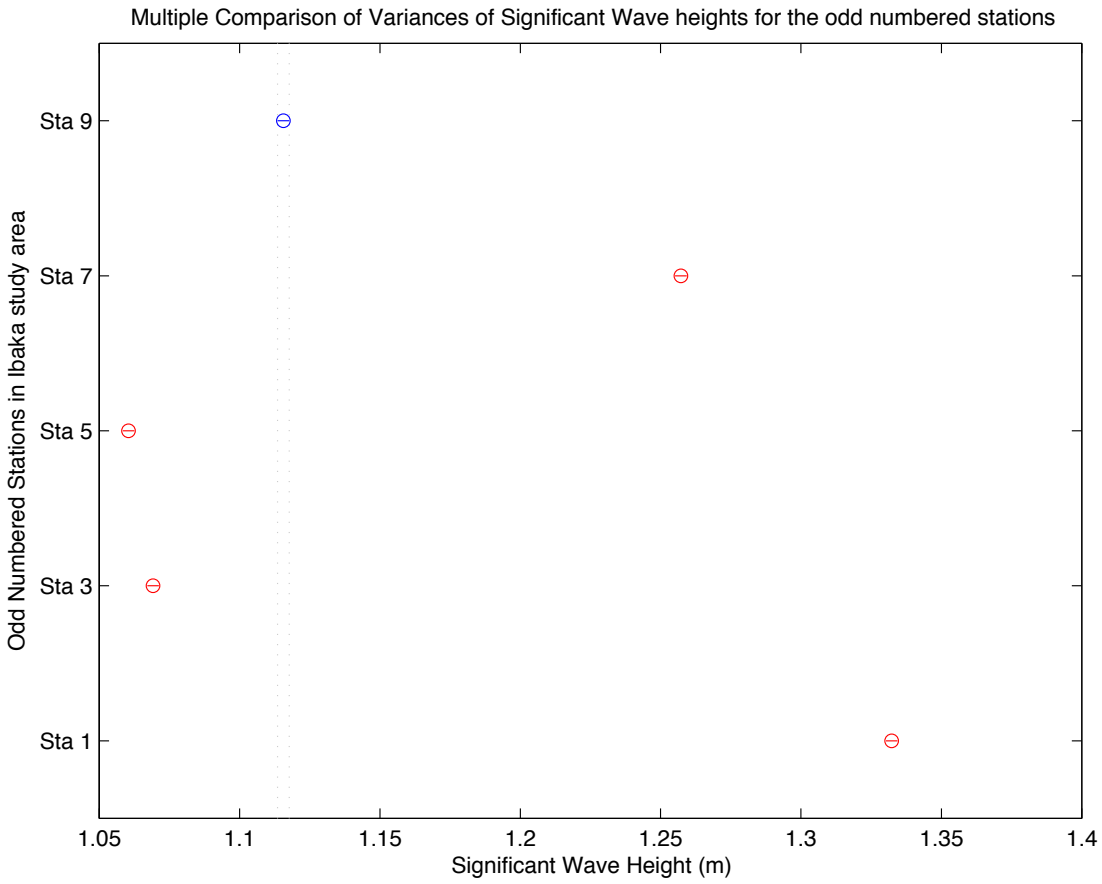

Figure 54. Multiple comparison tests to determine the statistical significance of the variances of the five odd-numbered stations' significant wave heights. The significant wave heights are averaged over one year. The blue color represents the particular model output station that was compared to the other stations at the time the output snapshot was taken from MATLAB. Dash lines show two standard deviations from the mean of the station output compared with others at this time.

Figure 55 shows the variances of cumulative seabed level changes for the five odd-numbered stations in Ibaka study area. In a statistical sense, these analyses illustrate that most individual stations model output differ significantly from the others.

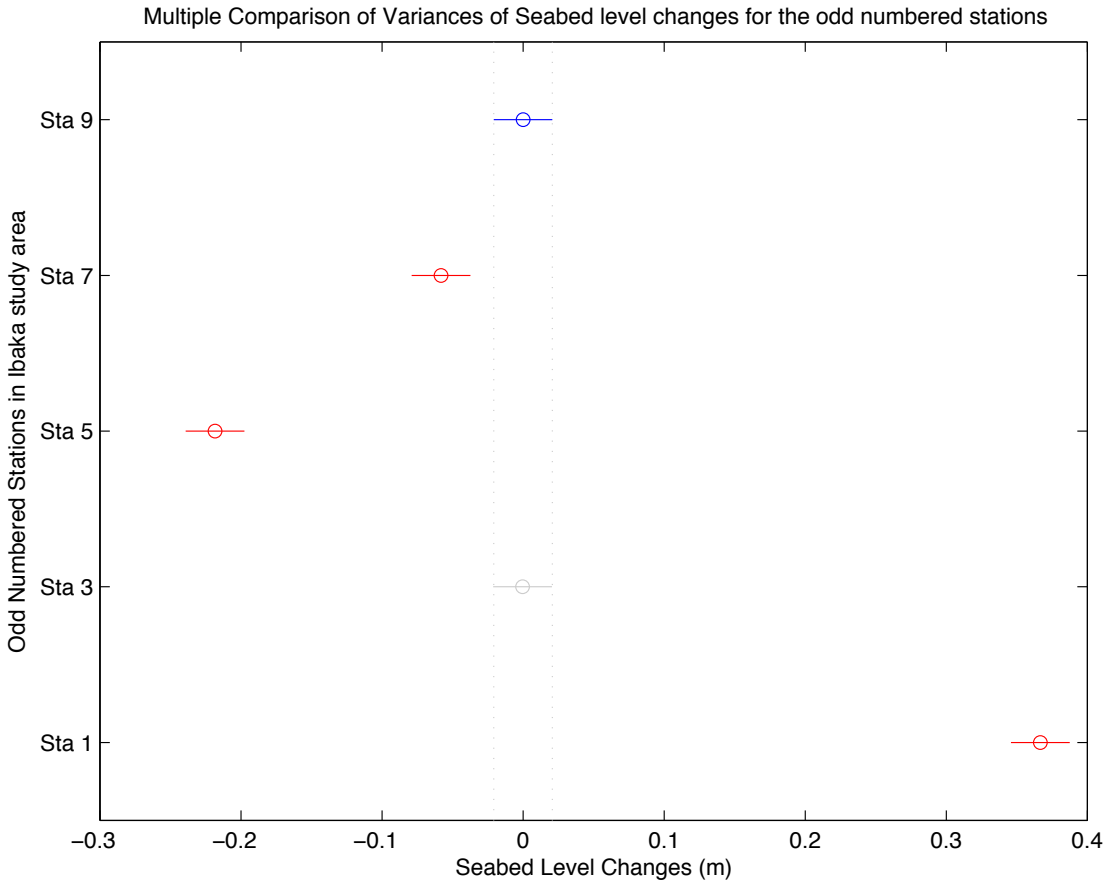

Figure 55. Multiple comparison tests to determine the statistical significance of the variances of the five odd-numbered stations' seabed level changes. The seabed level changes are one year cumulative. A morphology factor of 4 was specified for this run. The blue color represents the particular model output station that was compared to the other stations at the time the output snapshot was taken from MATLAB. Dash lines show two standard deviations from the mean of the station output compared with others at this time. Any station that is not statistically different from the selected station is dimmed out (gray color).

To further quantify the impact of wave action on sediment processes in Ibaka deep seaport domain, we examined the dissipation of offshore wave action in the bay. Two scenarios were studied: case one was without the channel while the second case had the channel dug. Figure 56 shows the map of total wave dissipation in the study area, when the channel had been dredged. The wave dissipation mechanisms considered here are bottom friction, depth-induced breaking, and white capping. This figure indicates that the presence of the ship channel enhances total wave dissipation, especially on the right flank of the channel. This focusing of dissipation on the right side of the channel can be attributed to the direction of wave propagation in the bay. The offshore wave propagates towards the north east of the domain. Dissipation decreases when the wave enters the deeper part of the channel. As the wave encounters a relatively shallower area on the sloping right flank of the channel, it feels the bottom and dissipation increases. It will be shown later that this increased dissipation results in bottom erosion.

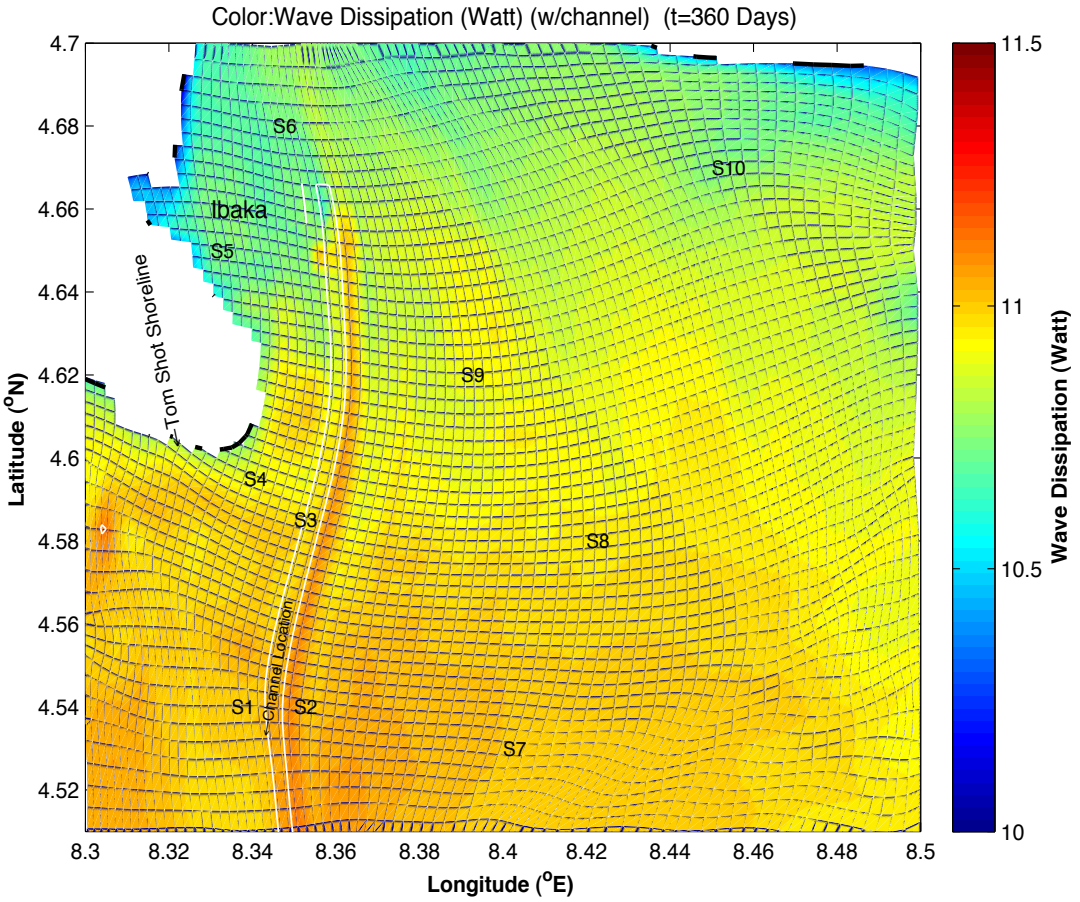

Figure 56. A map of wave dissipation in Ibaka bay study area. The white line depicts the deepest part of the dredged approach channel.

A difference map (with and without ship channel) of wave dissipation (not shown here) reveals that there is more dissipation of wave action when the channel is present; that is, the offshore wave energy is more dissipated when the channel is present than when the channel is absent in Ibaka deep seaport domain. Figures 57 and 58 show cross sectional graphs of wave energy that propagate from the offshore towards Ibaka bay. It is seen in these graphs that less wave action (more wave dissipation) reaches Ibaka bay when the channel is dredged.

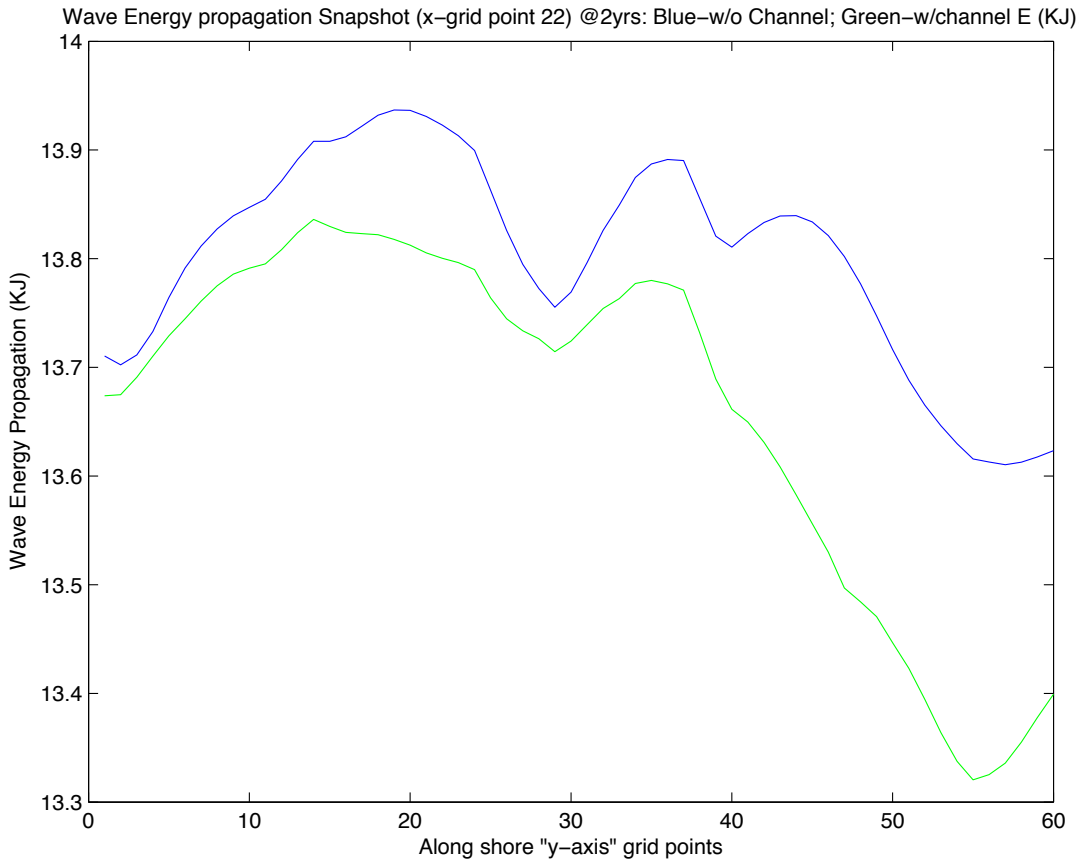

Figure 57. Cross sectional graph of wave energy propagation from offshore towards Ibaka bay at cross-shore grid point 22. Cross-shore grid point 22 is on the left flank of the channel. Blue line indicates energy propagation when there is no channel while green line represents energy propagation when the channel is dredged.

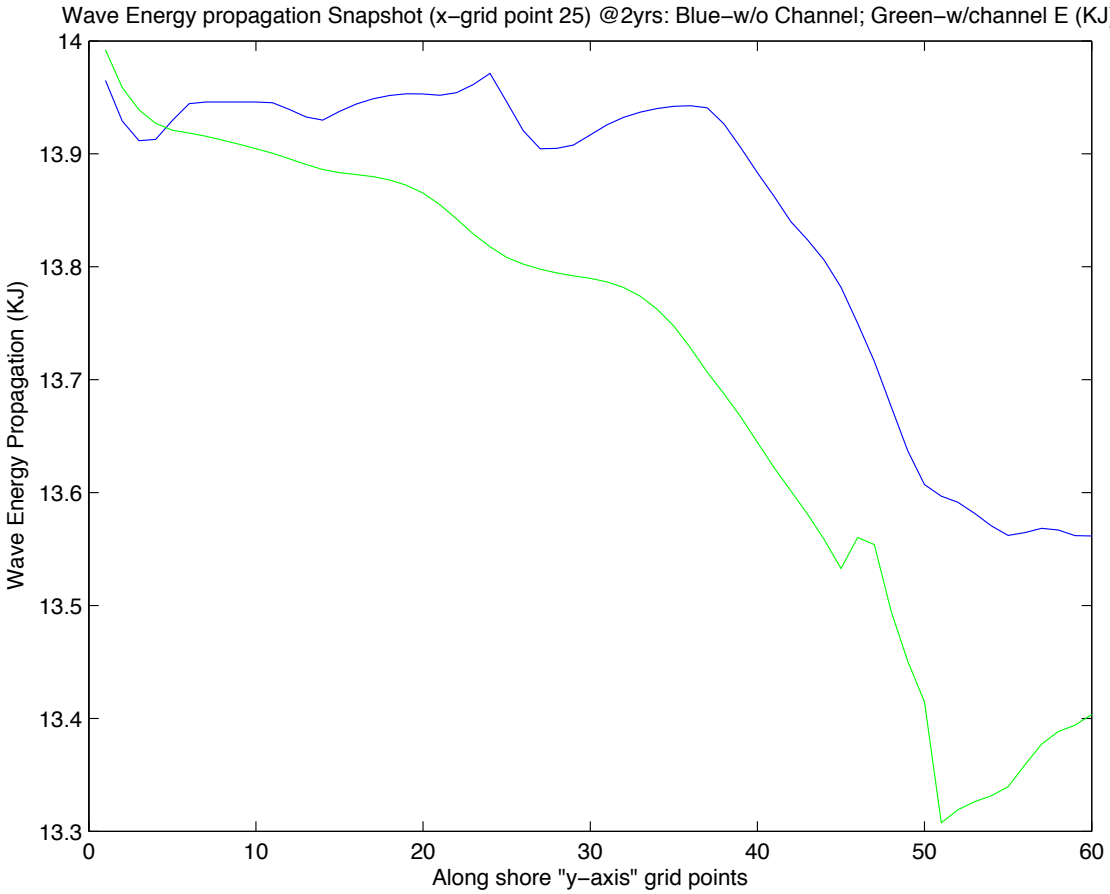

Figure 58. Cross sectional graph of wave energy propagation from offshore towards Ibaka bay at cross-shore grid point 25. Cross-shore grid point 25 is on the right flank of the channel. Blue line indicates energy propagation when there is no channel while green line represents energy propagation when the channel is dredged.

The effects of the ship channel on waves, circulation, and sediment processes were further investigated by looking at model parameters difference plots at some selected locations. Three model output parameters chosen for this investigation were current magnitudes, significant wave heights, and seabed level change. Difference is defined here as

model output without ship channel minus model output with ship channel. The difference result for stations 1 is shown in figure 59 below.

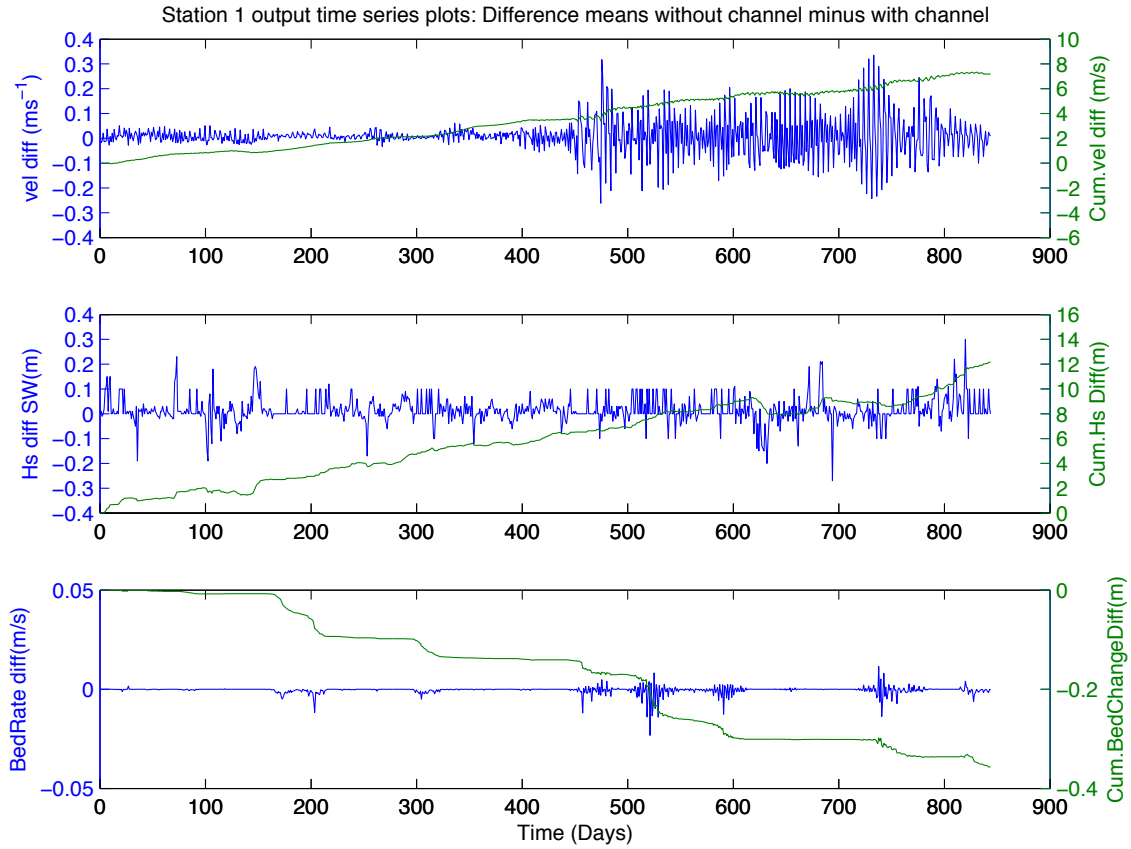

Figure 59. Plots of difference between model run without ship channel and model run with ship channel for current magnitude, significant wave height, and seabed level change at station 1. Difference is defined as output parameter obtained in a model run without ship channel minus the same output parameter in a model run with the dredged ship channel. Cumulative parameters shown on the right y-axis represent the total change in the parameter that could be observed over the time period of integration when the ship channel is dredged.

The time series graph in figure 56 clearly shows that the dredged ship channel is making a difference in the transformation of these model parameters. However, we are interested in

understanding what kind of difference the channel is making to the seabed: Is the dredging of the channel aiding erosion or accretion? Noting that station 1 is at the left side of the channel towards Tom Shot Island, previous results showed that both simulations without the channel and with the channel resulted in some accretion at that station. The cumulative seabed level change difference plot indicates that over the two-and-half year simulations (actually about 9 years because a morphology factor of 4 was specified for this run), there will be an additional sediment deposition of 0.4 meters when the ship channel is dredged. Remember that both individual run bed level changes give a positive number at this location. Mathematically, a small positive number minus a larger positive number gives a negative number. Having -0.4 meter as the difference value here means more accretion with the channel. By looking at the wave and current directional maps (wave directional map for the study area will be shown after these difference plots), we can infer that this extra sediment deposit will be transported towards Tom Shot Island and protect the island and the surrounding beach against erosion.

Figure 60 shows these difference plots at station 2. At station 2, we also found a favorable (minimal dredging requirements of the ship channel and harbor) condition when there is ship channel. This station is on the right flank of the ship channel. The result shows that there will be slight erosion there when the channel is dredged. Slight erosion of the ship channel is favorable than accretion.

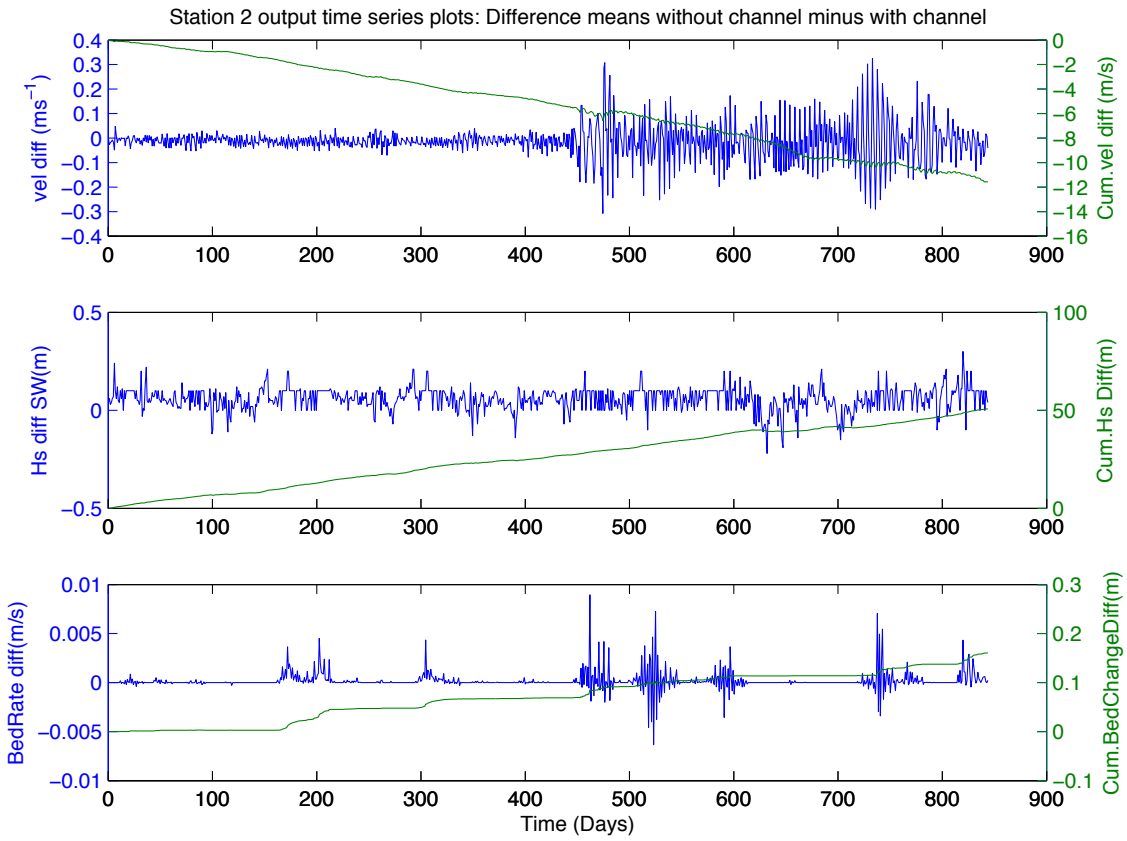

Figure 60. Plots of difference between model run without ship channel and model run with ship channel for current magnitude, significant wave height, and seabed level change at station 2. Difference is defined as output parameter obtained in a model run without ship channel minus the same output parameter in a model run with the dredged ship channel. Cumulative parameters shown on the right y-axis represent the total change in the parameter that could be observed over the time period of integration when the ship channel is dredged.

The difference plots is also shown in figure 61 for these variables at Station 8. Station 8 is further away from the channel location. Note the differences in scales between these three station outputs. The seabed level change difference graph indicates that there is virtually no change at this location. A seabed change of -0.01 meter over a period of nine years (remember the morphology factor of 4) is not physically significant.

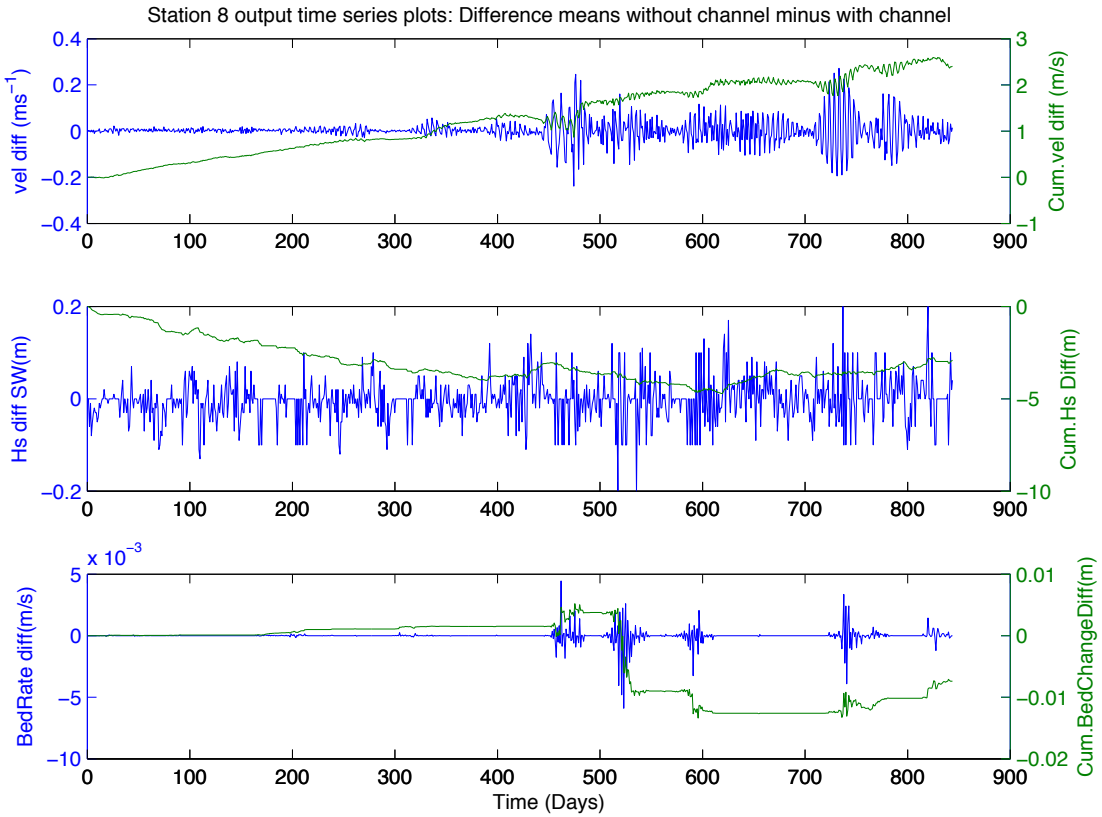

Figure 61. Plots of difference between model run without ship channel and model run with ship channel for current magnitude, significant wave height, and seabed level change at station 8. Difference is defined as output parameter obtained in a model run without ship channel minus the same output parameter in a model run with the dredged ship channel. Note the difference in scales between these three stations. Cumulative parameters shown on the right y-axis represent the total change in the parameter that could be observed over the time period of integration when the ship channel is dredged.

Figure 62 shows a map of wave direction in the study area when the ship channel is dredged. The wave refracts away from the ship channel and propagates towards Tom Shot Island.

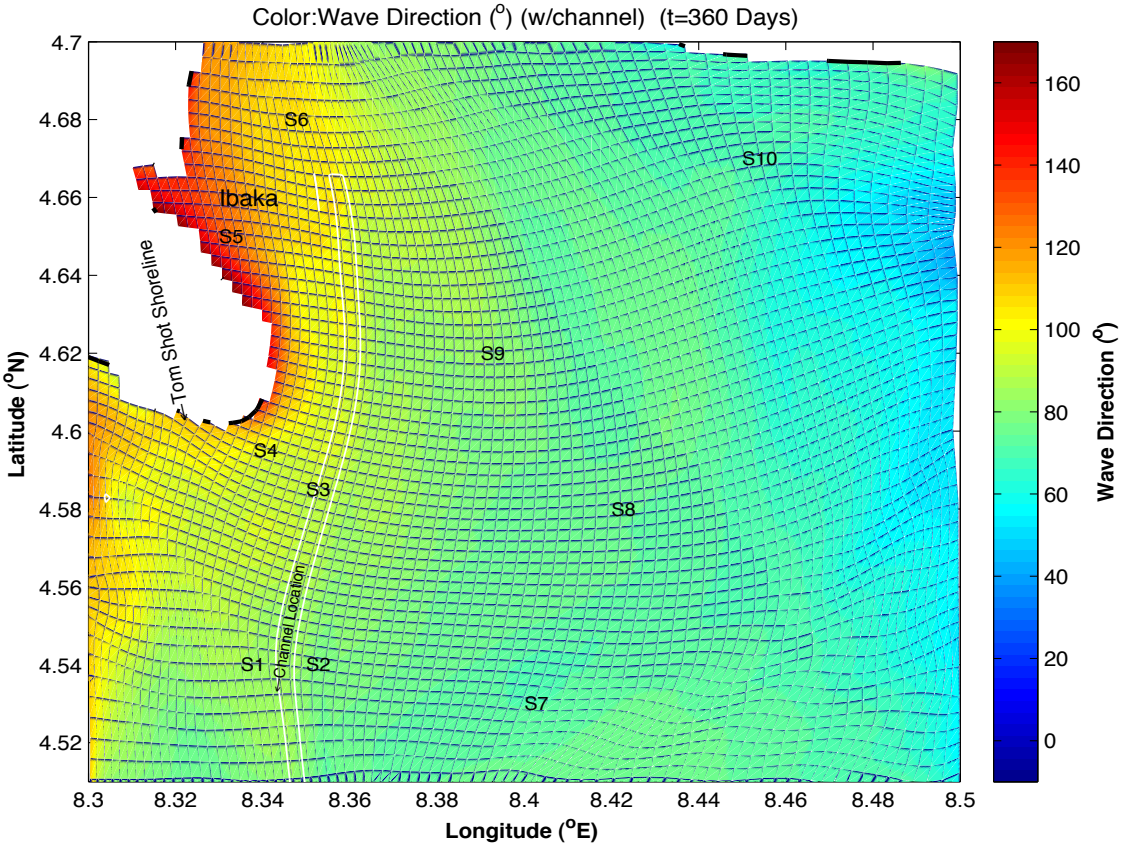

Figure 62. Map of wave direction in Ibaka when the ship channel is dredged. The angle convention here is a mathematical convention where 0^{o} points towards the east and the angle increases anti-clockwise. Offshore waves refract away from the ship channel and propagate towards Tom Shot Island.

The model results indicate that when offshore wave heights exceed 1.5 meters, such waves do not make any significant difference in circulation and sediment transport in Ibaka bay than waves between 1.3 and 1.5 meters. This is because the energy of those high waves is dissipated through depth-induced breaking and bottom dissipation. A closer look at the geometry and bottom topography of the study area (Figures 2 and 3) shows that there are bottom features (seamounts) near the offshore boundaries of this domain that reduce the wave heights to a certain level irrespective of the initial offshore wave height that approaches

the region. Also, Tom Shot Island blocks waves from the western side of the domain. South of the study area, there are canyons and an Island (Malabo). Figure 63 highlights Malabo in a contour map of the bathymetry and topography in a region of the Gulf of Guinea and southeastern Nigerian coast.

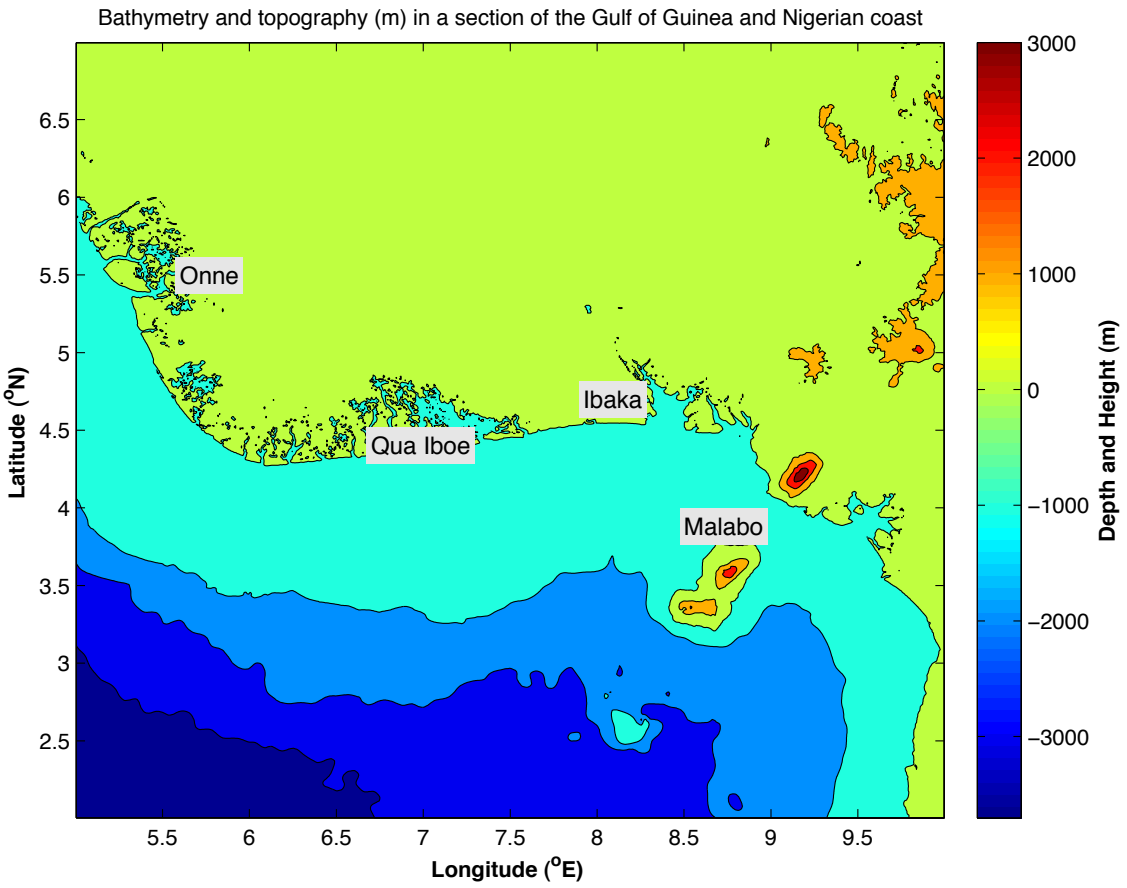

Figure 63. Contour map of the bathymetry and topography of a region in the Gulf of Guinea and part of Nigerian southeastern coastline. Malabo island, Ibaka, Qua Iboe, and Onne estuaries are also shown.

Malabo Island prevents direct waves from the southern Atlantic Ocean to reach Ibaka. The waves are broken as they hit the island. There is a canyon north of the island that should

provide a conducive environment for wave generation and growth but the re-generated waves encounter some underwater seamounts a few kilometers away from the canyon. The long continental shelf (≈120 km) in the southeastern region of Nigeria also plays a role in dissipating offshore wave energy that approaches Ibaka bay. Bays that are located closer to the shores in regions with wider continental shelf do not suffer the adverse effects of open ocean wave phenomena, such as storms, because the wide shelf will dissipate the larger wave heights. Awosika and his colleagues at the Nigerian Institute of Oceanographic and Marine research (NIOMR) have documented that near shore waves are milder at the Nigerian eastern coastal zone compared to the energetic wave climates found in the western coastal zone (Awosika and Ibe, 1994). In Nigeria, the width of the western continental shelf is about 30 kilometers while it widens up to 120 km in the eastern region.

Next, a map of bed level change was plotted as shown in figure 64. A comparison of figures 56 (page 104) and 64 indicate that bottom processes contributed to the wave dissipation. There is a discernable pattern between wave dissipation and seabed level changes in the study area. Erosion dominates regions of high wave dissipation.

Integration of the sediment fluxes over the study domain for a one-year time period gave a net sediment loss of 1.06×10^{-5} kg/m^2. This net loss agrees with the net ebb tidal current (figures 65 to 69) in the study area. There are two main sources of sediment namely: sediment fluxes from rivers into the bay at the northern boundary and sediment from tidal fluxes at the southern boundary. In these simulations, the specified river fluxes are small relative to the tidal fluxes. Thus, net sediment loss implies that the bay flushes out more sediment during the ebb cycle than the sediment supplied to it during the flood tidal cycle.

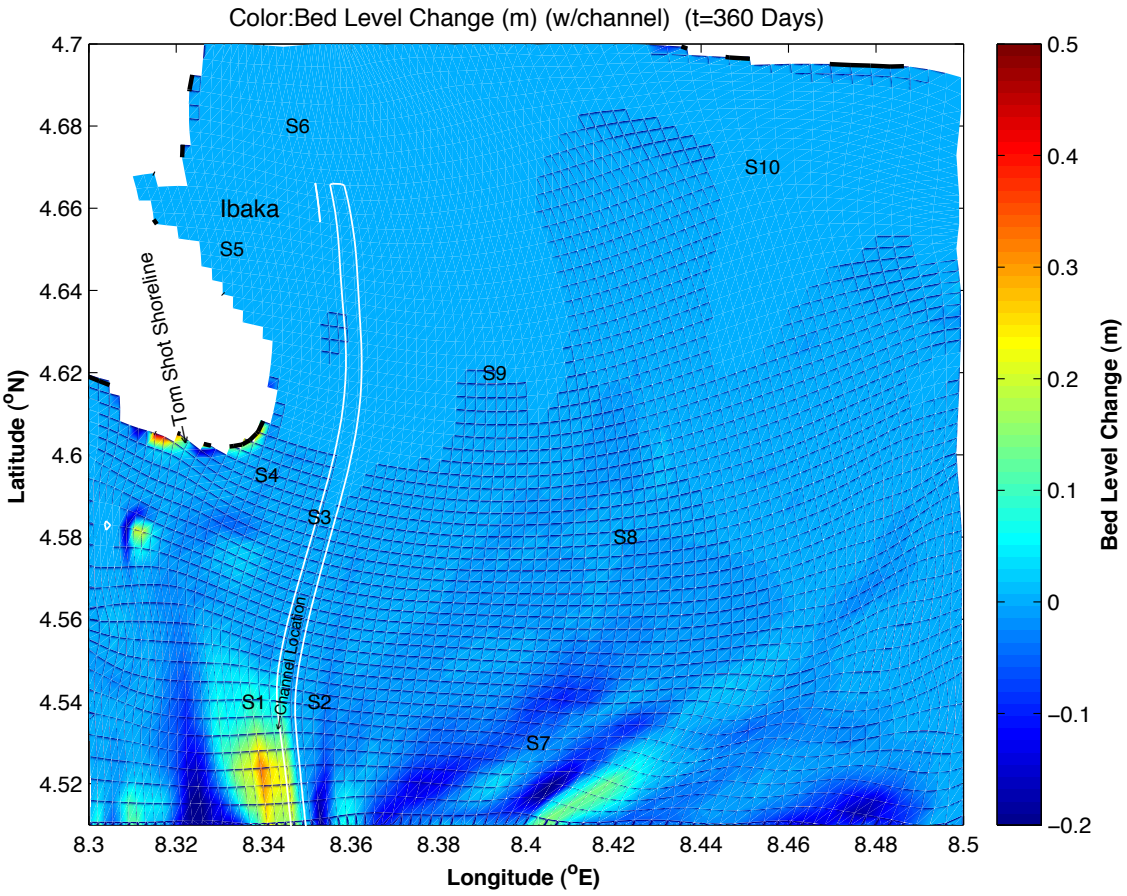

Figure 64. A map of seabed level change in Ibaka bay. A morphology factor of 4 was specified for this simulation. Crosshatches indicate the curvilinear computational grid. Comparison of this figure with figure 53 indicates a relationship between seabed level change and wave dissipation. White line denotes the channel.

Several runs were made to determine the residual circulation in the bay. Here, the residual current is defined as a one-year average of the current components. Each station graph is an average of five simulations. Figures 65 to 69 show the mean, running average (smoothed over an overlapping seven data points) and running standard deviation for the ten stations used in this analysis. It can be seen that the residual or net current is negative which means it is

directed towards the offshore. This is good news in the perspective of maintenance dredging of the channel and harbor. This circulation pattern can explain why the bay is termed a natural harbor, with the deepest non-dredged draft in Nigeria. Over time, sediment will not be deposited in the bay; rather there might be erosion. However, the residual current (averaged over one year) speed is relatively low compared to the rapidly varying onshore and offshore flood and ebb tidal current magnitudes as can be seen in the figures below.

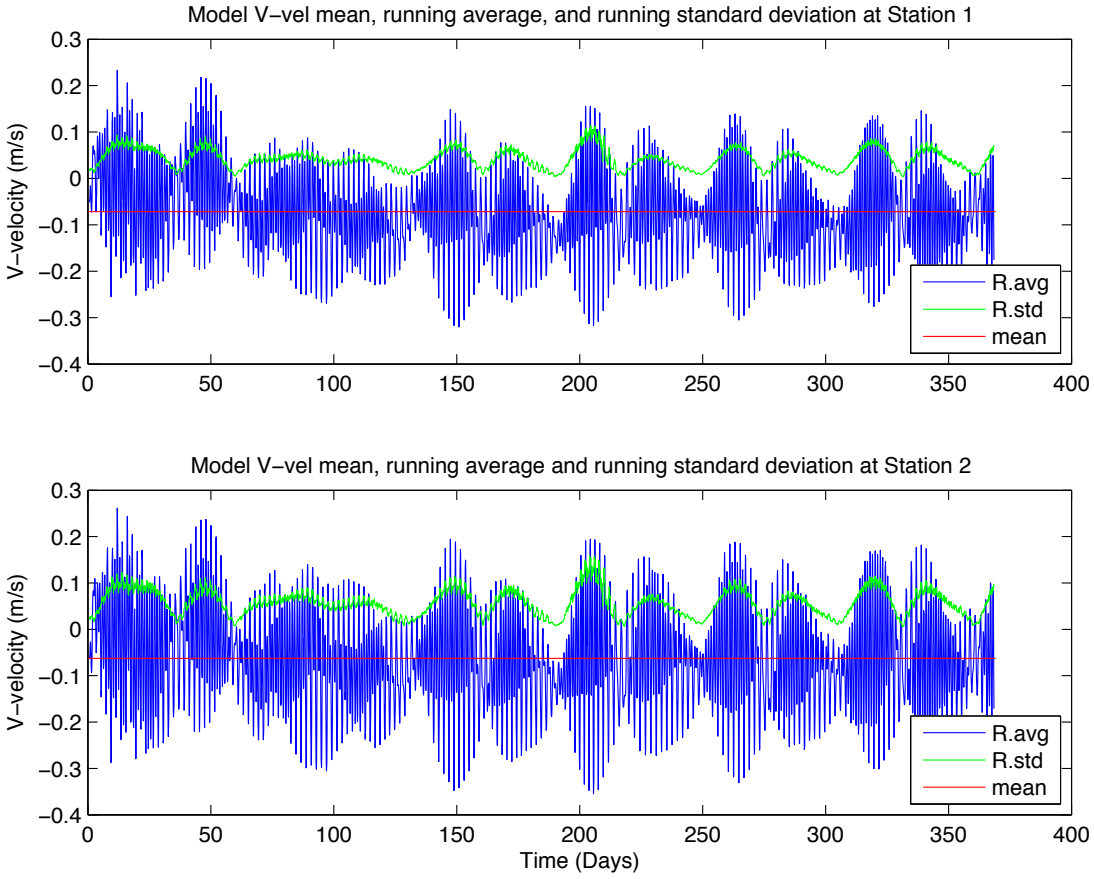

Figure 65. Running mean and running standard deviation of circulation at stations 1 and 2. The residual (one year averaged) current (red line) over this time period is directed towards offshore. The running average window is over seven overlapping data points.

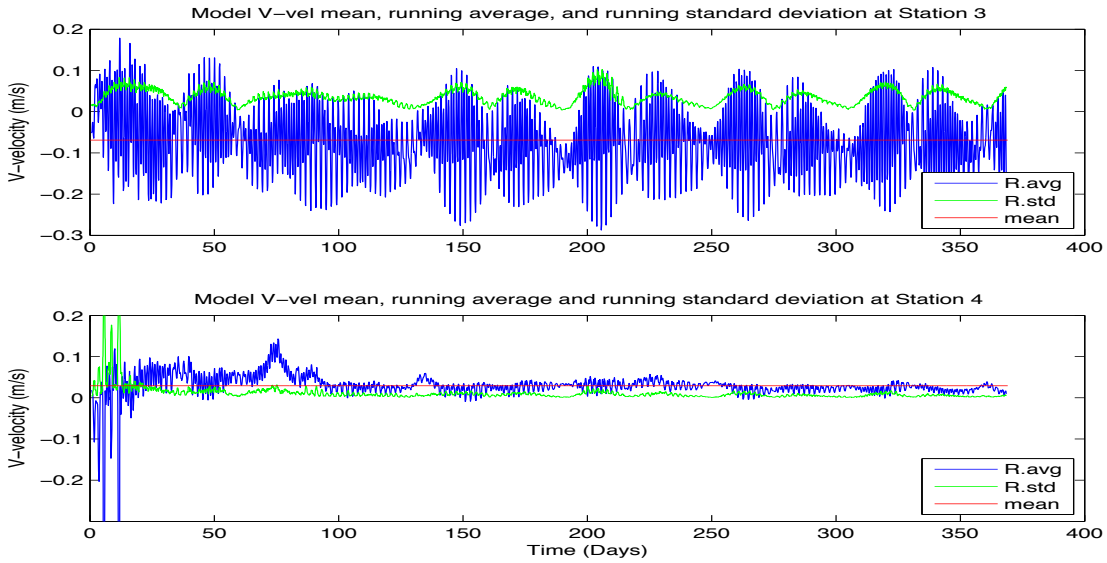

Figure 66. Running mean and running standard deviation of circulation at stations 3 and 4. The residual (one year averaged) current (red line) over this time period is directed towards offshore. The running average window is over seven overlapping data points.

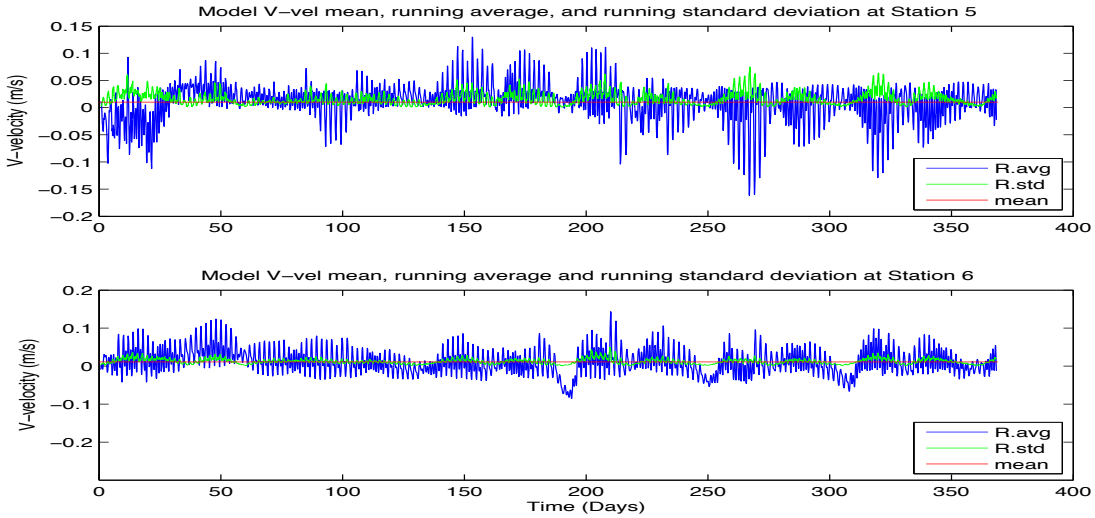

Figure 67. Running mean and running standard deviation of circulation at stations 5 and 6. The residual (one year averaged) current (red line) over this time period is directed towards offshore. The running average window is over seven overlapping data points.

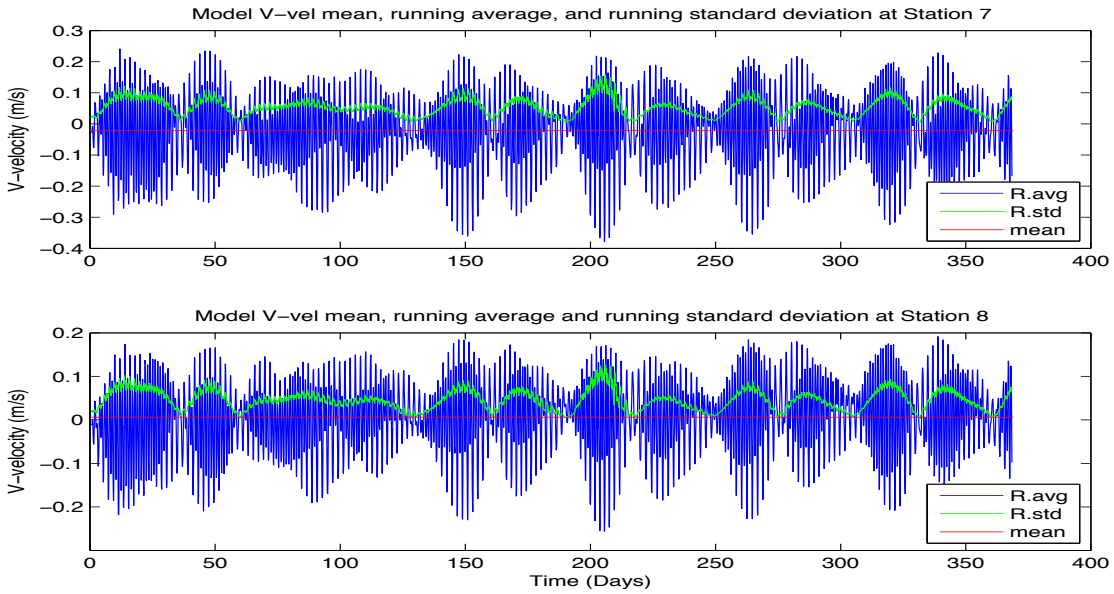

Figure 68. Running mean and running standard deviation of circulation at stations 7 and 8. The residual (one year averaged) current (red line) over this time period is directed towards offshore. The running average window is over seven overlapping data points.

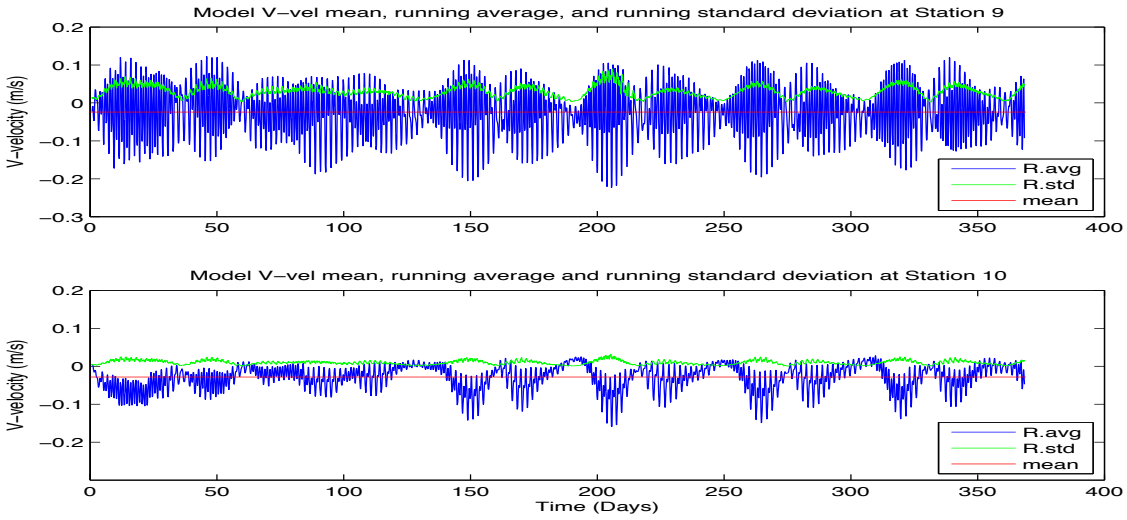

Figure 69. Running mean and running standard deviation of circulation at stations 9 and 10. The residual (one year averaged) current (red line) over this time period is directed towards offshore. The running average window is over seven overlapping data points.

We have seen from the analyses of the results in this chapter that the deep seaport project will be a cost-effective venture if all stakeholders could collaborate and design the ship channel to the specifications outlined in this study. The channel location and size used in this numerical experiment was chosen among seven channel designs. The required depth is reached at this selected (optimum) channel location with minimum dredging cost. Most importantly, the wave, current, and other environmental processes within the bay do not seem to fill this optimum channel rapidly. If an additional depth clearance of one meter is planned for during the initial deepening of the ship channel, the model results indicate that maintenance dredging will not be required for a period of five years. This will be a huge savings to stakeholders of this project. On the average, it costs more than $3 million to mobilize a dredge machine to site.

CHAPTER VII

SUMMARY, CONCLUSIONS, AND RECOMMENDATIONS

SUMMARY

This study examined the roles of wave action and circulation on sediment processes in Ibaka bay. Three main approaches were adopted in investigating these processes. First, a field experiment was conducted in the study area in December 2012. Some valuable wave, circulation, and sediment characteristics data and information were gathered during the field experiment. That information served as a guide in qualitative analyses of the model result. The sediment data gathered were used to initialize the sediment module. Secondly, physical oceanographic data within the vicinity of Ibaka bay were accessed from available archives and analyzed. SIMORC and GLOSS were the main archives I accessed that contained useful data for this research. The oceanographic data extracted from these archives included sea surface elevations, significant wave heights, mean wave period and direction, current speed and direction. Bathymetry data were extracted from Topex UCSD (University of California, San Diego) 30-arc seconds archive. The data from these archives were analyzed and then used to calibrate, validate, and verify the numerical model. Thirdly, NearCoM-TVD software was used as the base model for all numerical experiments. NearCoM-TVD is a quasi-three dimensional model that solves the shallow water wave equation numerically in two dimensions and also accounts for the vertical variations of the horizontal currents, due to waves, in an analytical manner. This makes it very efficient in long-term simulations of oceanographic processes in well-mixed bays and estuaries.

This dissertation documents an important (and oftenly neglected) area that should be incorporated during the planning and designing phases of coastal and environmental field studies. The field experiment component of this project suffered a huge setback because Ibaka local residents were not properly informed and carried along at every stage of the study. All time and available resources were channeled into the scientific and engineering aspects of the work. Appropriate communication channels were not established to inform and educate the local residents on the benefits of the project to the community. Some youths of Ibaka community protested against this noninvolvement and removed all the surface drifters from the bay, a few hours after deployment. Some exposed surface sampling equipment was never recovered from the local residents after seizure. Rebuilding trust and confidence among the local community and other stakeholders was time consuming and more expensive.

A nested modeling approach was used to transform the waves from offshore to the nearshore modeling boundary domains. Waves and winds from the National Center of Environmental Predictions (NCEP) were used to initialize a coarser and larger SWAN model and transformed wave output were taken from some points that coincided with NearCoM-TVD domain boundaries. The larger SWAN domain included Ekundu data station. Wave height and wave period model output taken at Ekundu were comparable to Ekundu measured wave height and wave period data found in SIMORC database. This larger SWAN model wave output served as the offshore boundary wave forcing for the nested, finer resolution NearCoM-TVD model. Ekundu current data was used for current initialization while a spatially constant but time varying wind was specified for NearCoM-TVD model. Coastgrid software and a FORTRAN program were used to design curvilinear grids for both SWAN and NearCoM-TVD models.

Sensitivity analyses of the model to some input forcing functions revealed that the NearCoM-TVD model was robust to changes in most input forcing functions that were tested. Perturbations of wave, current, and sediment characteristics did not result in a different pattern of the model output parameters. This analysis was also used to determine the optimum model grid and time resolutions for these simulations.

Model results indicate that wave action influences sediment transport and seabed changes in Ibaka deep seaport site. Other forcing functions such as currents, river fluxes, and wind also contributed to seabed level changes but their patterns did not correlate as that of significant wave heights. An intriguing result was the threshold value of significant wave height that initiated seabed sediment processes in Ibaka bay. Only significant wave heights above 1.0 meter caused sediment transport and seabed morphological changes in the bay.

The seasonal variability of wave, circulation, and sediment processes of Ibaka was also investigated. Statistical analyses of the measured data and model output showed a significant difference in rainy and dry season waves and currents, with a significant level (alpha) of 0.05. Aside from the statistical significance, this result also had physical significance because significant wave heights during the dry season (November to March) never reached the 1.0-meter critical value required for sediment transport in the bay.

An attempt was made to relate the critical bed shear stress with the mean free stream flow using common empirical formulas. Some level of success was achieved and a friction velocity (required to initiate sediment transport with respect to the sediment characteristics in the bay) of 1.1 cm/s resulted in a mean free stream flow of 25.1 cm/s (as shown in Gardner, 1989b) in most locations of the study area. However, it was found at a few locations and times that sediment transport was initiated with a mean free stream flow below 25.1 cm/s when

significant wave height was above 1.0 meter. One possible reason for this slight anomaly is that the formula used for this computation was derived for tidally dominated current regions. Currents in some locations in Ibaka bay seem to have same order of magnitude contributions from tides, waves, and river fluxes.

NearCoM-TVD model simulations were used to determine an optimum ship channel location and size for Ibaka deep seaport project. Model results using this optimum ship channel showed that deepening the channel, to accommodate vessels up to 200,000 DWT, will not cause frequent siltation in the channel or erosion of nearby beaches. Dredging and deepening of the ship channel effectively reduced the wave action that propagates from offshore towards the inner part of the bay. Some accretion or sediment deposition occurred on the left flank of the ship channel (towards Tom Shot Island) and slight erosion occurred on the right flank of the channel. The direction of the transformed wave aided in further transportation of the deposited sediment on the left flank of the channel towards the beach.

Finally, the instantaneous seabed level changes from NearCoM-TVD model output were integrated over the simulation time period. The result of the cumulative seabed changes indicated that it would take at least five years for sediment deposition in the ship channel to reach one meter high. Based on this result, we estimated a periodic maintenance dredging time window of five years for Ibaka deep seaport.

CONCLUSIONS

The following conclusions are drawn for this study:

Ibaka bay is a natural harbor. Tom Shot Island shields the bay against direct impacts of south-south-west swells coming from the Atlantic Ocean.

Significant wave heights above 1.0 meter are required for sediment transport and seabed level changes in Ibaka bay. Wave action plays a significant role in circulation and sediment processes in Ibaka. Significant wave height and seabed changes patterns are highly correlated ($r^2 = 0.91$).

Only rainy season (April to October) weather conditions produce energetic wave and currents that can drive sediment transport in Ibaka bay. Monthly averaged residual current in Ibaka is ebb (offshore) directed and this helps in flushing out fine sediment deposit out of the dredged ship channel.

Dredging of the ship channel to accommodate higher tonnage vessels (>200,000 Dead Weight Tonnage) will not propagate higher wave energy towards inner parts of Ibaka bay. Re-focusing of the wave energy due to the dredged ship channel does not cause significant beach erosion or channel infilling.

The geometry and bathymetric characteristics of Ibaka limits the maximum significant wave heights (less than 1.0 meter) that can get to the inner part of Ibaka bay, regardless of the magnitude of approaching offshore waves at the boundary of this study domain.

Periodic maintenance dredging of Ibaka ship channel and harbor will be minimal (with an estimated periodic dredging time window of five years), when compared to periodic maintenance dredging windows in other existing ports in Nigeria.

Involving and engaging the local community actively at every developmental stage of Ibaka deep seaport project is a worthwhile investment because the resources committed into this kind of communication and enlightenment projects will be insignificant relative to the cost of re-negotiating the entire project following local residents' protest and eventual obstruction of work.

Lastly, the involvement of undergraduate students at Akwa Ibom State University, Nigeria caused excitement and joy among the students. The students developed interest in experimental oceanographic work and requested that they be included in subsequent field trips on this project.

RECOMMENDATIONS

Finer bathymetric resolution is required for simulating finer features of physical processes of interest in this study. Stakeholders and development partners of Ibaka deep seaport project should collaborate and launch a bathymetric sampling campaign before the end of this year. Modeling with finer and optimum bathymetric resolutions will produce a better design of the port.

A fully three-dimensional model should be used with the finer bathymetric resolution to simulate the wave, circulation, and sediment processes in Ibaka bay. The results from this three-dimensional model (which is capable of explicitly simulating density driven or baroclinic currents) should be compared with model results from the quasi three-dimensional NearCoM-TVD model. Estimates of errors associated with quasi three-dimensional model could be obtained and then incorporated into future analyses of model output.

Longer records of quality controlled physical oceanographic data (wave, current, salinity, and temperature) in Ibaka bay should be acquired and archived properly. This will assist in model calibration, validation, and verification. Sediment characteristics (type, texture, and size distribution) in the bay also need to be understood better and applied as a varying quantity into numerical models. Sediment modeling and predictions are highly complex, and the data available, at the time of this research, are very limited for drawing conclusions with

high confidence. Additional field campaigns will significantly improve our understanding of the processes examined in this dissertation.

Traditional and modern communication instruments should be installed and properly managed to disseminate information clearly, and in a timely manner, to all stakeholders (including the local Ibaka residents) of the deep seaport project.

Dredged materials should be strategically placed to minimize adverse environmental consequences, due to disposal of the dredged materials. Beneficial use of the dredged materials should be maximized and economically used for projects such as Ibaka beach nourishment. The sediment is mainly medium and coarse sand, which is ideal for beach nourishment. Materials should be placed within the bay's depth of closure.

REFERENCES

Ajao, E. A. and Houghton R.W. (1998). "*Coastal Ocean Of Equatorial West Africa From 10^{o}N To 10^{o}S, Coastal Segment (17, E)"*. The Sea, Vol. 2, John Wiley And Sons Inc., Hoboken, NJ, pp. 605-631.

Akwa Ibom State Government (2012). *"State Government Official Website: Ibaka Deep Seaport Project"*. www.aksg.gov.ng/ibaka-project, Accessed December 12, 2012

Antia E. E. (2012). *"Personal Communication"*. Institute Of Oceanography, University Of Calabar, Nigeria.

Austin J. and Atkinson S. (2004). *"The Design And Testing Of Small, Low-Cost GPS-Tracked Surface Drifters"*. Estuaries, Vol. 27, No. 6, pp. 1026 - 1029.

Awosika L. F. (1994). *"Impact Of Global Climate Change And Sea Level Rise On Coastal Resources And Energy Development In Nigeria"*. Proceedings From The International Workshop On Impact Of Global Climate Change On Energy Development, March 28-30 1994.Lagos, Nigeria, pp. 80–88.

Awosika, L. F. (1995). *"Storm Surge Of August 1995 And Flooding Of The Victoria Island On 17 August 1995"*. An Unpublished Paper, pp. 1-13.

Awosika, L. F., Dublin-Green C.O., Folorunsho R., Adekoya, E.A., Adekanmbi, M.A., and Jim-Saiki, J. (2000). "*Study Of Main Drainage Channels Of Victoria Islands In Lagos, Nigeria And Their Response To Tidal And Sea Level Changes*". CSI-UNESCO Special Report, pp. 1–108.

Awosika, L. F., Ibe, A.C., and Ibe, C.E. (1993). "*Anthropogenic Activities Affecting Sediment Load Balance Along The West African Coastline".* In Proceedings: Coastlines Of Western Africa, Coastal Zone 93. American Association of Civil Engineers, New York, NY, pp. 81-93.

Awosika, L. and Ibe, A. (1994). "*Geomorphic Features Of The Gulf Of Guinea Shelf And Littoral Drift Dynamics*". In Proceedings, International Symposium On The Results Of The First IOCEA Cruise In The Gulf Of Guinea, May 17-20, 1994. Center For Environment And Development In Africa, pp. 14-18

Balson, P.S. and Collins, M.B. (2007). "*Coastal And Shelf Sediment Transport*". Geological Society of London, Special Publications, Vol. 274, pp. 1-5.

Barthel, V. and Funke, E.R. (1989). "*Hybrid Modelling As Applied To Hydrodynamic Research And Testing".* In: Recent Advances In Hydraulic Physical Modelling, R. Martins (Ed), NATO ASI Series E: Applied Sciences*,* Vol. 165, Kluwer Academic Publishers, Boston, MA.

Berkhoff, J.C.W. (1972). "*Computations Of Combined Refraction-Diffraction*". Proceedings Of 13th International Conference, Coastal Engineering, ASCE, New York, NY, pp. 471–490.

Birkemeier, W.A. and Dalrymple, R.A. (1975). "*Nearshore Water Circulation Induced By Wind And Waves*". Proceedings of Modeling '75, ASCE, San Francisco, CA, pp. 5-12.

Booij, N. (2012). "*An Improved New Release of Simulating Waves Nearshore: SWAN 40.91*". Delft University of Technology, Delft, The Netherlands, pp. 1-108.

Booij, N. (2012). "*The SWAN Support Package: A Review Of Wave Diffraction Models And Their Application In SWAN Model*". Digital Hydraulics, Delft, The Netherlands.

Booij, N., and Holthuijsen, L.H. (1987). "*Propagation Of Ocean Waves In Discrete Spectral Wave Models".* J. Computational Physics, Vol. 68, pp. 307–326.

Booij, N., Holthuijsen, L.H., and Herbers , T.H.C. (1985). "*A Numerical Model For Wave Boundary Conditions In Port Design*". Proceedings Of International Conference On Numerical And Physical Modeling Of Ports and Harbours," BHRA, Birmingham, pp. 263–268.

Booij, N., Ris, R.C. and Holthuijsen, L.H. (2012). "*A Third-Generation Wave Model For Coastal Regions*". Version 40.91. http://swanmodel.sourceforge.net. Accessed July 15, 2012.

Booij, N., Ris, R.C. and Holthuijsen, L.H. (1999). "*A Third Generation Wave Model For Coastal Regions. 1. Model Description And Validation*". J. Geophys. Res., Vol. 104, pp.7649-7666.

Brackbill, J.U. and Saltzman, J.S. (1982). "*Adaptive Zoning For Singular Problems In Two Dimensions*". J. Computational Physics, Vol. 46, pp. 342-368.

Brown, J. and Wolf, J. (2009). "*Coupled Wave And Surge Modelling For The Eastern Irish Sea And Implications For Model Wind-Stress".* Continental Shelf Research, Vol. 29, pp. 1329-1342.

Building Nigeria's Response To Climate Change (BNRCC), (2011). http://nigeriaclimatechange.org/. Accessed February 10, 2013.

Carbajal, N. and Montaño-Ley, Y. (2011). "*Transport Of Sediments In Water Bodies Of The Gulf Of California, Sediment Transport In Aquatic Environments*", Dr. Andrew Manning (Ed.), ISBN: 978-953-307-586-0, InTech, DOI: 10.5772/21585. Available from: http://www.intechopen.com/books/sediment-transport-in-aquatic-environments/transport-of-sediments-in-water-bodies-of-the-gulf-of-california. Accessed October 10, 2013.

Dean, R. G. (2001). "*Coastal Processes; Chapter 8: Sediment Transport*". Port Chester, NY, USA. Cambridge University Press, pp. 210–264.

Eckart, C. (1952) "*The Propagation Of Gravity Waves From Deep To Shallow Water*". Circular 20, National Bureau of Standards, pp. 165-173.

Elgar, S. and Guza, R.T. (1985). "*Shoaling Gravity Waves: Comparisons Between Field Observations, Linear Theory And A Nonlinear Model*". J. Fluid Mech., Vol. 158, pp. 47-70.

Ebbesmeyer, C. C. and Coomes, C.A. (1993). "*Historical Shoreline Recoveries Of Drifting Objects: An Aid To Future Shoreline Utilization*". IEEE Proceedings, Victoria, Canada, Oceans '93, Oceanic Engineering Society, Vol. 3, pp. 14-19

Ewa-Oboho, I. (2012). "*Personal Communication*". Department Of Oceanography, Akwa Ibom State University, Uyo, Nigeria.

Ewans, K., Forristall, G.Z., Prevosto, M., and Olagnon, M., (2013). "*Response Sensitivity To Swell Spectra Off West Africa*". Proc. 32nd Int'l. Conference On Offshore Mech. And Arctic Eng., OMAE 2013-11252, pp. 11252-11261.

Flather, R.A. (2000). "*Existing Operational Oceanography*". Coast. Eng. Vol. 41(1–3), pp.13–40.

Folorunsho, R. (2006). "*Meteorologically Induced Storm Surge In The Gulf Of Guinea: Consequences On Coastal Resources And Infrastructure*". Nigerian Institute For Oceanography And Marine Research, Lagos, Nigeria, pp. 1-10.

Folorunsho, R. and Awosika, L.F. (1995). "*Meteorologically Induced Changes Along The Nigerian Coastal Zone And Implications For Integrated Coastal Zone Management Plan*". Proceedings Int'l Conf. "Coastal Change 95" BORDOMER – IOC Bordeaux 1995, pp. 804-811.

Forristall G.Z, Ewans, K., Olagnon, M., and Prevosto, M. (2013). "*The West African Swell Project (WASP)*". ASME 2013 32nd International Conference On Ocean, Offshore And Arctic Engineering. Vol. 2B, OMAE2013-11264, pp. 11264-11271.

Fredsoe, J. and Deigaard, R. (1992). "*Mechanics Of Coastal Sediment Transport (Advanced Series On Ocean Engineering)"*. World Scientific, Vol. 3, pp. 1113-1151.

Gardner, W. (1989b). "*Periodic Resuspension In Baltimore Canyon By Focusing Of Internal Waves*". J. Geophysical Research, Vol. 94, No. C12, pp. 18185–18194.

Geeraerts, J., Kortenhaus, A. Gonzalez-Escriva, J.A., De Rouck, J. and Troch, P. (2009). "*Effects Of New Variables On The Overtopping Discharge At Steep Rubble Mound Breakwaters - The Zeebrugge Case Coast*". Eng. Vol. 56, No.2, pp. 141-153.

Gent, P.R. (2011). "*The Gent-Mcwilliams Parameterization: 20/20 Hindsight*". Ocean Modeling, Vol. 39, pp. 2-9.

Gent, P.R., Willebrand, J., Mcdougall, T.J., and McWilliams, J.C. (1995). "*Parameterizing Eddy-Induced Tracer Transports In Ocean Circulation Models*". J. Physical Oceanography, Vol. 25, pp. 463-474.

George, R. and Largier, J.L. (1996). "*Description And Performance Of Fine Scale Drifters For Coastal And Estuarine Studies*". J. Atm. And Oceanic Technology, Vol. 13, pp. 1322-1326.

González, M., Medina, R., Gonzalez-Ondina, J., Osorio, A., Méndez, F.J. and García, E. (2007). "*An Integrated Coastal Modeling System For Analyzing Beach Processes And Beach Restoration Projects, SMC*". J. Computers and Geosciences, Vol. 33, pp. 916-931.

Grant, W.D. and Madsen, O.S. (1979). "*Combined Wave And Current Interactions With A Rough Bottom*". J. Geophys. Res., Vol. 84, No. C4, pp. 1797–1808.

Grunnet, N., Lohier,S. and Deigaard, R. (2008). "*Study Of Sediment Bypass At Coastal Structures By Composite Modeling*". Proc. 31st International Conference On Coastal Engineering (ASCE), Hamburg, Germany, World Scientific, Vol. 2, pp. 1876-1887.

Haller, M.C., Dalrymple, R.A., and Svendsen, I.A. (1997). "*Rip Channels And Nearshore Circulation*". Proc. On International Conference On Coastal Research, Coastal Dynamics '97, Plymouth, UK, pp. 101-111.

Holthuijsen, L.H., Herman, A. and Booij, N. (2004). "*Phase-Decoupled Refraction-Diffraction For Spectral Wave Models*". Coastal Engineering Vol. 49, pp. 291-305.

Horsburgh K.J. and Wilson, C. (2007). "*Tide–Surge Interaction And Its Role In The Distribution Of Surge Residuals In The North Sea*". J. Geophys Res. Vol. 112, C8, pp. 1083-1089.

Houghton, R.W., (1976). "*Circulation And Hydrographic Structure Over The Ghana Continental Shelf During The1974 Upwelling*". J. Phys. Oceanography., Vol. 6, pp. 909-924.

Humbyrd, C.J. and Madsen, O.S. (2010). "*Predicting Movable Bed Roughness In Coastal Waters*". Department Of Civil And Environmental Engineering, Massachusetts Institute Of Technology, Cambridge, MA 02139, Coastal Engineering, Vol. 32, pp. 1032-1043.

Ibe, A.C. and Quelennec, R.E. (1989). "*Methodology For Assessment And Control Of Coastal Erosion In West Africa And Central Africa*". UNEP Regional Sea Reports And Studies No. 107. United Nations Environmental Program, New York, NY, pp. 1-100.

Johnson, D., Stocker, R. Head, R., Imberger, J. and Pattlaratchi, C.B. (2003). "*A Compact Low-Cost GPS Drifter For Use In The Oceanic Nearshore Zone, Lakes And Estuaries*". J. Atm. And Oceanic Technology, Vol. 20, pp. 1880-1884.

Jonsson, I.G. (1998). "*Wave Action Flux: A Physical Interpretation*". Department Of Hydrodynamics And Water Resources (ISVA), Technical University Of Denmark, Lyngby, Denmark. J. Fluid Mech. Vol. 368, pp. 155-164.

Kaihatu, J.M., Linda, S.L., and Thompson, E.F. (1989). "*Effects Of Entrance Channel Dredging At Morro Bay, California*". Coastal Research Engineering Center, Department Of The Army, Vicksburg, MS, pp. 1-77.

Kämpf, J. (2009). "*Ocean Modelling For Beginners (Using Open-Source Software)*". School Of Environment, Adelaide, Australia, Springer Heidelberg, Australia.

Kämpf, J. (2009). "*Advanced Ocean Modelling (Using Open-Source Software)*". School Of Environment, Adelaide, Australia, Springer Heidelberg, Australia.

Komarova, N.L. and Newell, A.C. (2000). "*Nonlinear Dynamics Of Sand Banks And Sand Waves*". J. Fluid Mech., Vol. 415, pp. 285-321.

Kranenburg, W., Ribberink, J., and Uittenbogaard, R. (2011). "*Sand Transport By Surface Waves: Can Streaming Explain The Onshore Transport?"* University of Twente, Enschede, The Netherlands. Proc. Of Int'l Conference On Coastal Engineering, Vol. 32, pp. 11-18.

Lin, L., Mase, H., Yamada, F., and Demirbilez, Z. (2006). "*Wave Action Balance Equation Diffraction (WABED) Model: Tests Of Wave Diffraction And Reflection At Inlets*". Coastal Inlet Research Program Technical Note, ERDC/CHL CHETN-III-73, U.S. Army Engineer Research And Development Center, Vicksburg, MS, pp. 1-52.

Lin, W., Sanford, L.P. and Suttles, S.E. (2002). "*Wave Measurement And Modeling In Chesapeake Bay*". Continental Shelf Research, Vol. 22, pp. 2673-2686.

Liu, P. L.F. (1994) *"Model Equations For Wave Propagation From Deep To Shallow Water*". In Advances In Coastal And Ocean Engineering, Vol.1, pp. 125-158.

Longuet-Higgins, M.S. and Stewart, R.W. (1960). "*Changes In The Form Of Short Gravity Waves On Long Waves And Tidal Currents*". J. Fluid Mech., Vol. 8, pp. 565-583.

Longuet-Higgins, M.S. and Stewart, R.W. (1961). "*The Changes In Amplitude Of Short Gravity Waves On Steady Non-Uniform Currents*". J. Fluid Mech., Vol. 10, pp. 529-549.

Longuet-Higgins, M.S. and Stewart, R.W. (1962). "*Radiation Stress And Mass Transport In Gravity Waves*". J. Fluid Mech., Vol. 13, pp. 481-504.

Longuet-Higgins, M.S. and Stewart, R.W. (1964). "*Radiation Stress In Water Waves: A Physical Discussion With Applications*". J. Deep-sea Research, Vol. 11, pp. 529-562.

Manian, D., Kaihatu, J.M., and Zechman, E.M. (2012). "*Using Genetic Algorithms To Optimize Bathymetric Sampling For Predictive Model Input*". J. Of Atmospheric And Oceanic Tech., Vol. 29, pp. 484-477.

Michael, B.C. and Balson, P.S. (2007). "*Coastal And Shelf Sediment Transport: An Introduction*". Geological Society, London, Special Publications 2007, Vol.274, pp. 1-5. doi: 10.1144/GSL.SP.2007.274.01.01.

Moeini, M.H. and Etemad-Shahidi, A. (2009). "*Wave Parameter Hindcasting In A Lake Using The Swan Model*". Scientia Iranica, Vol. 16, pp. 156-164.

Morteza, K., Imanian, H., and Falconer, R.A. (2006). "*Numerical Modeling Of Morphological Development In Tidal Basins Using Unsteady Criteria For The Initiation Of Motion*". Proceedings Of The 7th Int'l Conf. On HydroScience And Engineering, Philadelphia*, PA, Sept. 10-13, 2006, pp. 33-39*.

"*National Oceanographic And Atmospheric Administration/ National Weather Service/ National Centers For Environmental Prediction*", 5830 University Research Court, College Park, MD 20740.

National Population Commission (NPC) (2011). "*Official Site Of Nigerian Population Commission: 2006 Census*". www.population.gov.ng. Accessed December 3, 2013.

National Ports Authority (NPA), Nigeria (2012). "Preliminary Report On The Causes Of Accidental Discharge In Nigerian Coastal Waters". www.nigerianports.org . Accessed September 22, 2013.

Nielsen, P. (1992). "*Coastal Bottom Boundary Layers And Sediment Transport (Advanced Series On Ocean Engineering)*". World Scientific, Vol. 4, pp. 863-881.

Nwogu, O. (1993). "*An Alternative Form Of The Boussinesq Equations For Nearshore Wave Propagation*". J. Waterway, Port,Coast. Ocean Eng, ASCE, Vol.119, pp. 618-638.

Ocean Monitoring And Forcasting: "MyOcean". http://www.myocean.eu.org/, Accessed November 11, 2012.

O'Donoghue, T. and van der A, D.A. (2012). "*Laboratory Experiments For Wave-Driven Sand Transport Prediction*". School of Engineering, University Of Aberdeen, Scotland. Jubilee Conference Proceedings, NCK-Days 2012, Aberdeen, Scotland, pp. 61-67. DOI:10.3990/2.171

Olagnon, M., Prevosto, M.,Van Iseghem, S., Ewans, K., and Forristall, George G.Z. (2004). "*WASP - West Africa Swell Project – Final Report And Appendices*". pp. 90 -192. Available from: http://archimer.ifremer.fr/doc/00114/22537/ Accessed July 13, 2013.

Olagnon, M., Ewans, K., Forristall, G.Z., and Prevosto, M. (2013). "*West Africa Swell Spectral Shapes*". Proc. 32nd Int. Conference On Offshore Mech. And Arctic Eng., OMAE 2013-11228, pp. 11228-11237.

Osuna, P and Wolf, J. (2005). "*A Numerical Study On The Effect Of Wave–Current Interaction Processes In The Hydrodynamics Of The Irish Sea*". In: Proceedings Of The 5th International Conference On Ocean Wave Measurement And Analysis. WAVES2005, Madrid, Spain, 3–7 July 2005, pp. 93-102.

Oumeraci, H. (1999). "*Strengths And Limitations Of Physical Modelling In Coastal Engineering - Synergy Effects With Numerical Modelling And Field Measurements*". Proc. Of The Hydralab -Workshop On Experimental Research And Synergy Effects With Mathematical Models, Eds.: K.-U. Evers, J. Grune, A. van Os, Coastal Research Centre, Hannover, Germany, ISBN: 3-00-004942-8, pp. 7-38.

Panchang, V.G., Pearce, B.R., and Briggs, M.J. (1990). "*Numerical Simulation Of Irregular Wave Propagation Over Shoals*". J. Waterw., Port, Coast., Ocean Eng., ASCE, New York, Vol. 116 No.3, pp. 324–340.

Panigrahi, J.K., Ananth, P.N., and Umesh,P.A. (2009). "*Coastal Morphological Modeling To Assess The Dynamics Of Arklow Bank, Ireland*". Int'l Journal Of Sediment Research, Vol. 24, pp. 299-314.

Pape, III, E.H. and Garvine, R.W. (1982). "*The Subtidal Circulation In Delaware Bay And Adjacent Shelf Waters*". J. Geophys. Res. Vol.87. pp. 7995-7970.

Patella, L. (2013). "*Western Dredging Association (WEDA) Midwest Chapter Meeting: Opening Remarks*". WEDA Email Broadcast, St. Louis, Missouri, April 17-19, 2013.

Paul, E.U. (2008). "*Beach Nourishments And Impacts On National, States And Local Economies In The United States*". An unpublished Coastal Ocean Engineering (OCEN 672) Class Project At Texas A&M University, College Station, Texas, pp. 1-20.

Perez, J.C., Bonner, J., Kelly, F.J., and Fuller, C. (2003). "*Development Of A Cheap, GPS- Based Radio-Tracked Surface Drifter For Closed Shallow Water Bays*". Proceedings Of The IEEE/OES Seventh Working Conference On Current Measurement Technology, San Diego, California, pp. 66-69.

Picaut, J. (1983). "*Propagation Of Seasonal Upwelling In The Eastern Equatorial Atlantic*". J. Phys. Oceanography, Vol. 13, pp. 18-37.

Plant, N.G., Edwards, K.L., Kiahatu, J.M., Veeramony, J., Hsu, L., and Holland, K.T. (2009). "*The Effects Of Bathymetric Filtering On Nearshore Process Model Results*". Coastal Engineering, Vol. 56, pp. 484-493.

Prevosto, M., Ewans, K., Forristall, G.Z., and Olagnon, M., (2013). "*Swell Genesis, Modelling And Measurements In West Africa*". Proc. 32nd Int. Conference On Offshore Mech. And Arctic Eng., OMAE 2013-11201, pp. 11201-11210.

Quaresma, V.S., Bastos, A.C., and Amos, C.L. (2007). "*Sedimentary Processes Over An Intertidal Flat: A Field Investigation At Hythe Flats, Southampton Water, UK*". Marine Geology, Vol. 241, pp. 117–136.

Rider, K.E., (2004). "*Shelf Circulation Patterns Off Nigeria*". Master Of Science Thesis, Texas A&M University, College Station, Texas, pp. 1-154.

Ris, R.C., Holthuijsen, L.H. and Booij, N. (1999). "*A Third-Generation Wave Model For Coastal Regions. 2. Verification*". J. Geophys. Res., Vol. 104, pp. 7667-7681.

Sandra Plecha, S., Silva, P.A., Oliveira, A., and Dias, J.M. (2011). "*Sediment Transport Modelling And Morphological Trends At A Tidal Inlet, Sediment Transport In Aquatic Environments".* Dr. Andrew Manning (Ed.), ISBN: 978-953-307-586-0, InTech, Available from: http://www.intechopen.com/books/sediment-transport-in-aquatic-environments/sediment-transport-modelling-and-morphological-trends-at-a-tidal-inlet. Accessed December 15, 2013

Shapiro, G.I., Van der Molen, J., and De Swart, H.E. (2004). "*The Effect Of Velocity Veering On Sand Transport In Shallow Sea*". Ocean Dynamics, Vol. 54, Issue 3-4, pp. 415-423.

Sheremet, A. and Stone, G.W. (2003). "*Wave Dissipation Due To Heterogeneous Sediments On The Inner Louisiana Shelf*". Proceedings of Coastal Sediments'03*,* Clearwater Beach, FL*,* pp. 120-121.

Shi,F.,Svendsen,I.A., Kirby, J.T., and Smith, J.M. (2003). "*A Curvilinear Version Of A Quasi-3D Nearshore Circulation Model*". Coastal Engineering, Vol. 49 (1-2), pp. 99-124

Shi, F., Kirby, J.T., and Hanes, D. (2007). "*An Efficient Mode-Splitting Method For A Curvilinear Nearshore Circulation Model*". Coastal Engineering, Vol. 54, pp. 811-824.

Shi, F., Hanes, D.M., Kirby, J.T., Erikson, L., Barnard, P., and Eshleman, J. (2011). "*Pressure-Gradient-Driven Nearshore Circulation On A Beach Influenced By A Large Inlet-Tidal Shoal System*". J. Geophys. Res., Vol. 116, pp. 1029-1046. DOI:10.1029/2010JC006788.

Shi, F., Kirby, J.T. Hsu, T., and Chen, J. (2012). "*NearCoM-TVD: A Hybrid TVD Solver For Nearshore Community Model*". Center For Applied Coastal Research, University Of Delaware, Newark, DE, pp. 1-43

Shi, F. (2013). "*CoastGrid For Matlab (To Make A Boundary Fitted Grid)".* Center For Applied Coastal Research, University of Delaware, Newark, Delaware. Available from: http://coastal.udel.edu/~fyshi/coastgrid/coastgrid.html. Accessed March, 10, 2013.

Sivahkolundu, K.M., Mani, J.S., Idichandy, V.G., and Kathiroli, S. (2009). "*Estuarine Channel Stability Assessment Through Tidal Asymmetry Parameters*". Journal Of Coastal Research, Vol. 25, No. 2, pp. 315–323. (West Palm Beach, FL) ISSN 0749-0208.

Sleath J.F.A. (1990). "*Velocities And Bed Friction In Combined Flow*". Proc. 22nd International Conference On Coastal Engineering, ASCE, Delft, The Netherlands, Vol.1, pp. 450–463.

Soulsby, R.L. (1997). "*Dynamics Of Marine Sands: A Manual For Practical Applications*". Thomas Telford, London, UK, pp. 1-272.

Soulsby, R.L. (1987). "*The Relative Contributions Of Waves And Tidal Currents To Marine Sediment Transport*". Hydraulic Research Ltd., Wallingford, Oxfordshire, UK. Report SR 125, pp. 1-41.

Soulsby, R.L. and Clarke, S. (2005). "*Bed Shear-Stresses Under Combined Waves And Currents On Smooth And Rough Beds*". Hydraulics Research, Wallingford, Oxfordshire, UK. Report TR 137, pp. 1-32.

Stive, M. J.F. and Wind, H.G. (1982). "*A Study Of Radiation Stress And Set-Up In The Nearshore Region*". Coastal Engineering, Vol. 6, pp. 1-25.

Sutherland, J. and Obhrai, C. (2009). "*COMIBBS Composite Modelling Report*". HR Wallingford Report TR173, Which Is Also HYDRALAB-III Report JRA1-08-05, pp. 1-61.

Svendsen, I.A, Haas, K., and Zhao, Q. (2003). "*Quasi-3D Nearshore Circulation Model, SHORECIRC.*" Center For Applied Coastal Research, University Of Delaware, Newark, DE, pp. 1-36.

System Of Industry Metocean Data For The Offshore And Research Communities (SIMORC). http://www.simorc.org/ Accessed March 24, 2012.

Sybrandy, A.L. and Niller, P.P. (1990). "*The WOCE/TOGA SVP Lagrangian Drifter Construction Manual*". Scripps Institution Of Oceanography, University of California, SIO Reference 90-248, San Diego, California.

Van der A, D.A, Ribberink, J.S., van der Werf, J., and O'Donoghue, T. (2010). "*New Practical Model For Sand Transport Induced By Non-Breaking Waves And Currents*". Proceedings Of Int'l Conference On Coastal Engineering, No. 32, pp. 331-342.

Van Dongeren, A.R., Sancho, F.E., Svendsen, I.A., and Putrevu, U. (1994) "*SHORECIRC: A Quasi 3-Dimensional Nearshore Model*". Proc. 24th Int'l. Conference On Coastal Eng., ASCE, Kobe, No. 24, pp. 2741-2754.

Van den Boogaard, H., Gerritsen, H., Caires, S., and van Gent, M. (2009). "*Composite Modelling By Applying An Inverse Technique In Analysing Interactions Between Beaches And*

Structures". Proc. 8th Int'l. Conference On Hydroinformatics, Concepcion, Chile, January 12-16, 2009, pp. 178-188.

Van den Boogaard, H., Gerritsen, H., Caires, S., and van Gent, M. (2009b). "*Wave Attack On Sea Defences – Potential Benefits Of A Composite Modelling Approach*". Proceedings 33rd IAHR Congress, Vancouver, August 2009, Paper 10443, pp. 1006-1013.

Wang, X.H. and Craig, P.D. (1993). "*An Analytic Model Of Tidal Circulation In A Narrow Estuary*". J. Marine Research, Vol. 51, No. 3, pp. 447-465.

Williams, A.B. and Benson, N.U. (2010). "*Interseasonal Hydrological Characteristics And Variabilities In Surface Water Of Tropical Estuarine Ecosystems Within Niger Delta, Nigeria*". Environ. Monit. Assess. Springer Science And Business Media B.V. (2010) Vol. 165, pp. 399-406.

Wolf, J. (2009). "*Coastal Flooding – Impacts Of Coupled Wave-Surge-Tide Models*". Natural Hazards, Vol. 9 No.2, pp. 241-260.

Wolf, J., Hargreaves, J.C., and Flather, R.A. (2000). "*Application Of The SWAN Shallow Water Waves Model To Some Uk Coastal Sites*". Proudman Oceanographic Laboratory (POL) Report No. 57, pp. 1-51

Zhang, J. and Liu, H. (2009). "*Currents Induced By Vertical Varied Radiation Stress In Standing Waves And Evolution Of The Bed Composed Of Fine Sediments*". International Journal Of Sediment Research, Vol. 24, pp. 214-226.